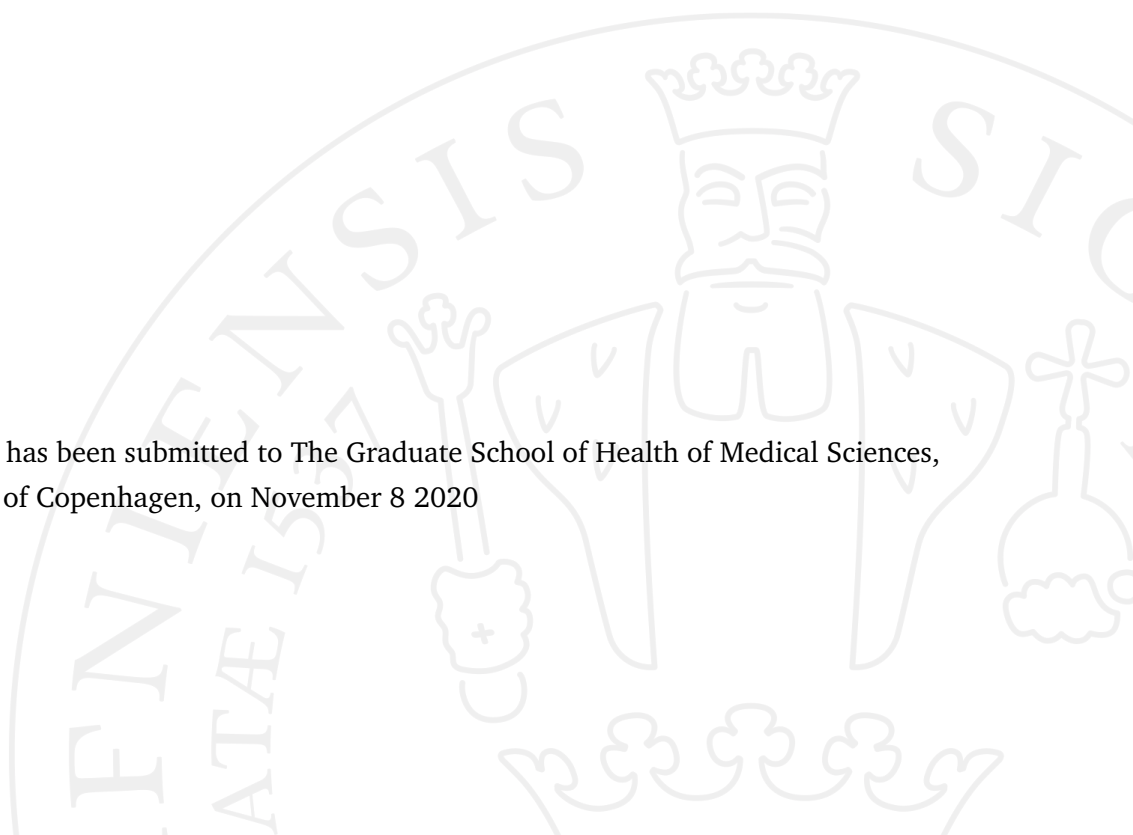UNIVERSITY OF COPENHAGEN

PhD Thesis

Utilizing 7 Tesla MRI
and automated segmentation

– A new era in the presurgical evaluation of patients with severe epilepsy

Giske Opheim

Giske Opheim

PhD Thesis title: *Utilizing 7 Tesla MRI
and automated segmentation*

Main supervisor: Lars H. Pinborg

Primary co-supervisor: Olaf B. Paulson

Co-supervisors:

Melanie Ganz-Benjaminsen

Patrick M. Fisher
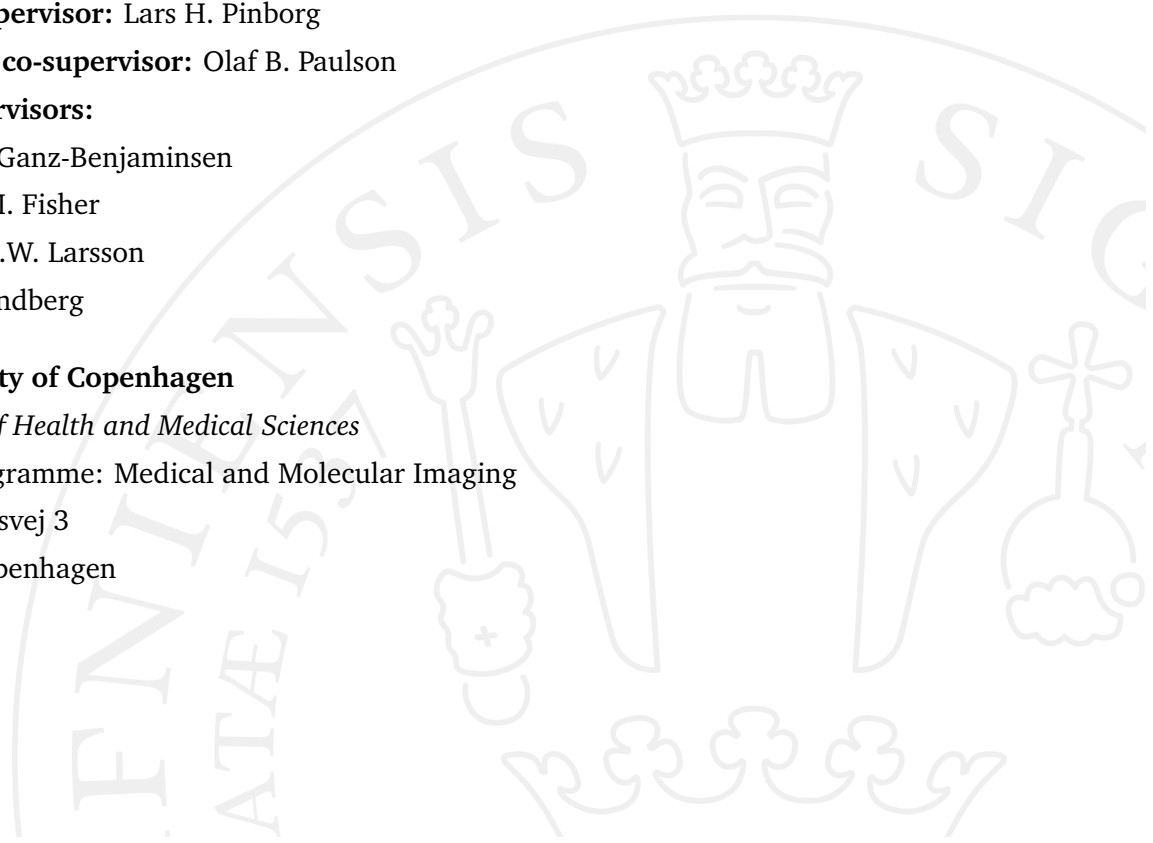
Henrik B.W. Larsson

Ulrich Lindberg

University of Copenhagen

Faculty of Health and Medical Sciences

PhD Programme: Medical and Molecular Imaging

Blegdamsvej 3

2100 Copenhagen

Preface

This project was carried out between August 2017 and October 2020, at Neurobiology Research Unit, Neuro Centre, Copenhagen University Hospital Rigshospitalet, Denmark.

The PhD student was first enrolled in the Clinical Medicine PhD programme at the PhD school of Faculty of Health and Medical Sciences, University of Copenhagen. Due to reorganization of the PhD school, the enrollment later switched to the Medical and Molecular Imaging PhD programme.

Both 3 Tesla (T) and 7T magnetic resonance imaging (MRI) scans were acquired at Hvidovre Hospital; 3T as part of standard clinical workflow, and 7T MRI as a clinical project-specific workflow.

The thesis is in synopsis form, and based on three articles. The first article is based on a study that is continued after preliminary results were included as part of the Master's thesis of Ane Kloster, now MD, whom I co-supervised in 2019. We therefore share first authorship in this article. This article is still in preparation, as we planned to include Norwegian data. The analyses performed during my research stay there were initially delayed due to COVID-19 travel restrictions. Thereafter, COVID-19 has had effects on elective patient treatments, which is still pressuring clinical workflow at many hospitals. This has delayed the retrieval of the clinical data necessary to complement and finish analyses.

The second article is based on data acquired during the PhD project. The manuscript was under review, and subsequently rejected (October 28th, 2020). Due to the tight schedule until thesis submission deadline, this manuscript

has not yet been reformatted according to requirements in the targeted journal. The third article has been formally accepted (October 29th, 2020) for publication, but is under embargo at the time of thesis submission.

List of manuscripts in the thesis

Article 1:

Ane Kloster, Giske Opheim, Emil Holm, Philip Fink-Jensen, Bo Jespersen, Camilla G. Madsen, Karen B. Larsen, Olaf B. Paulson, Melanie Ganz, Lars H. Pinborg, "*Automated hippocampal segmentations in histopathologically classified HS ILAE type 1 and 2*", 2020, **In preparation**

Article 2:

Giske Opheim, Erik B. Dam, Oula Puonti, Ane Kloster, Martin Prener, Raghavendra Selvan, Minna H. Litman, Helle J. Simonsen, Olaf B. Paulson, Lars H. Pinborg, Melanie Ganz, "*Exploring radiomic features in clinical 3T and 7T MRI of mesial temporal sclerosis in an open presurgical patient cohort.*", 2020, **In preparation**

Article 3:

Giske Opheim, Karin Markenroth-Bloch, Anja van der Kolk, et.al., "*7T Epilepsy Task Force consensus recommendations on the use of 7T in clinical practice*", 2020, **Accepted for publication.**

Acknowledgements

The first thank you goes to my main supervisor Lars H. Pinborg. Thank you for all the new, valuable knowledge, and for enduring the many calls and emails from me - it is a lot of work guiding a student with a technical background in a pure clinical environment. Also, thank you, Olaf B. Paulson, who together with Lars gave me the opportunity to continue as a PhD student after teaching me about neuroscience during my master's in Beijing. In this thesis, he was my principle co-supervisor, and also a research companion, a mentor in good clinical practice and oyster tasting, and a wine connoisseur. Melanie Ganz-Benjaminsen, one of my co-supervisors, I acknowledge as my main technical supervisor throughout this thesis. She also referred me to the Machine Learning in Imaging Projects (MLIP) course at Dept. of Computer Science (DIKU) at UCPH - which led to new collaborators and the core of the analyses in article 1 and 2. Also, thank you to my other co-supervisors, Patrick Fisher, Ulrich Lindberg and Henrik Larsson for complementing a solid supervisor team.

Next, I thank Erik B. Dam and Raghavendra Selvan at the MLIP course at DIKU. They inspired and taught me specific analysis tools and research mindset, which also helped me when searching for errors and writing a manuscript. The work from MLIP also involved collaboration with Oula Puonti, a collaborator and friend who has a unique ability to share knowledge, brainstorm technical analysis aspects, and teach important tricks to students - including how to move on after making errors.

For the students (now doctors) and pillars behind the data acquisition, Ane Kloster and Martin Prener: Thank you for being an incredible work force, and helping out with 7T MRI scans. Ane is also a shared first-author in article 1,

Summary

Epilepsy is a common chronic neurological disease that affects 1% of people of all ages worldwide. About one third of patients suffer from drug-resistant seizures, and in those with focal seizure onset, surgery may be the only cure. With MRI, the clinicians look for epileptogenic lesions that help localize the seizure origin. Mesial temporal sclerosis (MTS) is the most common epileptogenic lesion found in MRI in drug-resistant epilepsy. The histopathological substrate of MTS is hippocampal sclerosis (HS). HS can be further divided into subtypes, that are desired to identify before surgery. Automated MRI segmentation and 7T MRI are emerging techniques with a great potential to improve detection of epileptogenic lesions, and also to add new and unique information to the epilepsy surgery evaluation process. Automated MRI segmentation tools may identify changes in volume and shape not possible to identify by visual assessment. 7T MRI may both help visually detect and subclassify epileptogenic lesions, and the high-resolution images may also improve automated MRI segmentations.

In the first article, we tested if automated hippocampal subfield segmentations in 3 Tesla (T) MRIs could identify specific patterns of hippocampal subfield volume loss that correspond to histopathological classification in patients with HS. We found excellent correspondence with HS diagnosis, but failed to identify subfield volume patterns that allow us to separate patients with two different HS subtypes. This study will be complemented with additional and independent data from the Norwegian epilepsy surgery program, which will allow us to further test whether patterns of MRI volume changes are better markers of seizure outcome and memory function than the histopathological classification. The collaboration was put on hold by the COVID-19 pandemic.

In the second article, we compared standard quantitative hippocampal features between clinical 3T and 7T MRI in mesial temporal sclerosis (MTS) and non-MTS patients. Counter-intuitively, we found equally discriminative ability in the two MRI field strengths. Two main limiting factors were lack of histological ground truth and detailed understanding of differences in segmentation algorithm performance between 3T and 7T MRI.

The third article presents the first consensus-based recommendations for setting up and evaluating 7T MRI in epilepsy – a project I co-initiated and coordinated between teleconferences, and finalized manuscript draft in. This work was based on experiences from the 7T Epilepsy Task Force – an international group of 21 world-leading centers within this field. The article is intended as a handheld for centers that are new to 7T MRI in epilepsy.

In conclusion, the three studies provide information that is important to consider when implementing 7T MRI, automated segmentation and the combination thereof, in the presurgical evaluation of drug-resistant epilepsy patients. Our findings also demonstrate that in the cross-field between clinical and engineering considerations, more research is warranted to fully uncover characteristics in segmentation performance and potential of contributions from 7T MRI when compared to 3T. Lastly, having a consensus-based set of guidelines will hopefully help when setting up an epilepsy-specific 7T MRI protocol.

Resumé in Danish

Epilepsi er en almindelig kronisk neurologisk sygdom, der rammer 1% af mennesker i alle aldre verden over. Omkring en tredjedel af patienterne lider af lægemiddelresistente anfald, og hos patienter med fokal anfaldsstart kan kirurgi være den eneste kur. Med magnetisk resonans billeddannelse (MR) ser klinikerne efter epileptogene læsioner, der hjælper dem at lokalisere anfaldsoprindelsen. Mesial temporal sklerose (MTS) er den mest almindelige epileptogene læsion, der findes i MR ved lægemiddelresistent epilepsi. Det histopatologiske substrat for MTS er hippocampus sklerose (HS). HS kan yderligere opdeles i undertyper, som er ønskeligt at identificere inden operationen. Automatiseret MR-segmentering og 7 Tesla (T) MR er nye teknikker med et stort potentiale til at forbedre påvisning af epileptogene læsioner og også tilføje ny og unik information til evalueringsprocessen for epilepsikirurgi. Automatiserede MR-segmenteringsværktøjer kan identificere ændringer i volumen og form, der ikke er mulig at identificere ved visuel vurdering. 7T MR kan både hjælpe visuelt med at detektere og underklassificere epileptogene læsioner, og billeder med høj opløsning kan også forbedre automatiserede MR-segmenteringer.

I den første artikel testede vi om automatiserede hippocampussegmentateringer på 3T MR kunne identificere specifikke mønstre af volumentab i hippocampale subfields, der svarer til histopatologisk klassificering hos patienter med HS. Vi fandt fremragende korrespondance med HS-diagnose, men kunne ikke identificere mønstre i volumentab, der giver mulighed for at adskille patienter med forskellige HS-undertyper. Denne undersøgelse vil blive suppleret med yderligere og uafhængige data fra det norske epilepsikirurgiprogram, som gør det muligt for os at også teste om mønstre af MR-volumenændringer er bedre markører for krampeanfald og hukommelses-

funktion end den histopatologiske-klassificering. Samarbejdet blev sat på hold af COVID-19 pandemien.

I artikel 2 sammenlignede vi standard kvantitative hippocampale parametre i klinisk 3T og 7T MR hos patienter med og uden MTS. Vi fandt, kontraintuitivt, stor lighed i de to MR-feltstyrkers evne til at adskille de to patientgrupper. To begrænsende faktorer var mangel på histopatologisk information, samt detaljeret forståelse af forskelle i segmenteringsalgoritmens ydeevne mellem 3T og 7T MR.

Den tredje artikel præsenterer de første konsensusbaserede anbefalinger til opsætning og evaluering af 7T MRI i epilepsi - et projekt jeg co-initierede og koordinerede mellem telekonferencer, samt færdigstillede manuskriptet til. Dette arbejde var baseret på erfaringer fra 7T Epilepsy Task Force - en international gruppe med 21 verdensledende centre inden for dette felt. Artiklen er beregnet som en guide til centre, der er nye indenfor 7T MR i epilepsi.

Samlet set giver de tre studier information der er vigtig at overveje ved implementering af 7T MR, automatiseret segmentering, og kombinationen deraf, i den prækirurgiske evaluering af lægemiddelresistente epilepsipatienter. Vores fund viser også, at det på tværs af feltet mellem kliniske og tekniske overvejelser er nødvendigt med mere forskning for fuldt ud at afdække karakteristika i segmenteringsydelse og potentiale for bidrag fra 7T MR sammenlignet med 3T. Afslutningsvis, hjælper det forhåbentlig feltet at have et konsensusbaseret sæt retningslinjer, når hospitaler vil oprette en epilepsispecifik 7T MR-protokol.

Abbreviations

BOLD = blood oxygen-level dependent

CA = Cornu Ammonis

CSF = cerebral spinal fluid

DG = Dentate Gyrus

EEG = Electroencephalography

EMU = epilepsy monitoring unit

ESI = Electrical Source Imaging

FCD= focal cortical dysplasie

FDG = Fluor-deoxyglucose

FLAIR = fluid-attenuation inversion recovery

FS = FreeSurfer

GC-DG = Granular-cell dentate gyrus

HC = Healthy controls

HMPAO = Hexamethylpropyleneamine oxime

HS = Hippocampal sclerosis

IcEEG = Intracranial electroencephalography

ILAE = International League Against Epilepsy

MCD = malformations of cortical development

MDT = multidisciplinary team

MeanSig = Mean Signal Intensities

MEG = Magnetoencephalography

MPRAGE = magnetization-prepared rapid acquisition gradient echo

MR = Magnetic Resonance

MRI = Magnetic Resonance Imaging

MSI = Magnetic Source Imaging

MTS = Mesial Temporal Sclerosis

PET = Positron Emission Tomography

RF = radio frequency

SPECT = Single-Photon Emission Computed Tomography

std = standard deviations

StdSig = Standard deviations of signal intensities

Tc = Technetium

TE = echo time

TLE = temporal lobe epilepsy

TR = repetition time

TSE = turbo spin echo

WH = Whole-hippocampal

Contents

Introduction

1.1 Emerging changes in the evaluation of surgical candidacy in severe epilepsy

In the presurgical evaluation of epilepsy - where a multidisciplinary team reaches decisions regarding surgical treatment of individual patients with severe seizures - there is high demand on confidence in clinical investigations and expert decisions. The clinicians consider clinical findings, patient history and her/his subclinical experiences, and evaluate the probability of having precisely localized the seizure origin. The localization work-up is related to the need for concluding to what degree the individual patient will be relieved of seizures after surgical treatment [Ryvlin and Rheims, 2008].

During the evaluation process, which will be introduced in detail in section 2.1.2, several methods, including structural, functional and metabolic neuroimaging, are assessed in both qualitative and semi-quantitative manners. By qualitative, we mean, e.g., to visually inspect structural magnetic resonance (MR) imaging (MRI) scans for cortical or subcortical abnormalities. By semi-quantitative, we mean, e.g., using advanced algorithms to calculate cortical thickness from the structural MRI scan, and subsequently, qualitatively assessing whether a region with abnormal cortical thickness is likely to be the cause of seizures.

In 2019, Zijlmans et.al. published a review on changing concepts in presurgical evaluation for epilepsy surgery [Zijlmans *et al.*, 2019]. They explored how a range of new techniques such as post-processing of MRI [Jack Jr *et al.*, 1992; Wang *et al.*, 2015; Hong *et al.*, 2016], can give non-redundant information for diagnostic support and guidance of the surgical resection plan. MRI scans can also serve as input to analysis pipelines that utilize post-processing information to automatically detect a lesion [Mo *et al.*, 2019; Wagstyl *et al.*, 2020], predict surgery outcome and memory deficits in a patient with a certain

epilepsy subtype [Bernhardt *et al.*, 2015; Memarian *et al.*, 2015], or to simply discriminate between specific epileptogenic lesion subtypes [Scanlon *et al.*, 2013; Coan *et al.*, 2014b]. All these methods are semi- or fully quantitative, and have the common ability to provide objective support to the already complex presurgical decision-making. As shown in figure 1.1, the number of published studies based on automated segmentations is increasing. Notwithstanding the fact that epilepsy is a progressive network disorder, there will be no surgical treatment if the hypothesis of (primary) seizure origin is not pinned down with high certainty. Finding a structural epileptogenic lesion remains the most important individual correlate to the correct area to resect, and thus, early surgery success [Téllez-Zenteno *et al.*, 2010; Najm *et al.*, 2013]. Since the use of such techniques have great clinical potential, some are already being commercialized for the use MRI scans at conventional 1.5 or 3 Tesla (T) field strengths. Two examples are NeuroQuant [CoreTechLabsInc., 2020] and NeuroReader [Brainreader-Aps., 2020], which both function by giving the clinicians a report with cortical and subcortical morphometric measures, including volumetric asymmetry.
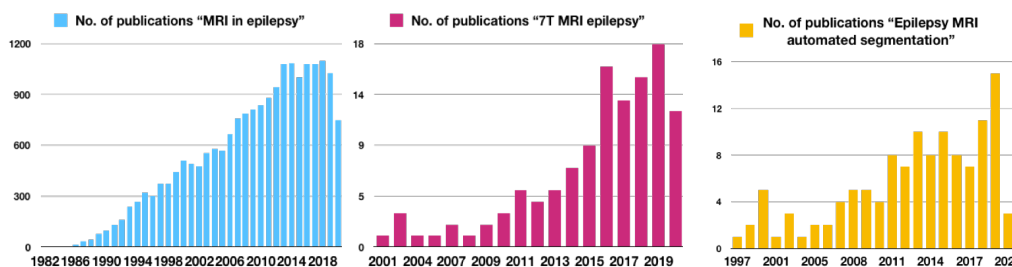
Figure 1.1.: Illustration of increased relative focus on MRI (blue), 7T MRI (red) and automated segmentations (yellow) in epilepsy. The barplots represent amount of publications found on PubMed (https://pubmed.ncbi.nlm.nih.gov) with the search terms as stated above each plot. While MRI has contributed to the understanding and diagnosis of epilepsy for almost four decades, both 7T and automated segmentation has been utilized for around two decades. Recent developments of 7T MRI hardware and software, the first FDA and CE approved 7T MRI system, and development of computational methods along with increased computational power likely explain these trends.

As another way of supporting the diagnostic process, the Zijlmans review also highlighted the increase in clinical studies using 7T MRI [Kwan *et al.*, 2016; Veersema *et al.*, 2016; De Ciantis *et al.*, 2016]. Investigations of the contributions of 7T MRI in the clinic have first of all focused on utility when performing the visual qualitative radiological assessment. The potential added

value by including ultrahigh field MRI scans at 7T in the presurgical evaluation has been emphasized during the last decade [Henry *et al.*, 2011; Van der Kolk *et al.*, 2013; Veersema *et al.*, 2017; Voets *et al.*, 2017; Feldman *et al.*, 2019]. Particularly, in difficult-to-diagnose epilepsy subtypes, hereunder individual patients with no or very subtle lesions on 3T MRI, 7T may have a large diagnostic yield. There also seems to be a non-redundant contribution of 7T MRI in elucidating what has been shown to be a "false-positive" or non-clarified lesion on 3T MRI [Veersema *et al.*, 2017; Feldman *et al.*, 2019]. Nonetheless, it is still a new field among other studies on MRI in epilepsy (see figure 1.1), and the relatively few studies still vary with regards to 7T MRI specific sequences, selected patient subtypes and results.

In parallel, studies on the information yield from post-processing on the same structural 7T MRI scans have largely been performed on healthy subjects or populations with Alzheimers disease or depression [Kim *et al.*, 2011; Lüsebrink *et al.*, 2013; Wisse *et al.*, 2016; Brown *et al.*, 2019]. Such post-processing techniques have not until recent years been adapted to the characteristics of the 7T MR images, and still need to be validated in populations of patients with specific epilepsy subtypes. Recently, one study assessed the yield of post-processing of cortical structures on 7T MRI in 3T MRI-negative (no finding of diagnostic importance) patients [Wang *et al.*, 2020]. They found that post-processing of 7T MRI yielded clinically important information in a total of 43% of the patients. This was a 22% increase from the yield from visual inspection of 7T scans, and a 25% increased yield compared to post-processing of their 3T MRI data.

Temporal lobe epilepsy (TLE) constitutes around 60% of patients with focal epilepsy, and about 80% of TLE patients have mesial temporal sclerosis (MTS) where the hippocampus is the most commonly affected region [Wiebe and Jette, 2012]. As with other epilepsy types, MRI analyses with focus on hippocampal sclerosis (HS) diagnosis could provide quantitative diagnostic support in a range of ways, including cost-saving automatization of radiological workflow and non-redundant information yield in subtle cases. MRI analyses of hippocampus and its subregions, however, have only been utilized in a few 7T studies [Henry *et al.*, 2011; Santyr *et al.*, 2017; Voets *et al.*, 2017; Zhang *et al.*, 2019; Canjels *et al.*, 2020]. These studies vary with respect to methodology (visualization only, or manual or automated segmentation), targeted features and samples. One of the studies compared 7T results to 3T, and

suggest improved visualization of hippocampal architecture, but no increase in predictive value of whole-hippocampal volumetry compared to 3T [Zhang *et al.*, 2019]. Although an increased precision in hippocampal visualization and delineation is indicated by the studies, there is still a need to clarify to what extent automated MRI analysis and targeted clinical MRI features on 7T contributes compared to 3T MRI in diagnosed HS cohorts.

This thesis will focus on structural MRI, and is based upon three articles. In article 1, an automated MRI segmentation technique is utilized on a large retrospective patient cohort with 3T MRI only. Following, the same technique is used in article 2, where the segmentations are performed on a unique dataset of comparable 3T and 7T MRI clinical scans. In article 3, world-leading experts present the first consensus-based experiences and guidelines for setting up and utilizing 7T MRI in epilepsy patients referred to presurgical evaluation.

1.2 Specific aims of articles in the thesis

- **Aim of article 1:** To assess automated 3T MRI hippocampal subfield segmentations for groups with hippocampal sclerosis type 1 and 2.

- **Aim of article 2:** To explore a set of radiomic MRI features in the hippocampi of radiologically diagnosed MTS patients, and compare the findings in clinical 3T and 7T MRI scans.

- **Aim of article 3:** To provide a consensus-based set of guidelines on how to set up and evaluate a 7T MRI epilepsy scan protocol.

Background

2

This chapter will introduce general theoretical background relevant to the articles included in this thesis. While some background is introduced as part of the rationale in each article, this chapter will contain important definitions and a broader range of information about the main clinical and methodological aspects that are mentioned in one or more of the three articles. The purpose is to give readers with a general clinical and/or technical background, without the specific knowledge of readers in the targeted journals, a wider appreciation of the complex considerations in epilepsy and implementation of MRI in epilepsy diagnostics.

2.1 Epilepsy

Epilepsy is a brain disease where patients present with a predisposition for recurring seizures, and affects around 1% of the world population [Fisher *et al.*, 2014; Fiest *et al.*, 2017]. Causes of epilepsy include structural (developmental or injury), genetic, infectious, metabolic, immune and unknown [Fisher *et al.*, 2014; Scheffer *et al.*, 2017]. In the case of focal epilepsies, disorganized tissue (neurons) is involved in epileptogenesis - the generation of seizures. One theory is that this disorganized tissue is arranged in distinct zones involved in a cascade of events leading to seizures [Lüders *et al.*, 2006; Staba *et al.*, 2012; Zhang and Kwan, 2019]. These zones together make up the so-called epileptogenic zone, as depicted on figure 2.1.

Seizures arise from abnormal, hypersynchronous neuronal firing, which may or may not spread beyond brain regions of focal seizure origin [Fiest *et al.*, 2017]. The duration of a seizure can vary from seconds to many minutes, with a post-ictal state (period after electrographic seizure) lasting for up to several hours after more severe seizure types. Seizure symptoms will vary dependent on location of the focal origin. The symptoms will also vary dependent on seizure propagation pathway(s), and whether they spread quickly to the whole
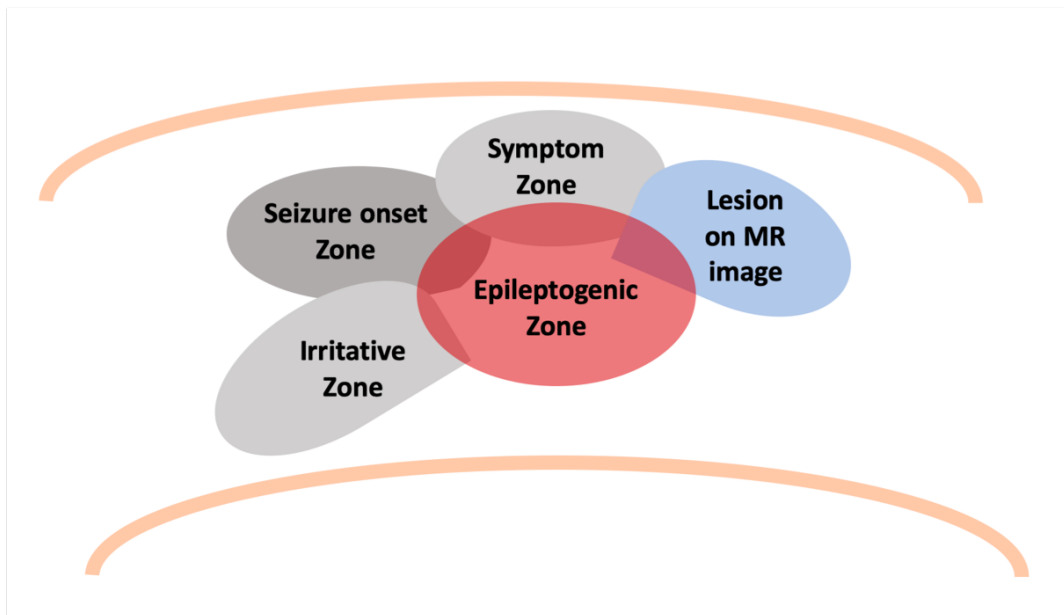
Figure 2.1.: Schematic illustration of the zone-model depicting the different functional zones (grey) adjacent to an epileptogenic lesion (blue), in a cortical area (beige lines). The epileptogenic zone (red) is a theoretical zone, which is thought to overlap across the other areas. It is sufficient removal of this zone which is crucial to obtain successful surgery outcome (see section 2.1.3).

brain or not. For instance, a seizure originating in the the occipital cortex may disturb vision. If such a seizure propagates to the motor cortex, the patient will present with motor symptoms - a simplified schematic is seen in figure 2.2. As mentioned in chapter 1, increasing efforts are made to better understand seizure propagation pathways and their predictive value to outcome. Seizures are classified based on whether the seizure onset is known, if they display with motor symptoms, affect awareness, and spread to the contralateral side [Fisher *et al.*, 2017; Scheffer *et al.*, 2017; Lüders *et al.*, 2019].

The seizure burden - related to seizure frequency, duration and type - varies between patients. It may also fluctuate in individual patients, meaning that a patient may be seizure free for months or years, and suddenly experience one or several seizures again. Living with epilepsy has often significant implications on quality of life, such as social anxiety, learning and concentration difficulties, and loss of driver's license [Langfitt, 1995; Sperling, 2004; Holmes, 2012; Strzelczyk *et al.*, 2017]. Additionally, there is the specific risk of injuries during a seizure, and the increased risk of sudden unexpected death [Shorvon and Tomson, 2011; Ryvlin *et al.*, 2011]. These risks apply to both patients who

still maintain a work/study life, as well as to patients fully disabled by their epilepsy.
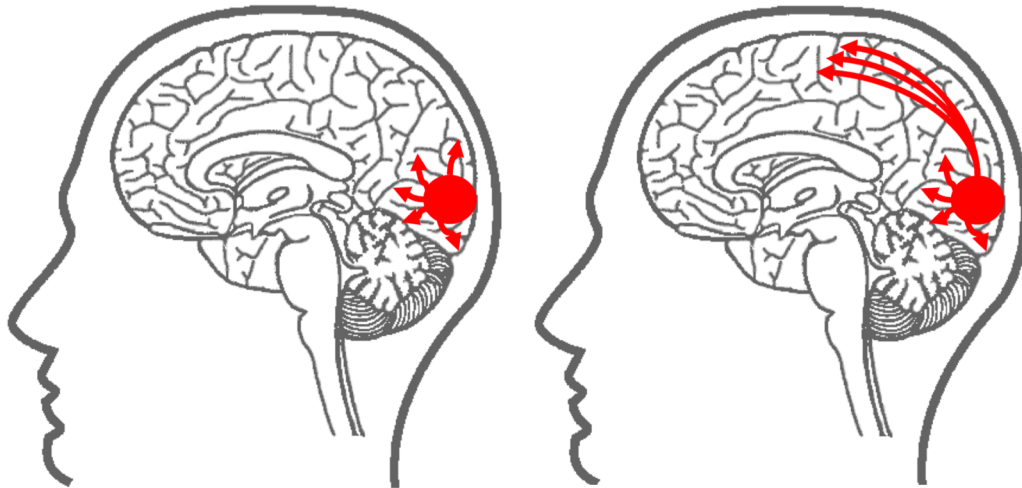
Figure 2.2.: Simplified illustration of a partial seizure (red) occurring in the occipital lobe. *Left:* seizure activity does not propagate outside adjacent cortical areas, and the patient likely only experiences transient visual symptoms. *Right:* The seizure hypothetically propagates to the motor area, and the patient simultaneously displays motor symptoms. If there was a spread to the whole brain, the patient would suffer from secondary generalized tonic-clonic seizures, and have affected awareness.

2.1.1 Drug-resistant focal epilepsy

Drug-resistant epilepsy has been defined as *"failure of adequate trials of two tolerated, appropriately chosen and used anti-epileptic drug schedules (whether as monotherapies or in combination) to achieve sustained seizure freedom"* [Fisher *et al.*, 2014]. World-wide, as many as one third of patients with epilepsy suffer from seizures in spite of optimized anti-epileptic drug treatment. Many patients respond partially or fully to the anti-epileptic drugs only for periods of time [Brodie *et al.*, 2012]. Also, many patients live with side-effects that are just as burdensome as the seizures themselves, such as severe sleepiness, tremble, or loss of libido. Not responding to two or more anti-epileptic drugs is one of the requirements for referral to presurgical evaluation [Ryvlin and Rheims, 2008].

2.1.2 Presurgical evaluation in drug-resistant focal epilepsy

An overview of the complex and iterative presurgical evaluation workflow of the multi-disciplinary team (MDT) is given in figure 2.3. The MDT is a group of neurologists, neurosurgeons, neuropsychologists, neurophysiologists, a radiologist and nursing staff specialized in evaluating patients with severe epilepsy.

Upon referral to a specialized epilepsy center, a patient will typically present with an MRI scan, a history of drug-resistant seizures and oftentimes a scalp electroencephalography (EEG). The specialized neurologist will often refer to a standardized MRI epilepsy protocol, as well as a neuropsychologist and admission to the Epilepsy Monitoring Unit (EMU). In the EMU, the patient is admitted as an in-patient for several days, while EEG and video-monitoring are assessed parallelly during seizures and inter-ictal stages [Kinney *et al.*, 2019; Baumgartner and Pirker, 2019].

When this first round of clinical findings are assembled, the neurologist meet together with the rest of the MDT. They discuss the concurrence of findings in the individual patient, and evaluate seizure burden and the patient's own motivation. In the ideal world, there is one MRI lesion corresponding to semiology plus laterality, and location determined on a EEG that displayed similar electrographic patterns on a number of seizures during the EMU admission. But this is rarely the case, and more clinical investigations are warranted.

In fact, around 15-30% of patients have no identifiable lesion on the structural MR images [Bien *et al.*, 2009; Duncan *et al.*, 2016]. While this may be aided by advanced MRI protocols [Duncan *et al.*, 2016], 7T MRI and/or post-processing combined with machine learning (see chapter 1), the current standard and recommendation is to investigate with ^{18}Fluor-deoxyglucose (^{18}FDG) Positron Emission Tomography (PET) and Technetium-^{99m} hexamethylene propylene amino oxine (^{99m}-Tc HMPAO) Single-Photon Emission Computed Tomography (SPECT) [Miller and Hakimian, 2013; Jette *et al.*, 2014; Tripathi *et al.*, 2016; Baumgartner *et al.*, 2019]. These are metabolic imaging methods, where a radioactive ligand is injected and used to trace regions with FDG-hypometabolism (inter-ictal PET) or increased perfusion
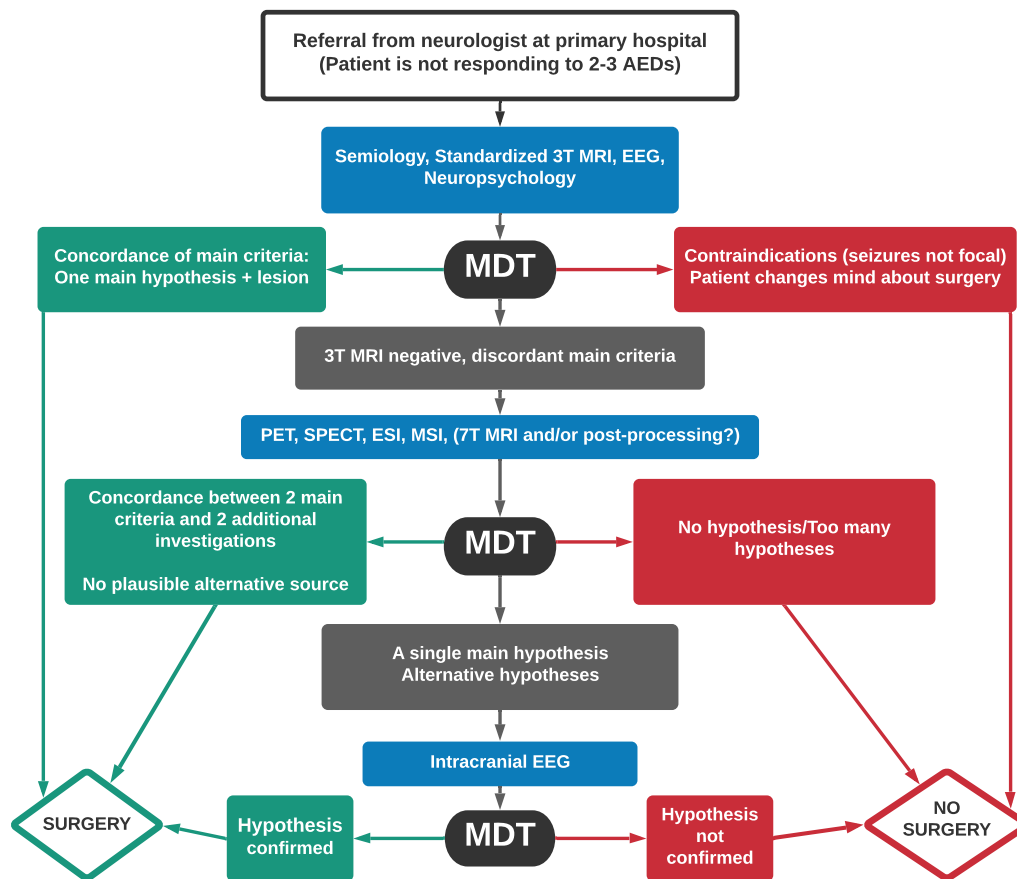
Figure 2.3.: Overview of the presurgical evaluation workflow. MDT = multidisciplinary team, EEG = electroencelography, MRI = magnetic resonance imaging, PET = positron emission tomography, SPECT = single-photon emission computed tomography, ESI = electrical source imaging, MSI = magnetic source imaging, T = Tesla, AEDs = anti-epileptic drugs.

(ictal SPECT), which is correlated with seizure onset zone (see figure 2.1). In addition, Electric Source Imaging (ESI) and Magnetic Source Imaging (MSI) may be recommended here. ESI and MSI are quantitative source localization techniques based on a neurophysiologist's registration of inter-ictal spikes on EEG and magnetoencephalography (MEG) data. Both have been shown to add significant diagnostic value: Foged et.al. recently demonstrated diagnostic added value of ESI in 34% of patients [Foged *et al.*, 2020]. In a review by Carrette et.al., a wide range of studies form evidence for sensitivity in localization of the irritative zone (see figure 2.1) with MSI in up to 75% of patients [Carrette and Stefan, 2019]. If two or more of these methods (SPECT, PET, ESI, MSI, EEG, semiology and MRI) concur, and there are no further plausible alternative hypotheses, a patient may be referred to surgery.

Still, up to 30-40% of patients proceed to invasive EEG-monitoring [Parvizi and Kastner, 2018], where intracranial EEG (IcEEG) electrodes are implanted into a number of brain regions in attempt to localize the seizure onset zone and, if confirmed, aids resection planning.

Clinical case example:

To give an example of the presurgical evaluation course in an individual patient, the following presents a fictive story of a patient with suspected TLE. A 23 years old female with first seizure onset at the age of 7, had started experiencing seizures again after being on her anti-epileptic medication. Her friends at football practice had seen her acting strangely, and when they tried talking to her, she was unresponsive. After the seizure she did not recall her friends asking her questions during the seizure. She recalled having a sensation arising from her stomach (an "epigastric aura") when she was home alone, and sometimes at the university. But she had no other recollection of seizures, other than being told in her post-ictal state (the period right after a seizure) when she was around friends and fellow students. This happened once a week, but may happen more often when she is alone. Her neurologists at the local hospital discussed referral to a tertiary epilepsy center, for evaluation of surgical candidacy. The patient was motivated, as she no longer had her driver's licence, and felt increased concentration difficulties at school.

At the epilepsy center, she was referred to a 3T MRI since her last one was acquired in the 1.5T MRI system ten years ago. The radiologist viewed the old MRI scans, but could not detect anything abnormal. In the new 3T MRI scans, he could see subtle signal changes and very slight flattening of the top of the left hippocampal head, but nothing clear enough to base a diagnosis on. Thus, it was concluded that the patient must be considered MRI negative. During the EMU recordings, that lasted for a whole week, she only had 3 seizures. Two of the seizures did indeed seem to originate on the left temporal lobe, but one seemed to start on the right side. All three times she experienced the gastric auras, and were able to notify nursing staff of this sign of an upcoming seizure. The nursing staff tested her awareness by response to tailored routine questions asked during the 3-minutes long seizure, e.g., "remember the colour

blue". The patient was unresponsive, and did not remember the task given to her.

At the subsequent conference, the MDT agreed that seizure semiology with epigastric aura suggested a mesial temporal symptomatogenic zone, and that MRI was considered normal though subtle changes in the left hippocampus were noted. The MDT further concluded that seizures during EEG were suggestive of an ictal onset zone in the temporal lobe, though laterality was not clear. The main hypothesis was that the epileptogenic zone was in hippocampus on the left side. The alternative hypothesis was hippocampus independently on both sides. To test these hypotheses she was referred to a new video-EEG (EMU), FDG-PET and ^{99m}-Tc HMPAO SPECT. The patient case was discussed again three months later. PET showed only subtle hypometabolism on the left basal temporal lobe. During the second EMU, she had two seizures, one indicating left temporal lobe, and one indicating right. The ictal SPECT showed one large hyperperfusion label mesially on the left side, but also several small ones in both temporal lobes. ESI indicated a source on the left basal temporal lobe, but more posteriorly than PET. She had also been scanned at 7T MRI as part of a research project. 7T MRI showed fewer digitations and a less visible molecular layer in left hippocampus, and slight increased signal on the 3D FLAIR image. Due to B_1 inhomogeneity, the basal parts of neither temporal lobes were possible to visually assess. Altogether, MRI was still considered negative. Post-processing of 3T and 7T MRI with segmentation of hippocampus and hippocampal subfields showed no significant volumetric reduction, except for CA1 from the 7T scans. The MRI texture measure was only slightly abnormal for left hippocampus on both 3T and 7T MRI.

The MDT could not determine whether all seizures were truly originating in left and fast-spreading to right, if this was a case of bilateral mesial TLE with subtle HS, or if there was an undetected cortical dysplasia (see section 2.4) in the left basal temporal lobe, as indicated by FDG-PET and ESI. The patient was referred to IcEEG, with nine depth electrodes being implanted, including two in each hippocampus and one in each amygdala, and three additional depth electrodes in the temporal cortex on the left side more lateral and posterior to hippocampus according to PET and SPECT. One year later, the MDT reconvened to discuss the IcEEG findings. The neuropsychologist met with the patient again, who had developed signs of depression, and experienced IcEEG implantation as quite traumatic. The recordings had shown clear seizure

onset in the left hippocampus during all six seizures, and also some inter-ictal activity in the basal temporal region on the left side. The patient was referred to a so-called Spencer resection, which is a tailored anterior temporolobectomy. At one-year postsurgical follow-up, she had experienced only two incidents of gastric auras and one seizure with affected awareness. This would be classified as ILAE class 2, see subsection 2.1.3.

2.1.3 Epilepsy surgery and outcome

In this thesis, epilepsy surgery refers to resective surgery. That involves neuro-surgical removal of the suspected epileptogenic tissue, or zone (see figure 2.1). Depending on the hypothesis, as mentioned in section 2.1.2, resecting the culprit region may involve selected lesionectomy (figure 2.4b), selected removal of complete structures such as the amygdala and hippocampus, or removal of larger parts of a lobe [Jette *et al.*, 2014], e.g., anterior temporo-lobectomy as on figure 2.4a. Sufficient removal of the epileptogenic zone responsible
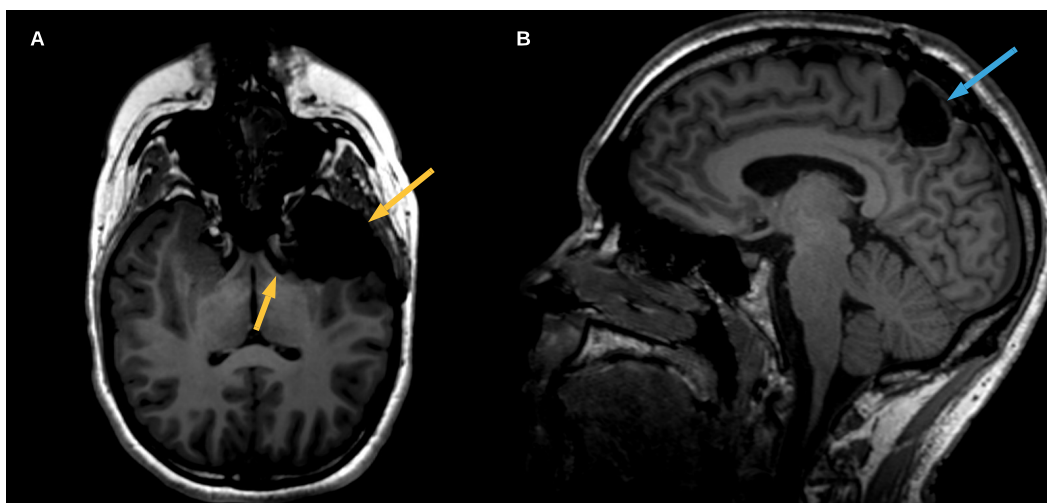
Figure 2.4.: Examples of post-operative MRI from two patients: **(A)** Left-sided anterior temporal lobectomy including removal of hippocampus, and **(B)** lesionectomy in the right parietal lobe. Both examples are from after second operations, where resection margins were expanded - both patients are now seizure free after 2-year follow-up.

for generating seizures is the best predictor of surgery outcome [Lüders *et al.*, 2006; Ryvlin and Rheims, 2016; Zhang and Kwan, 2019], i.e., seizure freedom. However, determining the resection margin can be cumbersome, and sometimes a patients need re-operation to become seizure free. Presurgically, both structural and functional neuroimaging, as well as IcEEG may guide the

diagnostic hypothesis and surgical plan. Of these modalities, visualization of the lesion on a structural MRI scan is to date the most important in vivo correlate to seizure freedom, since it indicates approximate area of the epileptogenic zone well (see figure 2.1) [Lüders *et al.*, 2006]. Notably, a recent study that analyzed the predictive value of several presurgical investigations claimed that MRI only held predictive value for up to 1-year follow-up, and that the relative predictive value of MRI after that was difficult to calculate [Goldenholz *et al.*, 2016]. To establish good basis for evaluating the contributions of MRI (radiological and/or post-processing) to diagnostic predictions in the future, West et.al. at the Cochrane Epilepsy Group suggest controlled studies including MRI in the presurgical work-up [West *et al.*, 2016].

Surgery outcome in temporal lobe epilepsy

As stated previously, surgery outcome, also termed post-surgical, postoperative, or seizure outcome, is the result of the epilepsy surgery: The seizure frequency before surgery is compared to the seizure frequency post-surgery.

Surgery outcome is most often classified by one of two systems: International League Against Epilepsy (ILAE) [Wieser *et al.*, 2001] or Engel [Engel, 1993] classifications. Both classifications define and describe four to six overall ranges of seizure frequency relative to that of the presurgical frequency. These ranges conceptually categorize into "free", "significantly reduced", "somewhat reduced" and "same or worse", as shown in table 2.1 for ILAE scores. One study in a series of 76 patients has shown excellent inter-rater reliability of the two classification systems [Durnford *et al.*, 2011]. In this thesis, we have referred to the ILAE surgery outcome classification system to parallel the use of HS ILAE subtype classification in article 1.

Conceptual categories	ILAE	Specifications
Free	Class 1	Completely seizure free without auras
Significantly reduced	Class 2	Only auras without other seizures
Somewhat reduced	Class 3	One to three seizure days per year with/without auras
Same or worse	Class 4-6	Less favorable seizure outcomes

Table 2.1.: Overview of categories for surgery outcome classification by ILAE. *In this thesis, namely article 1, we have referred to the ILAE surgery outcome classification system, as we also use ILAE classification for hippocampal sclerosis subtypes.*

In TLE with HS, the surgery outcome is considered excellent, with up to 75% of patients becoming seizure free [Muhlhofer *et al.*, 2017]. For negative MRI, which happens in approximately 30% of TLE patients, the pooled successful surgery outcome rate is around 51% [Wang *et al.*, 2016; Muhlhofer *et al.*, 2017]. In the latter group, the chances of seizure freedom depends highly on concordance of PET and electrographic (EEG or ESI) findings. With regards to resection strategy - anterior temporal lobectomy (ATL) vs selected removal of hippocampus and amygdala (SAH) - Mathon et.al. found that the methods had similar effects on surgery outcome [Mathon *et al.*, 2017].

HS Subtype	Prevalence	Surgery Outcome
HS type 1	60-80%	Good
HS type 2	5-10%	Poor
HS type 3	4-7.4%	Poor

Table 2.2.: Overview of prevalence and typical surgery outcome of hippocampal sclerosis (HS) types 1-3. A more severe degree of neuronal loss corresponds to better outcome. Classification of HS subtypes is further explained in section 2.2.

An atrophic hippocampus is found to be an overall good predictor of surgery outcome in TLE [Jardim *et al.*, 2016]. However, different HS ILAE subtypes also correlate with different surgery outcomes [Blümcke *et al.*, 2013], as seen in table 2.2. This is an important rationale behind the wish to accurately classify HS based on in vivo neuroimaging, namely MRI. An accurate in vivo classification would entail a more precisely informed surgery consent, along with enabling tailored postsurgical follow-up. This requires precise evaluation of degree of atrophy of the different hippocampal subfields (see table 2.3).

Of importance, HS is variably distributed along the hippocampal axis [Thom *et al.*, 2012], and remaining sclerotic tissue that are missed during localization and resection may be the cause of unsuccessful surgery outcome.

2.2 Histopathological assessment of hippocampal sclerosis

According to the ILAE, the subtypes of HS are classified according to patterns of neuronal cell loss [Blümcke *et al.*, 2013]. These patterns imply which

hippocampal subfields are predominantly presenting with the most severe reduction in neurons.

HS subfield	HS ILAE type 1	HS ILAE type 2	HS ILAE type 3
CA1	↑↑	↑↑	0-↑
CA2/3	0-↑	0-↑	0-↑
CA4	↑↑	0-↑	↑↑
DG	0-↑	0-↑	0-↑↑

Table 2.3.: Adapted version of table 1 the ILAE classification of HS article [Blümcke *et al.*, 2013]. ↑↑=severe neuronal loss, ↑=moderate neuronal loss, 0 =no visible neuronal loss, CA=cornu ammonis, DG=dentate gyrus, HS=hippocampal sclerosis.

There are also other characteristics such as dispersion of granular cells and mossy fibers [Schmeiser *et al.*, 2017], and within each HS subtype, specimens can present as heterogeneous [Blümcke *et al.*, 2013; Thom, 2014]. This entails that the degree of neuronal loss in a specific subfield may be close to equal between two subtypes, and that each combined pattern of subfield reduction determines the subtype (see table 2.3). HS ILAE type 1 is reckognized by severe neuronal loss in both CA1 and CA4, meaning most neurons (>80%) are lost. HS ILAE type 2 is classified as moderate-to-severe neuronal loss in CA1, and maximum of moderate (< 30%) neuronal loss in the other subfields. Notably, visual confirmation of neuronal loss depends on 30-40% reduction in principal cells in these subfields. HS ILAE type 3 presents with predominant moderate-to-severe neuronal loss in CA4, and up to moderate in the other subfields. Furthermore, ILAE states that HS subtype classification applies to anatomically intact specimens, and recommend evaluating with whole cross-sections with all subfields being present. As a consequence, the histopathological diagnosis is most often performed as "approximate" description during visual inspection of the hippocampal tissue. The typical histopathological description of hippocampal tissue does not include detailed description of reductions in all subfields, since it is not visible below 30-40%. A moderate degree of neuronal loss, such as with cases of CA4 in HS ILAE type 2, can be difficult to evaluate with the human eye.

In addition to the variability in the patterns described above, the degree of neuronal loss may also vary along the hippocampal axis (see dotted line in figure 2.5), and the sclerosis has been shown to extend posteriorly to the hippocampal tail [Thom *et al.*, 2012]. Normally, only an anterior part
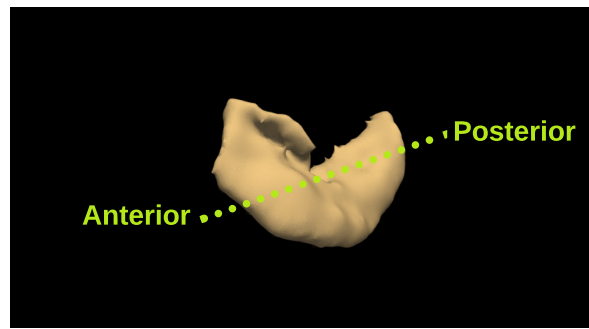
Figure 2.5.: A smoothed 3D rendering of left hippocampus based on the 3D MPRAGE scan acquired at 7T in our project. The green dotted line depicts the longitudinal axis from anterior to posterior end.

of the hippocampus is removed, and hence available for histopathological assessment.

At Copenhagen University Hospital Rigshospitalet, neuropathologists classify HS subtypes according to ILAE consensus classification [Blümcke *et al.*, 2013]. This is done by viewing several cross-sections of tissue, often by each subfield individually. Examples of specimens from HS ILAE type 1 and 2 are shown alongside a non-HS specimen in figure 2.6.

2.3 Magnetic Resonance Imaging

The first part of the current section is written based on knowledge from classes in basic and advanced MRI, and the handbooks by Brown [Brown et al., 2014] and Nishimura [Nishimura, 2010]. In following subsections, sources will again be cited continuously.

Magnetic resonance imaging (MRI) of the brain is a technique to obtain good soft tissue contrast due to the magnetic properties of the varying water content in different tissue types. The hydrogen protons in the water molecules, which are spinning, partially align with the static magnetic field (B_0) when a subject is placed inside the magnet - the scanner bore. Computer-steered radio-frequency (RF) waves can then be applied to excite the protons and push them out of steady-state. The spatially dependent RF field is referred to as the B_1 field. These RF waves are transmitted through an RF transmit coil, which can be placed outside in the gantry (3T MR scanners) or be close to the head in
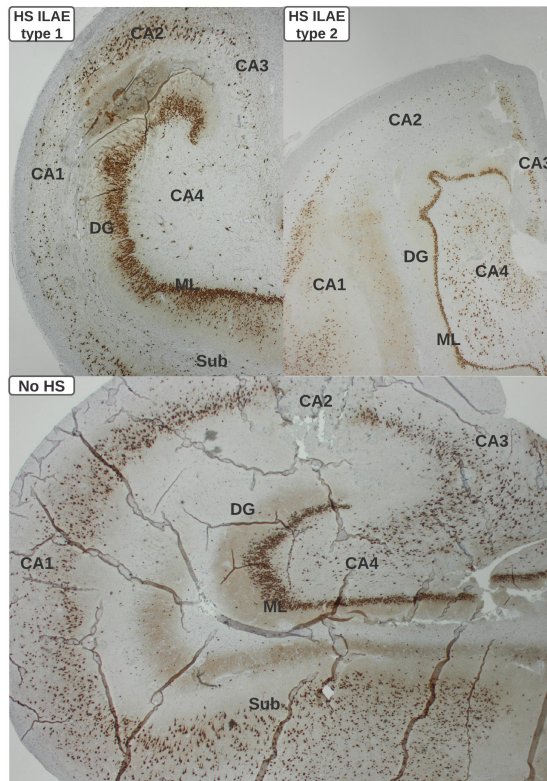
Figure 2.6.: Histopathological samples from HS ILAE type 1 (upper left), type 2 (upper right) and non-HS (bottom) specimens. CA=cornu ammonis, DG=dentate gyrus, ML=molecular layer, Sub=subiculum.*This figure is a copy of figure 2 in article 1, appendix A.1.*

combination with the RF receiver coil (7T MR scanners). In the RF receiver coil, currents are induced by the magnetic fields in the tissue as the tissue magnetization changes over time. The gradient system is also located inside the gantry. A combined overview of timings and amplitude of applied RF and gradient waveforms is referred to as the pulse sequence design, and is highly specific for each image type. A simplified overview of the parts of the MRI system is given in figure 2.7.

A pulse sequence is programmed according to what region(s) of the brain one aims to image and what contrast weighting that is requested. Contrast weighting translates into what tissue parameter is dominating the image. T_1 and T_2 parameters, two magnetization relaxation constants, have different magnetization relaxation rates in fat and water, so by adjusting repetition time (TR) and echo time (TE) (two basic pulse sequence parameters), one can determine if the more fatty tissue and/or cerebral spinal fluid (CSF) should display hyperintense signal.
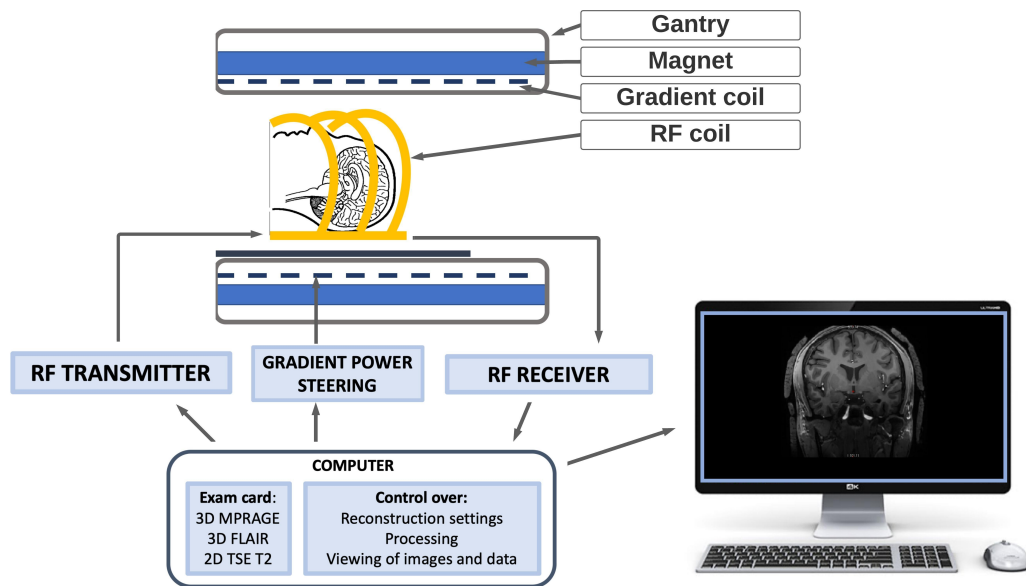
Figure 2.7.: A schematic overview of the MRI system. The sequences in the exam card represent the recommended MRI protocol for epilepsy at 1.5 or 3T systems. The image on the computer screen is a coronal slice of the 3D MPRAGE image acquired at 7T. RF=radio frequency, MPRAGE= magnetization-prepared rapid gradient echo, FLAIR=fluid-attenuation inversion recovery, TSE=turbo spin echo.

A commonly implemented MR sequence for T_1-weighted images is the 3D (whole-brain) magnetization-prepared rapid acquisition gradient echo (MPRAGE) sequence, which has short TR and short TE. A T_1-weighted image displays with dark grey matter and cerebral spinal fluid (CSF), and a slightly brighter white matter. The, also common, turbo spin-echo (TSE) sequence is used to acquire T_2-weighted images, with a long TR and long TE. The TSE T_2-images are most often acquired in a multislice 2D sequence in MR scan protocols in epilepsy, which is recommended by the International League Against Epilepsy (see subsection 2.3.1. Another recommended T_2-weighting sequence is the fluid-attenuation inversion-recovery (FLAIR) sequence, which similarly to TSE T_2 images display bright grey matter and dark white matter, but with the characteristical dark CSF signal, due to an inversion pulse that attenuates the "free water"-signal.

The resulting image characteristics are used for evaluation of different forms of signal changes, corresponding to different tissue properties. An abnormal tissue property may be the sign of pathology - more on this in section 2.4.

2.3.1 Clinical MRI protocol in epilepsy

Structural MRI in epilepsy is assessed to detect and characterize structural substrates of epileptogenic lesions, and to plan resective surgery [Rüber *et al.*, 2018]. The ILAE presented its newest recommendations for 3T MRI protocol in epilepsy [Bernasconi *et al.*, 2019] in 2019, see table 2.4. Although other minimal setup standards have been proposed [Cendes *et al.*, 2016], they are similar in terms of contrast weightings.

When utilized during presurgical workup, structural MRI will be evaluated by an expert neuroradiologist. She/he assess all MR images with the contrast-weightings in table 2.4, as any signal changes (or lack thereof) may inform of different characteristics in the individual brain, as described in section 2.4.

Contrast	Resolution	Recon.	Comments on usage
3D MPRAGE	1x1x1 mm	All three planes	Anatomy and morphology
3D FLAIR	1x1x1 mm	All three planes	Signal intensity
2D TSE T_2	0.4x0.4x2 mm	Only coronal	Mesial temporal structures
T_2* (and SWI)	-	-	Venous blood, hemorrhage, iron and calcifications
MPRAGE-Gd	-	-	Tumor, vascular pathology or infection

Table 2.4.: Summarized overview of the currently recommended 1.5 or 3T MRI protocol for epilepsy. T_2* (or susceptibility weighted imaging (SWI)) and MPRAGE-Gd (gadolinium) are optional, and the authors did not specify recommendations for settings in these sequences. *MPRAGE= magnetization-prepared rapid acquisition gradient echo, FLAIR=fluid-attenuation inversion recovery, TSE=turbo spin echo, Recon.=reconstruction planes*.

The 3D images are acquired sagittally and reconstructed in axial and coronal planes while perpendicularly angulated on the hippocampi or temporal lobes. This requires some training of the MR operator, as slightly misangulated images might hamper radiological assessment. The purpose is to provide the radiologist with slices that depict the biggest cross-sectional planes of hippocampus, according to radiological routine and preference specific to MRI in epilepsy.

The coronal 2D TSE T_2 is also angulated perpendicularly on the hippocampi or temporal lobes, see example figure 2.8 from the 7T MR protocol. At 7T, the field-of-view determines what regional slices should be selected. In the 3T protocol, the 2D TSE T_2 still covers the whole brain.
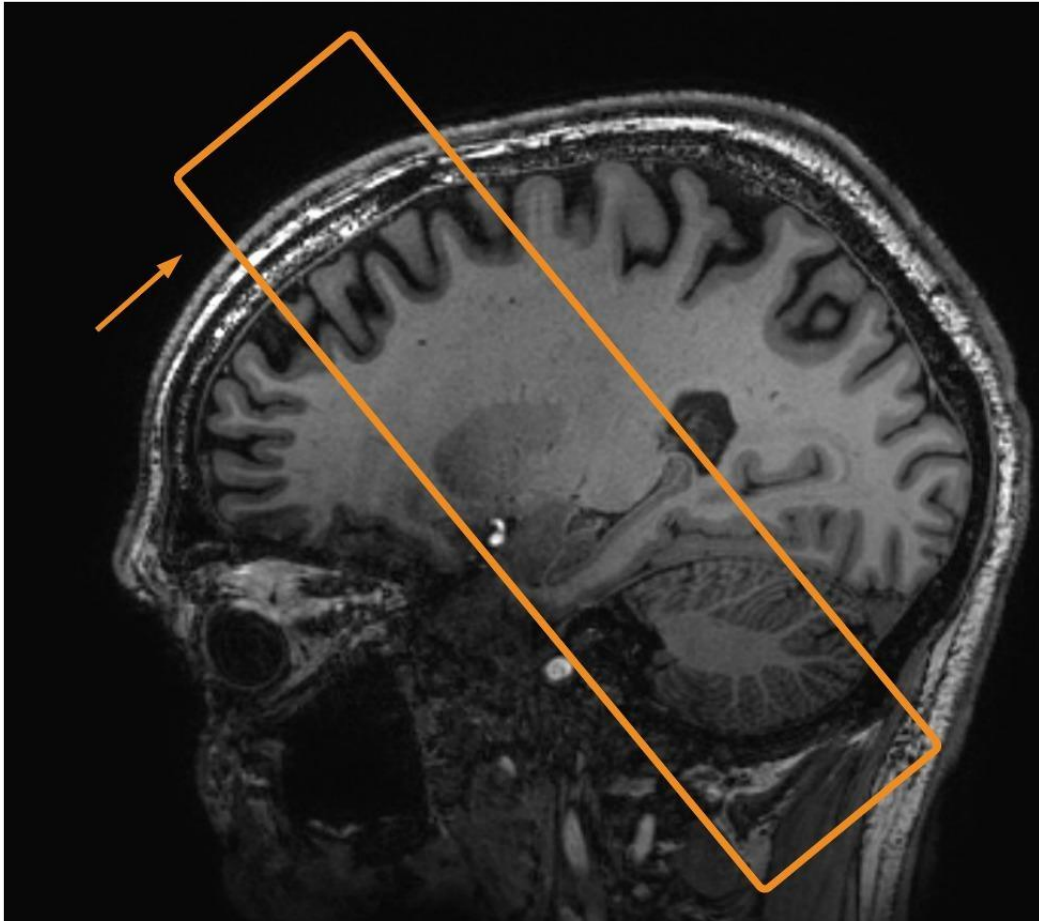
Figure 2.8.: Demonstration of placement of the field-of-view box (orange), as a typical multi-slice T_2 sequence focusing on hippocampus would be planned. The box is angulated to have the coronal view oblique to the hippocampus and temporal lobes. The orange arrow indicated the sampling direction. Additionally, this is how one angulates the coronal reconstructions of the 3D scans.

2.3.2 Moving to ultrahigh field MRI

As stated in articles 2 and 3, and also in chapter 1, there have been several demonstrations of the added value of 7T MR in epilepsy [Colon *et al.*, 2016; Veersema *et al.*, 2016; Veersema *et al.*, 2017; Colon *et al.*, 2018; Feldman *et al.*, 2019; Rondinoni *et al.*, 2019]. The advantages of clinical 7T MRI are related to the increased signal-to-noise ratio (SNR) and stronger susceptibility effects - due to the stronger magnetic field [Van der Kolk *et al.*, 2013; Balchandani and Naidich, 2015; Springer *et al.*, 2016; Obusez *et al.*, 2018; Trattnig *et al.*, 2018]. Susceptibility effects are what happens in the tissue when affected by a magnetic field, and tissues have different susceptibility properties. Increase

in SNR and susceptibility can either be utilized to acquire the same structural images as on 3T either faster than at 3T, or with higher spatial resolution and better contrast than what is obtainable at standard 3T MR systems in the clinic. To help limit acquisition times, and thus limit patient discomfort and scan costs, high-resolution 7T MR sequences are typically implemented with higher parallel imaging acceleration, whose performance greatly improves at higher magnetic fields [Wiesinger *et al.*, 2006].

There is, however, "no free lunch" when performing MRI scans. For instance, the susceptibility effects can in addition to increased image contrast entail undesired susceptibility artefacts in certain areas of the brain where the borders between two different tissues meet, e.g., in the brain right above the nasal cavities. This happens due to local distortions in the magnetic fields in such areas, and would lead to local signal loss (dark spots) in parts of the affected brain region.

Additionally, there are other issues that are more pronounced at 7T than at 3T, that have significant implications for clinical workflow and image assessment. According to the 21 centers in the 7T Epilepsy Task Force, the most significant issues are increased sensitivity to motion, and increased spatial inhomogeneity of the B_1 field (the RF transmit field, see section 2.3). Examples of the motion issue and B_1 field inhomogeneity issues are seen in figure 2.9. B_1 homogeneity can improve somewhat with the use of dielectric pads. Dielectric pads are thin "pillows" filled with high permittivity materials, that are placed on each side of the head. The ones used in 7T MR acquisitions in the current thesis are seen in figure 2.10. The spatial dependency of the B_1 field entails that when optimizing sequences to maximize global SNR, it may lead to local signal loss. Particularly at ultrahigh field strengths, it is difficult to ensure the same local flip angle centrally and laterally in the brain. One solution is to "help" the scanner by manually modifying the B_1 field magnitude, as demonstrated in figure 2.9c and d.
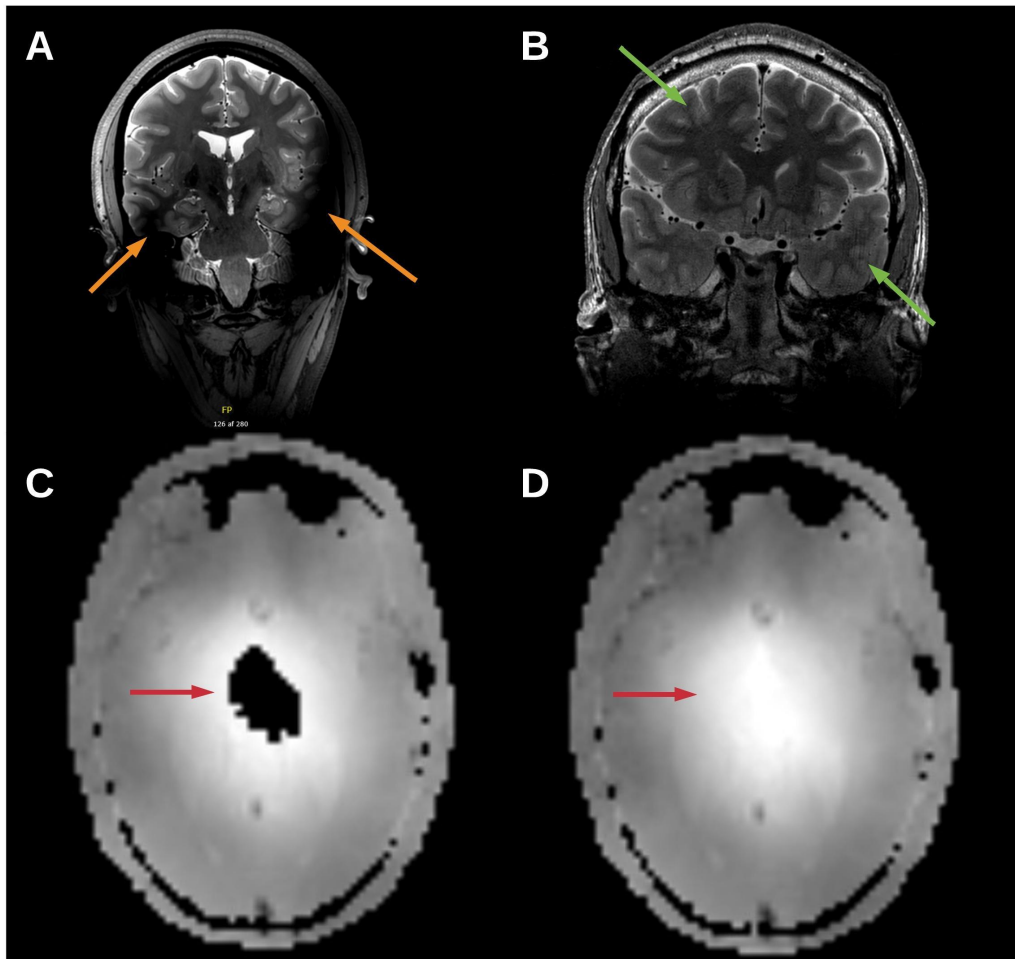
Figure 2.9.: Illustration of specific issues encountered at 7T. **A:** A coronal view of a 3D TSE T_2 image from patient in our cohort. This was before renewal of dielectric pads, when smaller and older pads were used. As reported by other sites in the 7T Epilepsy Task Force, the B_1 spatial inhomogeneities (indicated by orange arrows) are detrimental to radiological evaluation of lateral and basal parts of the temporal lobe. **B:** A 2D T_2 image from our cohort. Green arrows mark motion artefacts, which is a frequently occurring issue in multi-slice T_2 scans. **C:** B_1 magnitude map demonstrating a signal dropout in the central part of the scan. This issue translated to a very dark spot in 3D FLAIR and T_2 scans, particularly when the preferred contrast setting of most radiologists is used. Such dark spots hampers image assessment in the mesial brain structures, e.g., the hippocampi. The issue is mentioned in chapter 3 in article 3, appendix A.3. **D:** Same B_1 magnitude map from same subject, after manually scaling the so-called RF drive scale. Albeit inferring some signal loss laterally, the signal gain across hemispheres is evident, and alleviates the whole-brain assessment. However, it comes at the cost of prolonged total scan duration, as it takes a few extra minutes to adjust at the beginning of the MR protocol. *This solution have been automized by the Clinical MR scientist, Jan Ole Pedersen, at Philips, as it helps clinical workflow and reduces scan costs.*

The stronger magnetic field itself may induce dizziness when the epilepsy patient is moving into the 7T scanner bore, due to the B_0 field's effect on the balance organs during movement [Hansson *et al.*, 2020]. Other noticeable differences compared to 3T, is the longer scanner bore and smaller headcoil (see figure 2.10). Ultimately, the consequence of a patient not being prepared for these 7T-specific experiences can be increase in discomfort, leading to more motion artefacts and disruption of scans. Although they are not exclusive to 7T, and some patients also experience them at 3T, it is a good idea to spend extra time preparing patients for a 7T MRI scan. This is advocated for by the 7T Epilepsy Task Force, and is found in the subsequent recommendations in chapter 2 in article 3 (appendix A.3).

Figure 2.10.: *Top:* The Philips Achieva 7T MR scanner at Centre for Functional and Diagnostic Imaging and research, Hvidovre Hospital, Copenhagen, Denmark. *Bottom left:* The head coil (2Tx/32Rx) used for the regular single-transmit setup. This coil is also used in the only FDA and CE approve 7T MR system worldwide. *Bottom right:* One of two dielectric pads, measuring 19x19 cm, that we use in the 7T MRI scans in article 2.

2.4 Radiological assessment of MR images in epilepsy

The targeted lesion subtype in article 1 and 2 is HS, which in this thesis (and in article 2) is referred to as MTS when diagnosed radiologically. One of the MRI signs of HS is atrophy of the affected hippocampus, which can be seen on both MPRAGE and TSE T_2 or FLAIR images [Henry *et al.*, 2011; Malmgren and Thom, 2012]. Other signs related to the shape and size are disorganized internal architecture and reduced digitations (foldings on the superior part of the hippocampi). Another sign that reflects disrupted tissue is the hyperintense signal changes, also on TSE T_2 and FLAIR images. All signs can, in more subtle cases, be present without the others. In many cases, however, both atrophy and hyperintense T_2 signal are described [Malmgren and Thom, 2012], as examplified in figure 2.11.
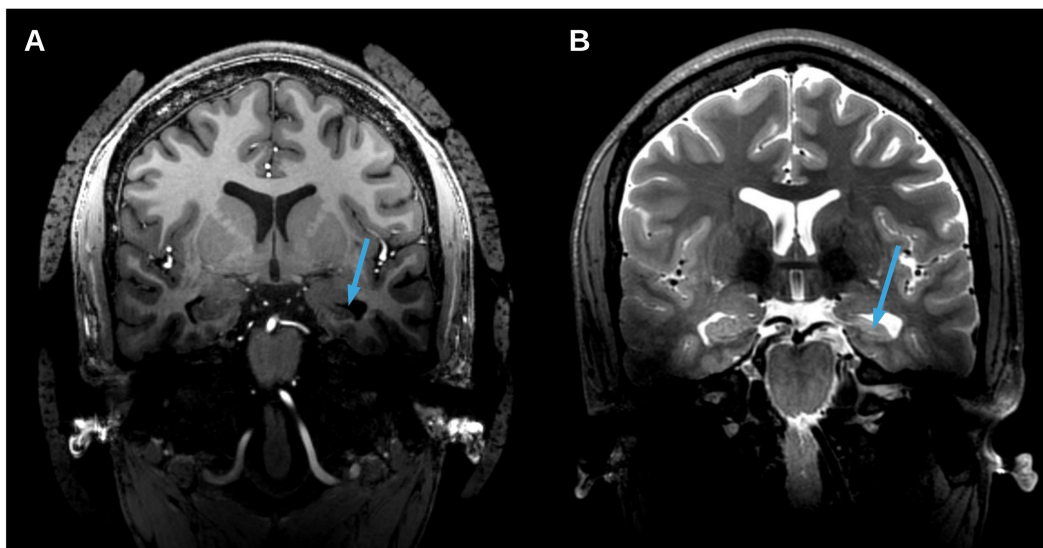
Figure 2.11.: Example of left-sided hippocampal sclerosis on coronal reconstructions of a 3D T_1-weighted **(A)** and a 3D T_2-weighted **(B)** 7T MRI image. As indicated by the blue arrows, the hallmarks of atrophy (reduced volume) and increased T_2 signal intensities are seen. A radiologist would evaluate the whole 3D volumes of these MR images.

As with HS, many types of malformations of cortical development (MCD), including focal cortical dysplasias (FCD) and polymicrogyria [Papayannis *et al.*, 2012], can be very subtle and difficult to detect even for other neuroradiologists specialized in epilepsy. Typical for the specialized neuroradiologist, is to look through both the lobe with suspected seizure onset and the whole

brain in all three image planes [Friedman, 2014]. When detecting a region with suspicious signal changes, typically all three main image contrasts are evaluated side-by-side to determine whether it is pathological. If so, a closer inspection may or may not enable distinguishing between likely subtypes of a lesion.

The radiologist also provides a general description of the whole-brain anatomy, looking for any other conspicuous abnormal findings. Such findings may include incidental findings of non-/pathological type, e.g., enlarged ventricles or a overall asymmetry in hemispheres. These findings may or may not be relevant to the epilepsy diagnosis, and will consequently be discussed when the MDT meets at a presurgical evaluation meeting.

Regarding radiological assessment of 7T MRI in epilepsy, the reader is referred to chapter 4 in article 3 (appendix A.3). Although the radiological assessment at large remains the same as described earlier in this section, there are several new details in both normal anatomy and appearance of lesions to look out for. These general considerations are also summarized in section 4.3.

Overview of methods

3

In this chapter, methods for the three articles will be presented. In articles 1 and 2, the same segmentation software and statistical tests are used for the 3T MRI and 7T MRI data. The 7T-specific pre- and post-processing for article 2 will be presented in 3.2.3, but otherwise the sections for article 1 will be used as subsequent references. The same 3T MRI sequences in table 3.1 were used in article 1 and 2. Lastly, the data collection workflow in article 3 will be presented in more details in section 3.3 than in the article.

3.1 Article 1

This article is based on a subgroup of a large, retrospective cohort with procedural 3T MRI scans performed during their enrollment in presurgical workup. After rigorously assessing quality of MRI scans, excluding other pathology affecting segmentations, and controlling the quality of segmentations of around 200 TLE patients, we ended up with a total patient population of n=60. The subgroup in subsection 3.1.1 is included on the basis of available hippocampal histology samples from resective surgery. The hippocampal tissue was classified according to ILAE HS classification guidelines [Blümcke *et al.*, 2013].

3.1.1 Patients and controls

The resulting patients (HS ILAE type 1 (n=25), type 2 (n=18)) patients were described by severe neuronal loss in subfields CA1 and CA4, and neuronal loss predominantly in CA1, respectively. Eight (n=8) patients were determined as having no HS. Additionally, nine HS patients were excluded, as shown in the overview in figure 3.1.

As control material to the patient group as a whole, we used healthy subjects (n=52). These were obtained from the Center for Integrated Molecular Brain Imaging (CIMBI) database [Knudsen *et al.*, 2016].
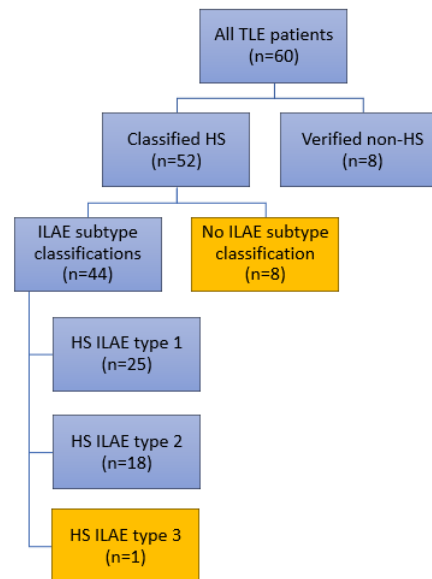
Figure 3.1.: Overview of included temporal lobe epilepsy (TLE) patients, from the point of completing quality assessment of MRI scans and segmentation output. Patients were divided into verified hippocampal sclerosis (HS) and classified ILAE subtypes. Eight (n=8) patients had no subtype classificaton, and were therefore excluded. Further, only one patient had subtype 3, which is redundant in group comparisons, and was therefore also excluded. Eight patients with histopathologically verified non-HS were used as patient controls, in addition to the 52 healthy subjects not depicted in this overview. *This figure is a copy of figure 1 in article 1 in appendix A.1.*

3.1.2 Automated segmentation and data extraction

The T_1-weighted images were processed using FreeSurfer [Fischl, 2012] v.6.0 prior to using the FreeSurfer hippocampal subfield segmentation tool [Iglesias *et al.*, 2015]. The algorithm used for hippocampal segmentation is based on a probability atlas that is derived from manual segmentations on both ex vivo and in vivo MRI. Simplified, the algorithm segments the subfields based on *a priori* information from the probability atlas when given an input scan. The hippocampal subfield segmentation tool is an individual tool that is run in addition to the standard brain reconstruction algorithm in FreeSurfer, that is based on the T_1-weighted MR images.

The hippocampal segmentations can be done on T_1-weighted or T_2-weighted images, or a combination (multispectral). We ran the multispectral mode (combined T_1- and T_2-weighted MR images) to increase accuracy of boundary tracing during hippocampal segmentations [Iglesias *et al.*, 2015].

An example of hippocampal labels overlaying a T_1-weighted image, and corresponding label outlines on a T_2-weighted image from the same subject, is seen on figure 3.2. Placements of hippocampal label outputs were visually quality checked. Volumes for the whole-hippocampal (WH) region and the hippocampus proper regions of CA1 and CA4 were exported and used for further analyses.

3.1.3 Statistical analysis and comparisons

We calculated absolute asymmetry ratios $|\frac{L-R}{L+R}|$, where L stands for left and R for right, to have a comparable parameter that unified left- and right-sided HS.

All patient subgroups were compared against each other as well as to healthy controls. This was done with a two-tailed Wilcoxon rank-sum test, which is insensitive to distribution type. The significance threshold corrected for multiple comparisons with Bonferroni correction became

$$p < \frac{0.05}{3(\text{regions}) \times 2(\text{hemispheres})} = 0.0083,$$

where regions are CA1, CA4 and WH.

3.2 Article 2

This study was based on data acquired during ongoing enrollment in presurgical evaluation. The patients were referred to 7T MRI scans both directly from their neurologists and after discussion of clinical indications during the presurgical meeting. This patient group therefore consists of a broader mix of epilepsy subtypes (see details in the methods chapter in appendix A.2) of

that in article 1. As part of standard presurgical work-up, all patients had been referred to clinical 3T MRI, as described in section 2.3.1. 7T MRI referrals started in December 2017.
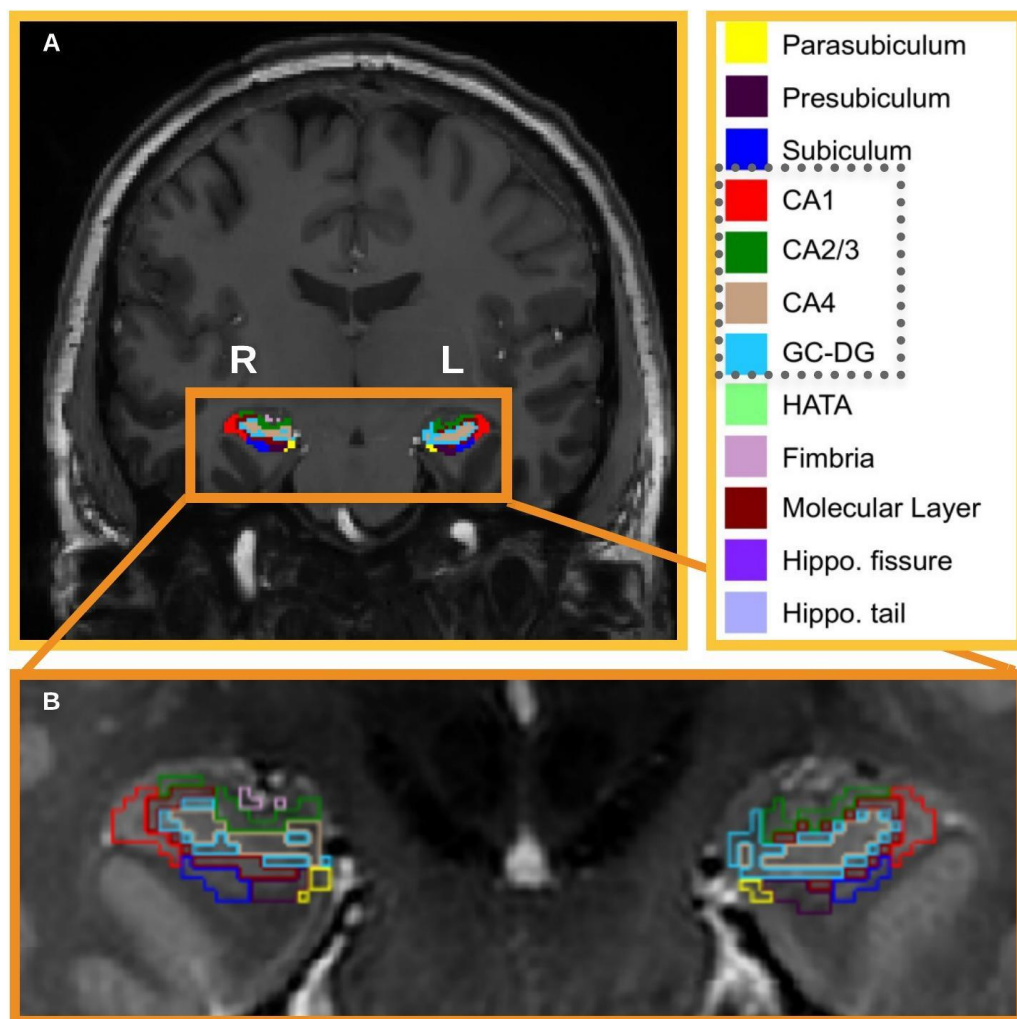
Figure 3.2.: *Top left:* Overlay of hippocampal subfield labels on a coronal slice of the 3D MPRAGE scan from a healthy control subject. *Bottom:* Overlay of outline of corresponding labels on corresponding 2D TSE T_2 scan. *Top right:* Color codes for the hippocampal subfield labels. The whole-hippocampal volume is the total volume from all labels in this box. The dotted box surrounds the four subfields that make up the ILAE HS subtype classification (see chapter 2). L=left, R=right, CA=cornu ammonis, GC-DG=granular-cell dentate gyrus, HATA=hippocampal-amygdala transfer region, Hippo.=hippocampal. *This figure is a copy of figure 2 in article 2, appendix A.2.*

3.2.1 MRI data

The 3T scans were acquired on a Siemens Prisma system (Siemens Ltd., Erlangen, Germany), with a 32-channel receive coil. The 7T MRI scans were acquired on an actively shielded Philips Achieva 7T system (Philips Ltd, Best, The Netherlands) and a quadrature 32/2 Rx/Tx coil (Nova Medical, Wilmington, MA). To compensate for B_1 inhomogenities (see sections 2.3 and 2.3.2), we used dielectric pads on both sides of the temporal lobes. An example is seen in figure 2.10. Sequence parameters from the two scans are shown in table 3.1.

Image	3T scan specifications	7T scan specifications
T_1-weighted	Sag./3D MPRAGE/1x1x1 mm	Sag./3D MPRAGE/0.7x0.7x0.7 mm
T_2-weighted	Cor./2D TSE T_2/0.5x0.4x3 mm	Sag./3D TSE T_2/0.7x0.7x0.7 mm

Table 3.1.: Scans used in article 2. Sag.=Sagittal sampling direction, Cor.=coronal sampling direction, MPRAGE= magnetization-prepared rapid gradient echo, TSE=turbo spin echo. *This table is a copy of table 1 in article 2, appendix A.2.*

3.2.2 Patient population

Sixty-eight patients were referred to 7T MRI from presurgical evaluation. One was excluded before acquiring 3T MRI data, and 12 were excluded during 7T MR safety screening. Of the 55 patients that were scanned at both 3T and 7T whose datasets were processed, one 7T MR scan was excluded due to poor quality, one due to large ventricles hampering segmentation, and five were excluded due to hippocampal subfield segmentations failing quality control.

The resulting patient subgroups were divided into a group of radiologically diagnosed MTS (n=15), and a pooled group of non-MTS diagnoses (n=33). For details of subtypes of radiological diagnoses within the non-MTS group, the reader is referred to section 2 in appendix A.2.

The purpose of this study was to compare group differences in 3T- and 7T MRI-based data, and the same two patient groups were used in both data sets, hence the patients served as their own controls.
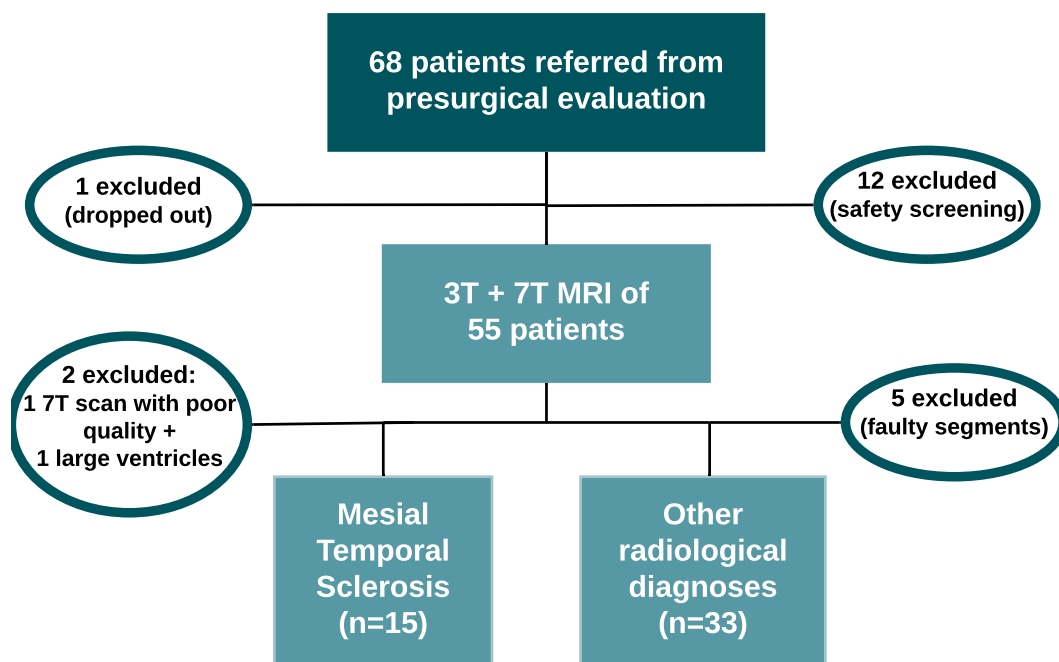
Figure 3.3.: Overview of patient inclusion since the point of referral. After safety screening, one drop-out, scan and segmentation quality assessment and evaluation of secondary pathologies affecting the segmentation, the resulting groups were mesial temporal sclerosis (MTS, n=15) and non-MTS(n=33). *This figure is a copy of figure 1 in article 2 in appendix A.2.*

3.2.3 7T MRI-specific pre- and post-processing

Due to the aforementioned B_1 inhomogeneities and spatially uneven signal intensity distribution, all 7T T_1-weighted images went through a specific pre-processing scheme, as recommended in a published abstract at the International Society for Magnetic Resonance in Medicine (ISMRM) 2020 proceedings [Opheim *et al.*, 2020]. This was done to correct for the spatially dependent signal variation (the "bias-field") and decrease the noise, which enables the FreeSurfer pipeline to complete segmentation with a higher rate of datasets passing quality control. A demonstration of the improvements entailed by this pre-processing is seen in figure 3.4.

Specifically, the bias-field correction was done in SPM12 (Wellcome Department of Cognitive Neurology) [Friston *et al.*, 1995], where a down-sampling factor of 3 was used together with light regularization and a 60 mm full-width half-maximum. A spatially adaptive non-local means (SANLM) filter
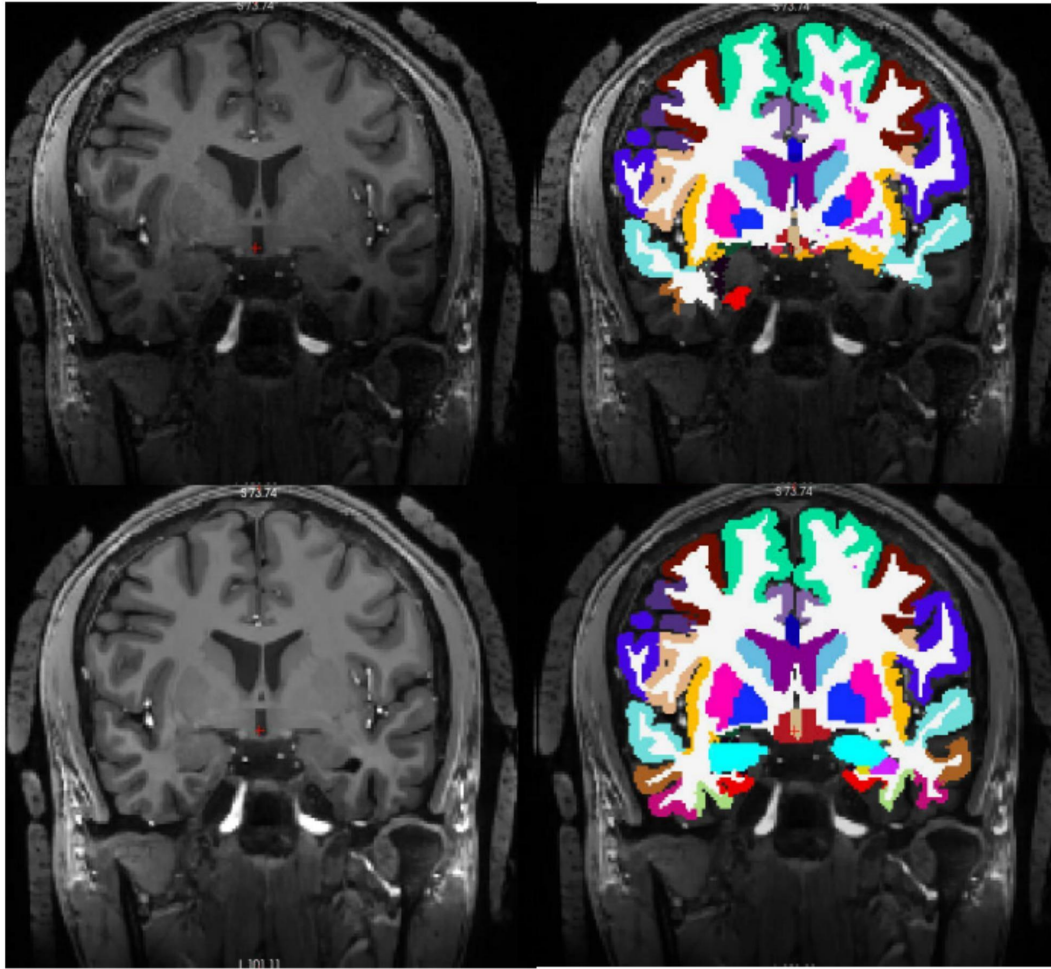
Figure 3.4.: Demonstration of effect of 7T-specific preprocessing on segmentation output, showing coronal slices of 3D MPRAGE scans (left) and labels of cortical parcellations from FreeSurfer v6.0 (right). *Top:* Raw image without any preprocessing, showing darker temporal lobe areas as a result of B_1 inhomogeneity. The cortical parcellations consistently failed in segmenting the middle and inferior temporal structures, and also had more errors in subcortical areas as well. In this case, the hippocampi were left out, which affected quality of the output of the hippocampal subfield segmentation tool as well. *Bottom:* Image after preprocessing, showing more uniform and smooth appearance of signal intensity across the whole brain. The cortical parcellations clearly improved segmentation quality, which resulted in good-quality hippocampal subfield segmentations. Some errors are still present in inferior temporal structures, which may be fixed with manual efforts.

provided in the SPM12 CAT12 toolbox [Gaser and Dahnke, 2016] was used for denoising.

The pre-processed T_1-weighted images were processed with the same FreeSurfer version and segmentation pipeline as described in 3.1.2, albeit adapted to sub-

millimeter images with a separate software patch dedicated to high-resolution scans [*Conf2hires* 2019]. The 7T TSE T_2-weighted images (see table 3.1) were similarly added to the hippocampal subfield segmentation pipeline.

3.2.4 Data extraction

In this study, we exported volumes for WH and the regions CA1, CA2/3, CA4 and molecular-layer granular-cell dentate gyrus (GC-DG). Furthermore, binary masks for the corresponding regional labels were created and exported. These masks were placed on the co-registered TSE T_2 images to retrieve mean and standard deviations (std) of the signal intensities, along with entropy values from the five hippocampal regions, which is an indirect measure for texture. Entropy is based on the variation of T_2 signal intensity distributions inside any region of interest [Gonzalez *et al.*, 2004]. Volumes, mean and std of T_2 signal intensities as well as entropy values were exported for further analyses. The asymmetry values were calculated with the same absolute asymmetry ratio as in section 3.1.3.

3.2.5 Statistical group comparison

For 3T and 7T MRI, asymmetries in the MTS group were compared to asymmetries in the non-MTS group. As in article 1, we used the Wilcoxon rank-sum (Mann-Whitney) test followed by Bonferroni correction for multiple comparisons. Given the use of five hippocampal regions and four radiomic features of interest, the corrected significance threshold for this study became $p < 0.00125$.

As marked by the red dashed lines at figures 4.2c and 4.2f, we defined outliers in the non-MTS group as patients with a WH volume asymmetry ratio greater than the upper 97.5% of non-MTS group, and outliers in the MTS group are defined as patients with an asymmetry ratio less than the upper 97.5% of the non-MTS group (see red dashed line on figure 4.2c and f).

3.3　Article 3

The work in article 3 (appendix A.3) is accepted for publication, but the manuscript is still under embargo. This article is a "Views and Reviews" class. This entails a different workflow than in original research articles such as articles 1 and 2 in this thesis. Nevertheless, besides the work behind gathering groups into an international task force (mainly done by Anja van der Kolk and Maxime Guye), there are numerous discussion sessions involved in a consensus-based study. To form a solid basis for such discussions, a survey was sent to all centers in order to map similarities and differences in set-up and experiences across centers. Prior to the discussion sessions formed by the subdivided expert groups, several teleconferences were held in plenum to determine the outline and contents of the upcoming article. Details of this work will be described in the following subsections.

3.3.1　7T Epilepsy Task Force

The 7T Epilepsy Task Force in an international collaboration between 21 centers worldwide. The group concists of neurologists (epileptologists), neurosurgeons, neuroradiologists, neuroscientists, physicists and engineers, whose cumulative experience is based on over 2000 patient scans in clinical and/or research settings. All three human 7T MR vendors (Philips, Siemens and GE) are represented across the groups, including the first FDA (and now CE) approved 7T system (Siemens Terra).

3.3.2　The survey

All centers received a survey with three main sections; hardware and scan set-up, radiological perspectives and weighting of prioritized sequences, and a range of miscellaneous questions regarding their center, what patient types they scanned, and views on impact of 7T MRI in their epilepsy clinics. For the latter two parts, they were given opportunity to comment specifically or broadly on issues with MRI scanning at 7T. *A copy of a blank survey is found in appendix A.4.*

3.3.3 Reaching concensus

The data from the survey was summarized and presented to all participating groups for orientation and majority consensus voting. The data was summarized into:

- Clinical indications and patient experiences

- Hardware setup and scan protocol

- Radiological priorities and experiences

- Technical issues, how to solve them, and future directions

The sequences in the scan protocols across centers were given a score according to frequency of use (how many used, e.g., an 3D MPRAGE sequence) and radiological weighting, i.e., rated between 1 and 4.

Afterwards, all who volunteered were subdivided into smaller groups who carried out individual discussions regarding contents of the various article sections. These groups included a separate group who discussed background and literature review in the introduction.

Statement of responsibility: I have been responsible for creating the survey, coordinating teleconferences, preparing agendas, collecting and presenting survey data, coordinating discussion groups and finalizing the manuscript draft. All work has been in close collaboration with Anja van der Kolk and Maxime Guye, who co-initiated and gathered the 7T Epilepsy Task Force by reaching out to individual centers. Anja van der Kolk chaired the first teleconferences in plenum.

Summary of main results, dicussions and conclusions

<div style="text-align: right">4</div>

In the following sections, the main results, discussions and conclusions from the three articles in the present PhD thesis are summarized. Article 3 does not have a regular discussion section, but contextual limitations are found in the conclusive remarks in subsection 4.3.2.

4.1 Article 1

4.1.1 Results

We found significant differences in all regions (WH, CA1 and CA4) between both HS ILAE type 1 and 2, and the two control groups (non-HS and healthy controls), see table 4.1. Furthermore, the control groups displayed no significant differences in either of the three regions, and neither did HS ILAE type 1 versus type 2.

Comparison	Whole Hippocampus	CA1	CA4
HS1 vs non-HS	1.21×10^{-4}	3.29×10^{-4}	2.79×10^{-4}
HS1 vs HC	1.27×10^{-11}	1.23×10^{-9}	3.33×10^{-10}
HS1 vs HS2	7.58×10^{-1}	1.24×10^{-1}	7.77×10^{-1}
HS2 vs non-HS	8.98×10^{-5}	7.12×10^{-5}	7.12×10^{-5}
HS2 vs HC	3.97×10^{-10}	1.01×10^{-9}	3.34×10^{-10}
HC vs non-HS	4.80×10^{-1}	3.67×10^{-1}	9.91×10^{-1}

Table 4.1.: P-values from group comparisons with Wilcoxon rank-sum test and Bonferroni correction for multiple comparisons. Significant differences after Bonferroni correction are marked in yellow. HS=hippocampal sclerosis, MTS=mesial temporal sclerosis, HC=healthy controls, CA=cornu ammonis. *This table is an adapted version of table 2 in article 1, appendix A.1.*

When looking at the boxplots in figure 4.1, it is confirmed that the two patient groups with verified HS have the highest asymmetry ratios for all three regions,

according to expectations. There are only marginal differences between the two control groups. Between the HS patient groups (the two red colours), distributions for volume asymmetry ratios seem wider for HS ILAE type 1 (dark red) than for HS ILAE type 2 (light red). The HS ILAE type 2 distributions of WH volume asymmetry ratios are also consistently more separated from the control groups.
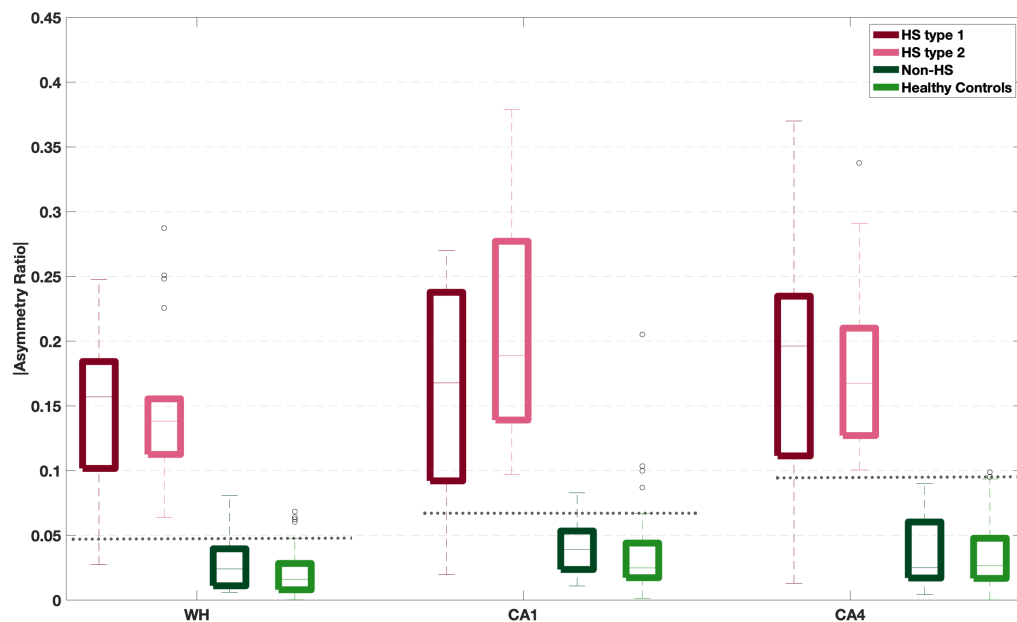
Figure 4.1.: Boxplots displaying distributions of asymmetry ratios in all five groups across the three hippocampal regions. Hippocampal sclerosis (HS) ILAE types 1 (dark red) and 2 (light red) display well separated and larger asymmetry ratios than non-HS patients (dark green) and healthy controls (light green). The dark grey dotted lines indicate threshold for abnormal asymmetry ratio determined by the upper adjacent whisker (approximately 99.3%) of the healthy population. MTS=mesial temporal sclerosis, WH = whole-hippocampal, CA=cornu ammonis. *This figure is identical to figure 4 in article 1, appendix A.1.*

There were 23/25 HS ILAE type 1 and 18/18 HS ILAE type 2 patients that displayed WH volume asymmetry ratios above the upper whisker (see grey dotted lines in figure 4.1) of WH asymmetries in healthy controls (0.048). With respect to CA1, 21/25 HS ILAE type 1 patients and 18/18 HS ILAE type 2 patients had abnormal asymmetry ratios compared to upper limit of CA1 asymmetry ratios in healthy controls (0.067). In CA4, 20/25 HS ILAE type 1 patients and 17/18 HS ILAE type 2 patients displayed asymmetry ratios above the upper limit of those in healthy controls (0.095).

When testing for differences between CA1 and CA4 volume asymmetry ratios, we found no significant differences between CA1 and CA4 volume asymmetry ratios within the HS ILAE type 1 group nor within the HS ILAE type 2 group.

4.1.2 Discussions and Limitations

As expected, we found significant group differences between the HS patient groups and the non-HS and healthy control groups. This corresponds well with the notion of HS in general displaying significant atrophy in the ipsilateral side. However, the wider distribution of WH volume asymmetry ratios in the HS ILAE type 1 group compared to those of type 2 is not consistent with type 1 having more severe neuronal loss [Blümcke *et al.*, 2013]. HS ILAE type 1 patients display four cases of CA1 volume asymmetry ratios that overlap with those of healthy controls, and five cases of overlap in CA4 volume asymmetry ratios. In these cases, neuronal loss is histopathologically confirmed. The overlap with healthy controls could be explained by gliosis that is maintaining the shape of the subfield, which would suggest that the segmentation algorithm is not delineating the borders of the subfield correctly.

Subsequently, we expected the HS ILAE type 2 group to display more overlap with the control groups, as it is less severe in both WH and CA4 neuronal loss than HS ILAE type 1 (see table 2.3), according to ILAE classification of HS subtypes [Blümcke *et al.*, 2013]. This lack of overlap could be explained either by samples having moderate neuronal loss, or by samples being misclassified as HS ILAE type 2, since HS ILAE type 1 (and the other types) can be difficult to assess if tissue is not intact. Further suggestive of misclassifications, are the abnormal distributions of HS ILAE type 1 (25/52, <49%) and type 2 (18/52, >34%), with a far higher proportion of HS patients being classified as ILAE type 2 compared to ILAE consensus literature [Blümcke *et al.*, 2013] (see table 2.3). Similarly as with HS ILAE type 1, the unexpectedly high CA4 volume asymmetry ratios in HS ILAE type 2 could also be explained by incorrect subfield border delineation.

Regarding lack of sensitivity to delineate both severe and minute changes in the small subfield regions, it is also suggested by other studies [Pardoe *et al.*, 2009; Brinkmann *et al.*, 2019], where manual segmentation is shown to be more accurate than the automated outputs, and automated subfield

segmentations tend to be overestimated also in healthy controls. The increase in estimation noise during delineation is also indicated by the slight increase in volume asymmetry ratios from WH to CA4 in our healthy population, as seen in figure 4.1.

Limitations

We only had one case of HS ILAE type 3 in this cohort, so it had to be excluded from group comparisons. As HS ILAE type 3 should have no to moderate neuronal loss in CA1, and less severe volume reduction in WH, a side-by-side comparison with a sizeable HS ILAE type 3 group would confirm suspicion of lack of segmentation sensitivity if WH and CA1 volume asymmetry ratios in this patient group were similar to those of type 1 and type 2. It was also limiting that neuronal loss is not possible to describe more precisely during histological assessments, although we cannot expect the volume and neuronal loss to display 1:1 correspondence. Since the probability atlas of the FreeSurfer hippocampal subfield segmentation is not specific to HS patients [Iglesias *et al.*, 2015], it is likely biased when delineating the disproportionally small hippocampal subfields relative to the WH region.

4.1.3 Conclusions

The detection rate of overall HS diagnosis seems excellent, and similar for both HS subgroups.

The inconsistensies in volume asymmetry ratios of CA1 and CA4 according to expectations from ILAE classifications are likely explained by a combination of segmentation inaccuracies in small subfields and true anatomical volume reductions due to neuronal loss. The latter could in turn be explained by some patients being misclassified as HS ILAE type 2. Expanding the analyses with close inspection of histopathological descriptions is warranted. Such an expansion could include re-evaluation of relative neuronal loss in CA4 specifically, but also automatic image analysis of the histological specimens.

When we have the independent dataset based on comparable 3T MRI protocol from our collaborator at the National Epilepsy Centre in Sandvika, Norway, we will add to the sample sizes of both HS subtypes. This will also allow us to compare results with an independent dataset, including the process of histopathological evaluation and its findings.

4.2   Article 2

4.2.1   Results

Group differences in 3T and 7T MRI sets

For 3T MRI, groups displayed significant differences in all five hippocampal regions for both our texture measure entropy and volume, see table 4.2 and figure 4.2. No other parameters were significantly different for any of the five regions, though standard deviations of T_2 signal intensities inside subfield CA2/3 were borderline significantly different (p=0.0016).

For 7T MRI, results were similar, except for lack of significant difference after Bonferroni correction for entropy in CA2/3 (table 4.2, figure 4.2). Additionally, a significant group difference was found in mean T_2 signal intensities in CA4.

Notably, when examining volume distributions in figure 4.2 (c and f), we find a more pronounced group separation for 3T than for 7T in subfield CA2/3.

4.2.2   Discussions and Limitations

Differences in volume asymmetries

As expected from ILAE classifications [Blümcke *et al.*, 2013], we found significant volume asymmetry differences between the visually diagnosed MTS and non-MTS groups. This is in good concordance with studies that utilized or investigated automated segmentations in MTS cohorts on 3T [Cendes *et al.*,

Comparison	3T MRI	7T MRI
Entropy WH	1.2×10^{-5}	1.4×10^{-5}
Entropy CA1	7.6×10^{-6}	2.2×10^{-6}
Entropy CA2/3	7.0×10^{-6}	1.1×10^{-2}
Entropy CA4	2.2×10^{-6}	3.3×10^{-6}
Entropy GC-DG	4.1×10^{-6}	3.5×10^{-5}
Volume WH	7.8×10^{-6}	9.6×10^{-6}
Volume CA1	2.2×10^{-6}	3.3×10^{-6}
Volume CA2/3	5.1×10^{-6}	9.2×10^{-4}
Volume CA4	5.7×10^{-5}	5.7×10^{-6}
Volume GC-DG	1.8×10^{-5}	6.3×10^{-6}
MeanSig WH	1.5×10^{-1}	1.6×10^{-2}
MeanSig CA1	3.3×10^{-1}	3.5×10^{-2}
MeanSig CA2/3	1.3×10^{-1}	1.9×10^{-3}
MeanSig CA4	4.8×10^{-1}	4.8×10^{-4}
MeanSig GC-DG	4.4×10^{-1}	1.9×10^{-3}
StdSig WH	1.6×10^{-1}	4.2×10^{-1}
StdSig CA1	4.3×10^{-2}	4.0×10^{-1}
StdSig CA2/3	1.6×10^{-3}	5.2×10^{-1}
StdSig CA4	3.9×10^{-2}	7.5×10^{-2}
StdSig GC-DG	1.8×10^{-1}	2.9×10^{-1}

Table 4.2.: Group comparison (MTS vs non-MTS) results . Significant differences after Bonferroni correction are marked in yellow. MeanSig=mean T_2 signal intensity, StdSig=standard deviations of T_2 signal intensities, MTS=mesial temporal sclerosis, CA=cornu ammonis, WH=whole-hippocampal, GC-DG=granular-cell dentate gyrus, T=Tesla, MRI=magnetic resonance imaging. *This table is an adapted version of table 2 in article 2, appendix A.2.*
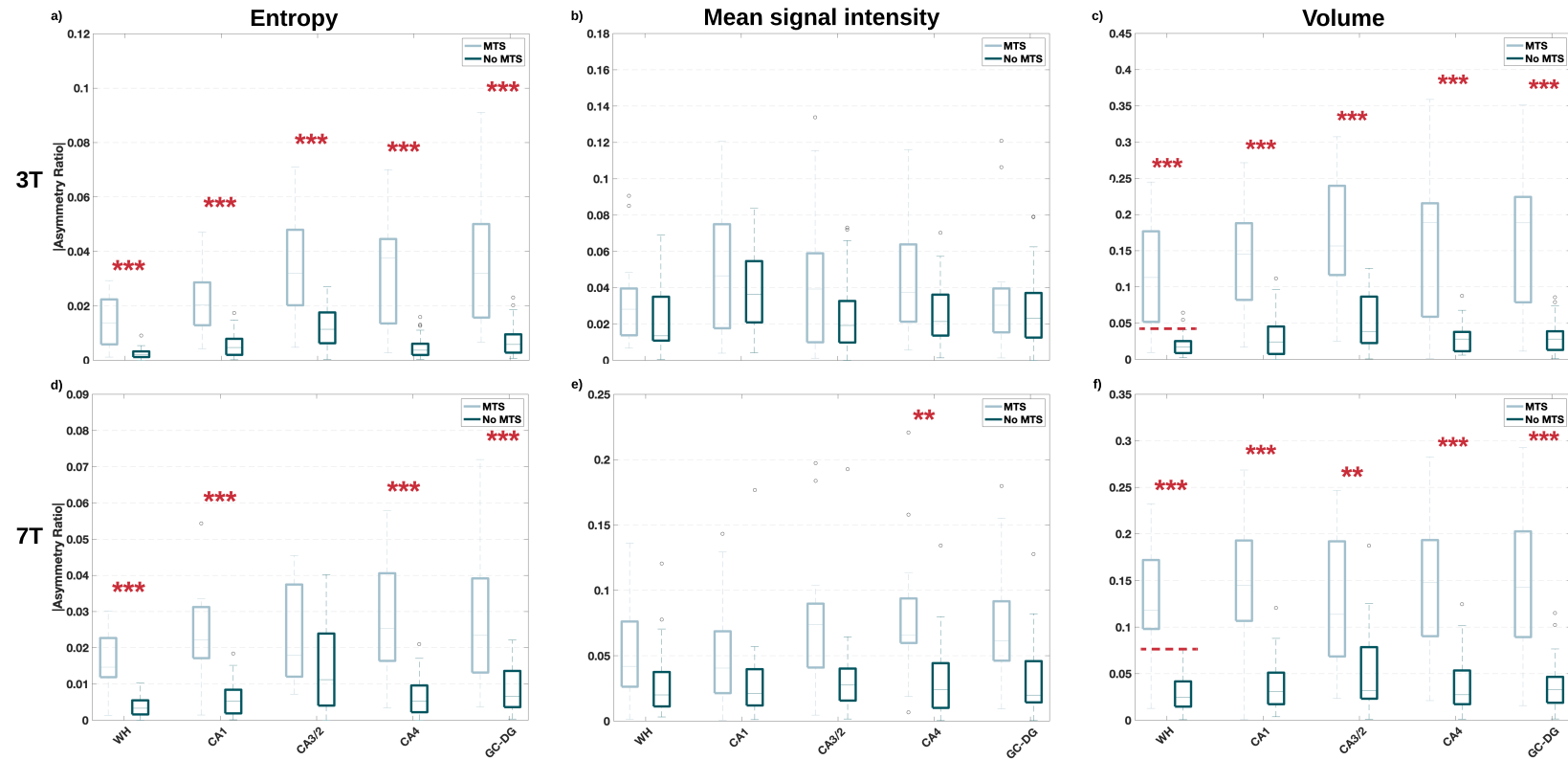
Figure 4.2.: Boxplots for entropy, mean signal intensity and volume asymmetry ratios across the two patient groups and five regions. a-c) (upper row) are 3T data, and d-f) (lower row) are 7T data. Statistical significance after Bonferroni correction is given as ** for p<0.00125 and *** for p<0.0005. The red dashed lines in c and f indicate the threshold for which we consider datapoints as outliers, and thus consider asymmetry ratios as abnormal in both groups. WH = whole-hippocampal, CA = cornu ammonis, GC-DG = granular-cell dentate gyrus. *This figure is a copy of figure 3 in article 2, appendix A.2.*

1993; Focke *et al.*, 2012; Coan *et al.*, 2014a; Steve *et al.*, 2014; Goubran *et al.*, 2016; Hadar *et al.*, 2018]. Likewise, it is in good agreement with segmentation studies on 7T MRI [Henry *et al.*, 2011; Santyr *et al.*, 2017; Gillmann *et al.*, 2018].

In the distributiones of volume asymmetries in figure 4.2 (c and f), both mean and max values are higher for 3T (c) than for 7T (f) in general. This is agreeing with an expected overestimation in segmentations performed on 3T MRI [Pardoe *et al.*, 2009; Brinkmann *et al.*, 2019]. Together with more well-separated group distributions for subfield CA2/3 for 3T compared to 7T, the differences in segmentation asymmetries may further indicate more precisely delineated hippocampal regions on 7T MRI.

According to ILAE classifications [Blümcke *et al.*, 2013] of HS and HS subtypes, we expected to find the largest volume asymmetries in WH, followed by CA1, CA4 and possibly CA2/3 and GC-DG in decreasing order, in the visually diagnosed MTS group. This seem somewhat opposite for our 3T data (figure 4.2c), although the most frequent HS subtypes should present with predominantly, but not exclusively, reduction in CA1 volume. For 7T data, CA1, CA4 and GC-DG volume asymmetries (figure 4.2f) seem largest, with a downwards shift in distributions of asymmetries for CA2/3. Without histopathology analyses, it can only be speculated how the true degree of neuronal loss in the hippocampal regions in our MTS patients connects to our findings in both MRI datasets.

Differences in mean T_2 signal intensities

Following the volume assymetries, we expected to find asymmetry differences in mean T_2 signal intensities in at least WH, CA1 and CA4 - the most prominent regions corresponding to neuronal loss in the most common HS subtypes Blümcke *et al.*, 2013.But only 7T-based subfield CA4 was significantly different after Bonferroni correction. This is not in accordance with previous 3T [Focke *et al.*, 2012; Coan *et al.*, 2014a; Steve *et al.*, 2014; Sánchez and Zapata, 2018] and 7T MRI studies [Henry *et al.*, 2011; Coras *et al.*, 2014]. As disruptions in hippocampal tissue should be significantly more pronounced in the MTS group, we cannot rule out that another T_2 signal intensity parameter would be more

sensitive. One example used in other studies is T_2 relaxometry [Bernasconi *et al.*, 2000], which reflects the T_2 relaxation rates based on intensities in all voxels in a region of interest. However, that would require multiple-spin-echo sequences (or multiple single spin-echo sequences with different echo times), and we only had one regular TSE T_2 acquisitions available.

Differences in texture

Our texture parameter entropy was significantly different for all five regions in 3T data, and all regions except for CA2/3 in 7T data. The similar asymmetries and differences we observe in 3T and 7T data do not support the notion that texture parameters should increase with field-strength [Larroza *et al.*, 2016]. Although, the higher texture changes in our subfield regions compared to WH, which is a sum of all 12 subfields including the hippocampal tail, may be meaningfully reflecting more texture changes corresponding to predominant neuronal loss in these areas.

Other 1.5 and 3T studies on texture changes in MTS further conclude that quantitative texture parameters are significantly different in both ipsi-and contralateral hippocampis of patients with MTS compared to non-MTS and healthy controls [Yu *et al.*, 2001]. Hence, texture changes can also be a consequence of seizures, even extending to adjacent temporal regions along the seizure propagation pathway in TLE [Yu *et al.*, 2001; Bonilha *et al.*, 2003; Sankar *et al.*, 2008]. As stated in subsection 4.2.1, it is notable that volume asymmetries in MTS and non-MTS are less separated for CA2/3 in the 7T data. For entropy, there is no significant difference in CA2/3 for 7T. Except for this apparent trend in CA2/3, which according to ILAE classifications should be less prominently affected in the most frequent HS subtypes, we conclude that the overall trends in group differences for 3T and 7T are the same.

Concordance of asymmetry outliers and clinical findings

The closer inspection of outliers in figure 4.2 (c and f), revealed important information for understanding the volumetric asymmetry variations in a clinical context.

The 7T data displayed no outliers above the interquartile range in the non-MTS group (see red dashed line on figure 4.2f), while 3T data displayed two outliers (see red dashed line oin figure 4.2c). The two patients had no other clinical findings supporting hypotheses of MTS.

There were four outliers in the 3T MTS group with WH volume asymmetry ratios within the range of the non-MTS, and three in the 7T MTS group - one of these were the same for both sets. This patient had no striking atrophy on a particular side, but in general small hippocampi, and the volumetric asymmetry was thus an unsuited index in this patient. That patient had described signal changes on the right side, but only entropy from 7T was abnormal, whose value was highest on the contralateral (left) side. As texture changes can occur on both sides [Yu *et al.*, 2001; Bonilha *et al.*, 2003], we regard it as a good marker for MTS, albeit non a good lateralizing marker.

Also, 1/3 of 3T MTS outliers diplayed abnormal CA1 volumetric asymmetries while WH was normal, and 2/2 of 7T outliers displayed abnormal CA1 volumetric asymmetries. We therefore speculate if there are still subtle contributions from increased sensitivity in 7T segmentations.

Altogether, there are some indications from the outlier inspection that point towards a benefit from 7T, as 11/15 (73%) at 3T and 12/15 (80 %) at 7T were concordant with radiological diagnosis.

Limitations

In this study, there are three main limitations: Potential bias in segmentations, lack of histology ground truth for all patients, and potential effects from comparing 2D T_2 images in the 3T dataset to 3D T_2 images in the 7T dataset.

The effects of any bias in segmentations is, to our knowledge, hitherto never investigated. We speculate whether the different spatial resolution, SNR and contrast in the two datasets, may cause 3T segmentations to be more similar to those of the probability atlas the hippocampal subfield segmentation tool they are based on. Vice versa, 7T-based segmentations may be more similar to "true" anatomy. Looking at the similar group comparison results, however, it has

likely not had an effect in our study. Furthermore, the lack of histology ground truth (i.e., ILAE classification of HS subtypes) is preventing us from reaching firm conclusions about the results with respect to variations in entropy and volumes in the subfields. Lastly, as seen in table 3.1, we are comparing 2D T_2 (3T) with 3D T_2 (7T) acquisitions. Although the in-plane spatial resolution in both is on the submillimeter range, the 2D 3T scan is anisotropic and from a multislice scan. Quantitative analyses on such scans may be influenced by slice profiling effects. We had a 2D T_2 scan for the 7T datasets as well, but this scan is too frequently affected by detrimental motion artefacts. The standard clinical 3T epilepsy protocol does not contain a 3D T_2 sequence. Nevertheless, such effects do not seem to have influenced our direct T_2 signal intensity parameter in this study, but may theoretically influence segmentations.

4.2.3 Conclusions

The clinical implications in this study are not on individual patient level, but may affect decisions on what MR field-strength to refer MTS patients to. Group differences between ordinary radiomic features across 3T and 7T may indicate that for patients with known MTS diagnosis, 7T MRI will likely not impact crude quantitative measures used during support of diagnostic workflow. Nonetheless, subtle indications from outlier analyses and trends in particular CA2/3 may still influence automatic detection algorithms, even if descriptive statistics show similar group results. Arguably, this is still speculative when lacking histopathological ground truth. Future studies with comparative 3T and 7T MRI sets and histology samples are warranted, as we need to understand the characteristic segmentation effects in MTS patient cohorts. In parallel, it would be valuable to further investigate automated detection accuracy differences in 3T and 7T.

4.3 Article 3

4.3.1 Recommendations

The results subsections below will present the summarized recommendations for all parts (clinical indications, scan protocol and general radiological con-

siderations) except for the lesion-specific radiological assessment and specific future directions, which can be found in the article 3 (sections 4 and 6) in appendix A.3. Before scanning patients at 7T MRI, the 7T Epilepsy Task Force recommends to pay special attention to implants and other potential safety hazards that may have been approved at 3T MRI, and therefore are easily forgotten by doctors, operators and patients alike.

Clinical indications

The main clinical indications for referring a patient in presurgical evaluation for severe epilepsy to 7T MRI are four-fold. **MRI negative at 3T:** Patients where no structural lesion has been detected at 3T. Due to the increased resolution, SNR and contrast, subtle structural lesion substrates may be easily missed at 3T, and be more readily detectable at 7T. **Known lesion at 3T:** Even for known lesions, 7T may both help discriminate lesion subtypes, and help delineate lesion borders more precisely. This indication is also impacted by 7T MRI's ability to sometimes resolve false-positives at 3T, e.g., when a periventricular space close to the cortex was suspected for a dysplastic change. **Electrode positioning:** Increased anatomical details of both lesions and adjacent structures may enable precise positioning of intracranial electrodes used for EEG measurements, therapeutic electrostimulation or laser ablation. **Eloquent areas:** Although the article focuses on structural lesions, there is consensus on the advantages by also utilizing 7T with its greater BOLD SNR performance for presurgical mapping prior to epilepsy resection surgery.

Preparing patients

Several factors can influence the patients' scanning experience at 7T. Even those who did not experience discomfort at 3T may experience several aspects of the 7T scan as uncomfortable. To increase patient comfort and thus also decrease risk of motion artefacts, we recommend preparing the patients for these 7T-specific factors: *longer bore and smaller headcoil*, *longer acquisition times*, *dizziness* and *peripheral nerve stimulation*. The latter two may also occur at 3T, but are uncommon.

Scan set-up

The acquisition recommended set-up for the eight most common sequences across centers is found in the table 4.3.

Table 4.3.: Summary of the eight most useful sequences as identified in a survey from 19/21 7T MRI centers experienced in examining epilepsy patients for research and/or diagnostic purposes. *This table is copied and minimally adapted from table 1 in article 3, appendix A.3.*

Sequence type		Orientation	In-plane spatial resolution in mm range (median)	Slice thickness in mm range (median)	Duration in mm:ss range (median)
Partial coverage					
$T_2w^\dagger$	TSE	Coronal[1]	0.25-0.70 (0.30)	1.00-3.00 (1.35)	3:36-8:48 (5:58)
T_2w	TSE	Axial[8]	0.40-0.70 (0.45)	0.75-3.00 (1.55)	3:39-12:00 (6.17)
T_2*w^6	GRE	Coronal	0.25-0.38 (0.30)	1.65-2.00 (2.00)	5:22-6:12 (5:58)
Whole-brain coverage					
3D T_1w	MPRAGE[4]	Sagittal	0.60-0.90 (0.73)	0.60-1.00 (0.73)	6:47-10.12 (8:27)
	MP2RAGE[2]	Sagittal	0.60-0.80 (0.70)	0.60-0.80 (0.70)	5:20-11:45 (6:21)
3D FLAIR[3]		Sagittal	0.70-1.00 (0.80)	0.70-1.40 (0.80)	5:54-10:38 (7:27)
3D T_2*w^7	GRE/SWI	Any	0.25-0.80 (0.50)	0.20-2.00 (0.90)	5:17-12:00 (8:27)
3D T_2w^5	TSE	Sagittal/Axial	0.50-0.80 (0.70)	0.69-2.40 (0.70)	5:32-10:59 (7:11)

†In a few centers, the multi-slice T_2-weighted TSE sequences were reconstructed to an even higher spatial resolution. 1-8: The order of importance as scored by the involved radiologists. Abbreviations: FLAIR, fluid attenuated inversion recovery; GRE, gradient recalled echo; MPRAGE, magnetization-prepared rapid acquisition gradient echo; SWI, susceptibility-weighted imaging; TSE, turbo spin echo; w, weighted. *This table is a copy of table 1 in article 3, appendix A.3.*

Patient-specific 7T MRI protocol

According to the clinical indications and lesion-specific evaluation purpose, the sequences in table 4.4 are a minimal protocol set-up we recommend at 7T MRI for epilepsy.

Table 4.4.: Summary of sequences of particular interest for certain (known and/or suspected) epileptic lesion types; often used acquisition parameters can be found in the text and in Table 4.3. *This table is copied and minimally adapted from table 2 in article 3, appendix A.3.*

Lesion type	Sequences of particular interest
TLE with known or suspected HS	3D T_1w MPRAGE or MP2RAGE 3D T_2w TSE 2D T_2w TSE focused on hippocampus and anterior temporal lobe
FCD (type I and II)	3D T_1w MPRAGE or MP2RAGE 3D FLAIR 3D T_2*w GRE or SWI +/- FWMS sequence +/- 2D T_2w TSE focused on suspected cortical lesion
LEAT	3D T_1w MPRAGE or MP2RAGE 3D T_2w TSE 3D T_2*w (GRE or SWI)
Polymicrogyria	3D T_1w MPRAGE or MP2RAGE 3D T_2*w (SWI or SWAN) +/- FSPGR
TSC	3D T 1 w MPRAGE or MP2RAGE 3D T_2*w (SWI or SWAN) 3D FLAIR
Vascular malformations	3D T_2*w (SWI)
MRI negative at 3T	3D T 1 w MPRAGE or MP2RAGE 3D FLAIR 3D T_2w TSE 3D T_2*w (GRE or SWI) +/- FWMS sequence +/- 2D T_2w TSE over regions indicated by, e.g., EEG

Abbreviations: FLAIR, fluid attenuated inversion recovery; FWMS, fluid and white matter suppressed; GRE, gradient recalled echo; MPRAGE, magnetization prepared rapid acquisition gradient echo; FCD, focal cortical dysplasia; HS, hippocampal sclerosis; SWAN, susceptibility-weighted angiography; SWI, susceptibility-weighted imaging; TSE, turbo spin echo; w, weighted; LEAT, long-term epilepsy-associated tumors (Gangliogliomas, DNET); DNET, dysembryoplastic neuroepithelial tumors; TSC, tuberous sclerosis complex; TLE, temporal lobe epilepsy.*This table is a copy of table 2 in article 3, appendix A.3*.

General recommendations for radiological assessment

A general recommendation for radiologists new to 7T MRI in epilepsy, is to get aqcuainted with scans from healthy subjects to familiarize with the characteristics of 7T MRI. Besides the already mentioned B_1 inhomogeneity (see section 2.3), which is more pronounced than on 3T, there are several other aspects that may present as a different "blueprint" than what a radiologist is used to. The images will show far more conspicuous vessels and an increased number of visible perivascular spaces and u-fibers, as well as increased contrast between cortical and subcortical structures. There will also be other artefacts that one should be careful not to mistake for abnormal anatomical structures, such as flow artefacts from the large vessels. When assessing images with suspected lesions of any kind, scroll carefully through the increased number of slices. These are very narrow at 7T, and lesions may still be subtle.

4.3.2 Conclusions

This article has presented the first international consensus-based recommendations for how to use 7T MRI in epilepsy. It would still be benfitial with controlled studies comparing use of optimized 3T protocols with optimized 7T protocols - i.e., the best from both worlds. Nevertheless, several clinical indications clearly exist for 3T MRI negative epilepsy patients or patients with 3T MRI lesions that require better characterization. Several non-structural sequences at 7T MRI also hold promise as future directions in epilepsy diagnostics. However, these functional and molecular methods need further clinical validation. The 7T Epilepsy Task Force hopes this article provided timely useful guidance when setting up a 7T MRI epilepsy protocol in the clinic.

Perspectives, future work and general conclusion

<div style="text-align: right">5</div>

In two studies in this PhD thesis, automated segmentation of the hippocampus is performed on retrospective 3T MRI data including histopathological ground truth material, as well as on 3T and 7T MRI data in an open patient cohort. In the third article, the first international consensus-based recommendations on how to set up and radiologically assess a 7T MRI protocol in epilepsy are presented. These studies adhere to the current changing concepts in presurgical evaluation, and highlight certain strengths and weaknesses of relevance when employing automated segmentation or 7T MRI in clinical work-up of patients with severe drug-resistant epilepsy.

5.1 Utilizing automated segmentations in presurgical evaluation

The study reflected in article 1, a manuscript still in preparation, showed that the automated segmentation of hippocampus is in very good agreement with the histopathological diagnosis of HS. The WH volume asymmetry ratio was abnormal compared to non-HS patients for 93% of the patients with HS. It will be interesting when the additional data from our collaborator at National Epilepsy Centre in Norway is available. Here, we will get to see if the findings are reproduced in an independent dataset, as well as supplementing the already unique sample sizes of two different HS subtypes. What remains to be understood in more detail, is to what extent it is reasonable that CA4 asymmetries for HS ILAE type 2 patients were not lower than CA1 asymmetries, and to what extent bias or noise in segmentations cause different segmentation precision in WH versus subfield regions. It may not be possible to assess the precise variations in neuronal loss in CA1 and CA4 without a more precise histopathological (qualitative or quantitative) description of neuronal loss in

individual subfields as well. But this is a cumbersome, if not infeasible, task without intact hippocampal specimens.

In the second article, we found essentially no differences between 3T and 7T in how well the asymmetries for any of the radiomic features agreed with visual diagnosis of MTS. Volume and texture were the only features that corresponded well to MTS diagnosis for the both MRI sets, albeit volume seem to be the only feature that held lateralizing value when inspecting outliers. Altogether, we concluded that 3T and 7T MRI can distinguish MTS from other epilepsy patients equally well in a group comparison. This is a new finding, and counterintuitive based on the multiple studies pointing to increased sensitivity from performing automated segmentations on submillimeter 7T MRI scans. While 7T MRI holds great promise in visual and automated analysis of other patient groups, the use of standard 3T MRI seems to offer the same separation between known MTS patients and other epilepsy subtypes.

This knowledge may be valuable to clinicians that have the opportunity to refer their epilepsy patients to 7T MRI scans – as well as for those without that opportunity, which still is the case for most epilepsy centers. It is also relevant when planning to add/further study hippocampal subfield segmentations as one of the emerging contributors to clinical decision support, and are contemplating whether to refer a patient with known MTS diagnosis to the costlier 7T MRI scan.

Based on article 2, future work includes understanding differences in segmentations on 3T and 7T based on closer examinations of the quantitative characteristics of the two datasets, i.e., investigate whether segments from 3T are more or less similar to the probability atlas compared to segments from 7T. We also plan to do analyses of histopathological correlations to verified HS next year, when a certain amount of MTS patients have gone through resective surgery. We would also like to investigate whether classification of MTS has different accuracies when based on 7T and 3T.

The hippocampal subfields segmentation tool [Iglesias *et al.*, 2015], an add-on tool to FreeSurfer (FS) software [Fischl, 2012], is widely used in other published studies. There are other methods, such as the ASHS tool by Yushkevich et.al. [Adler *et al.*, 2014; Yushkevich *et al.*, 2015], which comes with a separate 7T atlas [Wisse *et al.*, 2016]. But this method segments CA1-3 separately, and

CA4/DG jointly, making the FreeSurfer v 6.0 individual segmentation of CA1, CA2/3 (jointly), CA4 and DG more suitable for the specific purpose of investigating correlations with ILAE HS subtype classification. Given that neuronal loss varies along the longitudinal hippocampal axis (see section 2.2) [Thom *et al.*, 2012], segmentation methods that further divides the hippocampal subfields into head, body and tail may have increased clinical value [Shaw *et al.*, 2020]. Nonetheless, the most used methods are still limited by being based on atlases created from post-mortem samples from healthy and/or demented elderly people [Mueller *et al.*, 2018]. Until a specific epilepsy (MTS-based) atlas is developed, arguably, it is still prudent to understand how both 3T and 7T MRI segmentations in the current version of FS v.6.0 deviated from true anatomy.

Altogether, the methods still correlate well with radiological or histopathological diagnosis. Hence, they have a particular potential to support less experienced radiologists, but also to be included as a tool that helps separate MTS patients from other patients. This may be a valuable supplement in any busy radiological department, where analyses could be ready when the radiologists meet for work in the morning. All while acknowledging an error margin, which is indicated to be clinically significant in around 10% of cases [Brinkmann *et al.*, 2019].

5.2 Clinical impact of 7T MRI in epilepsy

A point frequently made by 7T MR sceptics, evolves around whether optimized 3T sequences in the newest scanners with the fastest scan encoding embedded available would be just as helpful as the submillimeter scans we know from 7T. It is worthwhile recognizing that any clinical MR protocol standard is seen as a "*one size fits most lesion types*", since standardization is important to claim clinical evidence. This does not mean that other sequences and hardware would not detect lesions not visible with the standardized setup. However, as also argued in the background chapter and in article 3, several studies have already demonstrated clinical yield of 7T both with standard structural sequences [Henry *et al.*, 2011; Colon *et al.*, 2016; Veersema *et al.*, 2016; Veersema *et al.*, 2017] and with specially developed heavily gray-matter specific sequences that sharpen the contrast between gray and white matter

[Chen *et al.*, 2018; Bannier *et al.*, 2018]. The latter sequences aid visualization in the cortical boundary areas where, e.g., subtle microdysplastic changes are easy to miss, or regions are relevant for implantation of EEG or stimulation electrodes. All such studies have used sequences with clinically acceptable scan duration. If performed with the same resolution and optimized SNR at 3T, they would require clinically *unacceptable* scan durations - both due to cost, and due to unavoidable patient movement.

In conjunction, another point is that 7T MR systems are hitherto seen as advanced engineering "toys": the clinical incentive is not evident enough to prioritize purchasing an expensive 7T MR system and in addition hire 7T MR engineers at the local epilepsy neuroimaging department. This claim is caused by a gap between the technical engineering side and the clinical side, that the 7T Epilepsy Task Force (among other initiatives [Düzel *et al.*, 2019; Clarke *et al.*, 2020]) is trying to minimize by unifying recommendations for 7T MRI setup. One of the patient groups that 7T MRI has the potential of having the largest clinical impact in, is patients with epilepsy [Van der Kolk *et al.*, 2013; Trattnig *et al.*, 2018].

There is, however, still missing studies that prospectively and controlled investigate the impact of 7T MRI on presurgical decisions.

5.3   Conclusion in general

The studies in this PhD thesis contribute to the fields of 7T MRI and automated MRI segmentations in epilepsy. In the first article, the uniqueness lies in the combination of using updated hippocampal segmentation tool in FreeSurfer and investigating a set of 3T MRI and histologically classified HS subtypes. That study will be complemented with additional and independent data from a collaborator institution in Norway. In the second article, the novelty is brought by the comparable clinical 3T and 7T MRI sets with MTS and non-MTS patients. These data allowed us to investigate group differences in both 3T and 7T MRI, where we, counter-intuitively, found equal discriminative ability in the two MRI field strengths. The third and last article presents the first consensus-based guidelines and recommendations for centers that are new to 7T MRI in epilepsy. This is a study we ourselves would have wanted to have available

when we started the PhD project, which also was the first clinical 7T MRI project in Denmark.

Bibliography 6

Adler, Daniel H, John Pluta, Salmon Kadivar, Caryne Craige, James C Gee, Brian B Avants, and Paul A Yushkevich (2014). „Histology-derived volumetric annotation of the human hippocampal subfields in postmortem MRI". In: *Neuroimage* 84, pp. 505–523.

Balchandani, P and TP Naidich (2015). „Ultra-high-field MR neuroimaging". In: *American Journal of Neuroradiology* 36.7, pp. 1204–1215.

Bannier, Elise, Giulio Gambarota, Jean-Christophe Ferré, Tobias Kober, Anca Nica, Stephan Chabardes, and Claire Haegelen (2018). „FLAWS imaging improves depiction of the thalamic subregions for DBS planning in epileptic patients". In:

Baumgartner, Christoph, Johannes P Koren, Martha Britto-Arias, Lea Zoche, and Susanne Pirker (2019). „Presurgical epilepsy evaluation and epilepsy surgery". In: *F1000Research* 8.

Baumgartner, Christoph and Susanne Pirker (2019). „Video-EEG". In: *Handbook of clinical neurology*. Vol. 160. Elsevier, pp. 171–183.

Bernasconi, Andrea, Neda Bernasconi, Zografos Caramanos, David C Reutens, Frederick Andermann, François Dubeau, Donatella Tampieri, Bruce G Pike, and Douglas L Arnold (2000). „T2 relaxometry can lateralize mesial temporal lobe epilepsy in patients with normal MRI". In: *Neuroimage* 12.6, pp. 739–746.

Bernasconi, Andrea, Fernando Cendes, William H Theodore, Ravnoor S Gill, Matthias J Koepp, Robert Edward Hogan, Graeme D Jackson, Paolo Federico, Angelo Labate, Anna Elisabetta Vaudano, *et al.* (2019). „Recommendations for the use of structural magnetic resonance imaging in the care of patients with epilepsy: A consensus report from the International League Against Epilepsy Neuroimaging Task Force". In: *Epilepsia* 60.6, pp. 1054–1068.

Bernhardt, Boris C, Seok-Jun Hong, Andrea Bernasconi, and Neda Bernasconi (2015). „Magnetic resonance imaging pattern learning in temporal lobe epilepsy: classification and prognostics". In: *Annals of neurology* 77.3, pp. 436–446.

Bien, Christian G, Miriam Szinay, Jan Wagner, Hans Clusmann, Albert J Becker, and Horst Urbach (2009). „Characteristics and surgical outcomes of patients with refractory magnetic resonance imaging–negative epilepsies". In: *Archives of neurology* 66.12, pp. 1491–1499.

Blümcke, Ingmar, Maria Thom, Eleonora Aronica, Dawna D Armstrong, Fabrice Bartolomei, Andrea Bernasconi, Neda Bernasconi, Christian G Bien, Fernando Cendes, Roland Coras, *et al.* (2013). „International consensus classification of hippocampal sclerosis in temporal lobe epilepsy: a Task Force report from the ILAE Commission on Diagnostic Methods". In: *Epilepsia* 54.7, pp. 1315–1329.

Bonilha, Leonardo, Eliane Kobayashi, Gabriela Castellano, Giselle Coelho, Eduardo Tinois, Fernando Cendes, and Li M Li (2003). „Texture analysis of hippocampal sclerosis". In: *Epilepsia* 44.12, pp. 1546–1550.

Brainreader-Aps. (2020). `https://brainreader.net/`. [Online; accessed 08-October-2020].

Brinkmann, Benjamin H, Hari Guragain, Daniel Kenney-Jung, Jay Mandrekar, Robert E Watson, Kirk M Welker, Jeffrey W Britton, and Robert J Witte (2019). „Segmentation errors and intertest reliability in automated and manually traced hippocampal volumes". In: *Annals of clinical and translational neurology* 6.9, pp. 1807–1814.

Brodie, MJ, SJE Barry, GA Bamagous, JD Norrie, and P Kwan (2012). „Patterns of treatment response in newly diagnosed epilepsy". In: *Neurology* 78.20, pp. 1548–1554.

Brown, Robert W, Y-C Norman Cheng, E Mark Haacke, Michael R Thompson, and Ramesh Venkatesan (2014). *Magnetic resonance imaging: physical principles and sequence design*. John Wiley & Sons.

Brown, SSG, JW Rutland, G Verma, RE Feldman, J Alper, M Schneider, BN Delman, JM Murrough, and P Balchandani (2019). „Structural MRI at 7T reveals amygdala nuclei and hippocampal subfield volumetric association with major depressive disorder symptom severity". In: *Scientific reports* 9.1, pp. 1–10.

Canjels, Lisanne PW, Walter H Backes, Tamar M van Veenendaal, Marielle CG Vlooswijk, Paul AM Hofman, Albert P Aldenkamp, Rob PW Rouhl, and Jacobus FA Jansen (2020). „Volumetric and Functional Activity Lateralization in Healthy Subjects and Patients with Focal Epilepsy: Initial Findings in a 7T MRI Study". In: *Journal of Neuroimaging*.

Carrette, Evelien and Hermann Stefan (2019). „Evidence for the role of magnetic source imaging in the presurgical evaluation of refractory epilepsy patients". In: *Frontiers in neurology* 10.

Cendes, Fernando, Frederick Andermann, Pierre Gloor, A Evans, M Jones-Gotman, Craig Watson, D Melanson, A Olivier, T Peters, I Lopes-Cendes, *et al.* (1993). „MRI volumetric measurement of amygdala and hippocampus in temporal lobe epilepsy". In: *Neurology* 43.4, pp. 719–719.

Cendes, Fernando, William H Theodore, Benjamin H Brinkmann, Vlastimil Sulc, and Gregory D Cascino (2016). „Neuroimaging of epilepsy". In: *Handbook of clinical neurology*. Vol. 136. Elsevier, pp. 985–1014.

Chen, Xin, Tianyi Qian, Tobias Kober, Guojun Zhang, Zhiwei Ren, Tao Yu, Yueshan Piao, Nan Chen, and Kuncheng Li (2018). „Gray-matter-specific MR imaging improves the detection of epileptogenic zones in focal cortical dysplasia: A new sequence called fluid and white matter suppression (FLAWS)". In: *NeuroImage: Clinical* 20, pp. 388–397.

Clarke, William T, Olivier Mougin, Ian D Driver, Catarina Rua, Andrew T Morgan, Michael Asghar, Stuart Clare, Susan Francis, Richard G Wise, Christopher T Rodgers, *et al.* (2020). „Multi-site harmonization of 7 tesla MRI neuroimaging protocols". In: *Neuroimage* 206, p. 116335.

Coan, AC, B Kubota, FPG Bergo, BM Campos, and F Cendes (2014a). „3T MRI quantification of hippocampal volume and signal in mesial temporal lobe epilepsy improves detection of hippocampal sclerosis". In: *American Journal of Neuroradiology* 35.1, pp. 77–83.

Coan, Ana C, Brunno M Campos, Guilherme C Beltramini, Clarissa L Yasuda, Roberto JM Covolan, and Fernando Cendes (2014b). „Distinct functional and structural MRI abnormalities in mesial temporal lobe epilepsy with and without hippocampal sclerosis". In: *Epilepsia* 55.8, pp. 1187–1196.

Colon, AJ, MJP van Osch, M Buijs, J vd Grond, Paul Boon, MA van Buchem, and PAM Hofman (2016). „Detection superiority of 7 T MRI protocol in patients with epilepsy and suspected focal cortical dysplasia". In: *Acta Neurologica Belgica* 116.3, pp. 259–269.

Colon, AJ, MJP van Osch, M Buijs, JVD Grond, A Hillebrand, O Schijns, GJ Wagner, P Ossenblok, P Hofman, MAV Buchem, *et al.* (2018). „MEG-guided analysis of 7T-MRI in patients with epilepsy". In: *Seizure* 60, pp. 29–38.

Conf2hires (2019). `https : / / ftp . nmr . mgh . harvard . edu / pub / dist / freesurfer/6.0.0-patch/hcp/conf2hires/`.

Coras, Roland, Gloria Milesi, Ileana Zucca, Alfonso Mastropietro, Alessandro Scotti, Matteo Figini, Angelika Mühlebner, Andreas Hess, Wolfgang

Graf, Giovanni Tringali, *et al.* (2014). „7 T MRI features in control human hippocampus and hippocampal sclerosis: An ex vivo study with histologic correlations“. In: *Epilepsia* 55.12, pp. 2003–2016.

CoreTechLabsInc. (2020). `https : / / www . cortechslabs . com / products / neuroquant/`. [Online; accessed 08-October-2020].

De Ciantis, Alessio, Carmen Barba, Laura Tassi, Mirco Cosottini, Michela Tosetti, Mauro Costagli, Manuela Bramerio, Emanuele Bartolini, Laura Biagi, Massimo Cossu, *et al.* (2016). „7T MRI in focal epilepsy with unrevealing conventional field strength imaging“. In: *Epilepsia* 57.3, pp. 445–454.

Duncan, John S, Gavin P Winston, Matthias J Koepp, and Sebastien Ourselin (2016). „Brain imaging in the assessment for epilepsy surgery“. In: *The Lancet Neurology* 15.4, pp. 420–433.

Durnford, Andrew J, William Rodgers, Fenella J Kirkham, Mark A Mullee, Andrea Whitney, Martin Prevett, Lucy Kinton, Matthew Harris, and William P Gray (2011). „Very good inter-rater reliability of Engel and ILAE epilepsy surgery outcome classifications in a series of 76 patients“. In: *Seizure* 20.10, pp. 809–812.

Düzel, Emrah, Julio Acosta-Cabronero, David Berron, Geert Jan Biessels, Isabella Björkman-Burtscher, Michel Bottlaender, Richard Bowtell, Mark V Buchem, Arturo Cardenas-Blanco, Fawzi Boumezbeur, *et al.* (2019). „European Ultrahigh-Field Imaging Network for Neurodegenerative Diseases (EUFIND)“. In: *Alzheimer's & Dementia: Diagnosis, Assessment & Disease Monitoring* 11.1, pp. 538–549.

Engel, Jerome (1993). „Update on surgical treatment of the epilepsies: summary of the second international palm desert conference on the surgical treatment of the epilepsies (1992)“. In: *Neurology* 43.8, pp. 1612–1612.

Feldman, Rebecca Emily, Bradley Neil Delman, Puneet Singh Pawha, Hadrien Dyvorne, John Watson Rutland, Jiyeoun Yoo, Madeline Cara Fields, Lara Vanessa Marcuse, and Priti Balchandani (2019). „7T MRI in epilepsy patients with previously normal clinical MRI exams compared against healthy controls“. In: *Plos one* 14.3, e0213642.

Fiest, Kirsten M, Khara M Sauro, Samuel Wiebe, Scott B Patten, Churl-Su Kwon, Jonathan Dykeman, Tamara Pringsheim, Diane L Lorenzetti, and Nathalie Jetté (2017). „Prevalence and incidence of epilepsy: a systematic review and meta-analysis of international studies“. In: *Neurology* 88.3, pp. 296–303.

Fischl, Bruce (2012). „FreeSurfer“. In: *Neuroimage* 62.2, pp. 774–781.

Fisher, Robert S, Carlos Acevedo, Alexis Arzimanoglou, Alicia Bogacz, J Helen Cross, Christian E Elger, Jerome Engel Jr, Lars Forsgren, Jacqueline A French,

Mike Glynn, *et al.* (2014). „ILAE official report: a practical clinical definition of epilepsy". In: *Epilepsia* 55.4, pp. 475–482.

Fisher, Robert S, J Helen Cross, Jacqueline A French, Norimichi Higurashi, Edouard Hirsch, Floor E Jansen, Lieven Lagae, Solomon L Moshé, Jukka Peltola, Eliane Roulet Perez, *et al.* (2017). „Operational classification of seizure types by the International League Against Epilepsy: Position Paper of the ILAE Commission for Classification and Terminology". In: *Epilepsia* 58.4, pp. 522–530.

Focke, Niels K, Mahinda Yogarajah, Mark R Symms, Oliver Gruber, Walter Paulus, and John S Duncan (2012). „Automated MR image classification in temporal lobe epilepsy". In: *Neuroimage* 59.1, pp. 356–362.

Foged, Mette Thrane, Terje Martens, Lars H Pinborg, Nizar Hamrouni, Minna Litman, Guido Rubboli, Anne-Mette Leffers, Philippe Ryvlin, Bo Jespersen, Olaf B Paulson, *et al.* (2020). „Diagnostic added value of electrical source imaging in presurgical evaluation of patients with epilepsy: A prospective study". In: *Clinical Neurophysiology* 131.1, pp. 324–329.

Friedman, Elliott (2014). „Epilepsy imaging in adults: getting it right". In: *American Journal of Roentgenology* 203.5, pp. 1093–1103.

Friston, Karl J, John Ashburner, Christopher D Frith, J-B Poline, John D Heather, and Richard SJ Frackowiak (1995). „Spatial registration and normalization of images". In: *Human brain mapping* 3.3, pp. 165–189.

Gaser, Christian and Robert Dahnke (2016). „CAT-a computational anatomy toolbox for the analysis of structural MRI data". In: *HBM* 2016, pp. 336–348.

Gillmann, Clarissa, Roland Coras, Karl Rössler, Arnd Doerfler, Michael Uder, Ingmar Blümcke, and Tobias Bäuerle (2018). „Ultra-high field MRI of human hippocampi: Morphological and multiparametric differentiation of hippocampal sclerosis subtypes". In: *PloS one* 13.4, e0196008.

Goldenholz, Daniel M, Alexander Jow, Omar I Khan, Anto Bagić, Susumu Sato, Sungyoung Auh, Conrad Kufta, Sara Inati, and William H Theodore (2016). „Preoperative prediction of temporal lobe epilepsy surgery outcome". In: *Epilepsy research* 127, pp. 331–338.

Gonzalez, Rafael C, Richard Eugene Woods, and Steven L Eddins (2004). *Digital image processing using MATLAB*. Pearson Education India.

Goubran, Maged, Boris C Bernhardt, Diego Cantor-Rivera, Jonathan C Lau, Charlotte Blinston, Robert R Hammond, Sandrine de Ribaupierre, Jorge G Burneo, Seyed M Mirsattari, David A Steven, *et al.* (2016). „In vivo MRI signatures of hippocampal subfield pathology in intractable epilepsy". In: *Human brain mapping* 37.3, pp. 1103–1119.

Hadar, Peter N, Lohith G Kini, Carlos Coto, Virginie Piskin, Lauren E Callans, Stephanie H Chen, Joel M Stein, Sandhitsu R Das, Paul A Yushkevich, and Kathryn A Davis (2018). „Clinical validation of automated hippocampal segmentation in temporal lobe epilepsy“. In: *NeuroImage: Clinical* 20, pp. 1139–1147.

Hansson, Boel, Karin Markenroth Bloch, Titti Owman, Markus Nilsson, Jimmy Lätt, Johan Olsrud, and Isabella M Björkman-Burtscher (2020). „Subjectively Reported Effects Experienced in an Actively Shielded 7T MRI: A Large-Scale Study“. In: *Journal of Magnetic Resonance Imaging*.

Henry, Thomas R, Marie Chupin, Stéphane Lehéricy, John P Strupp, Michael A Sikora, Zhiyi Y Sha, Kâmil Uğurbil, and Pierre-François Van de Moortele (2011). „Hippocampal sclerosis in temporal lobe epilepsy: findings at 7 T“. In: *Radiology* 261.1, pp. 199–209.

Holmes, Gregory L (2012). *Consequences of Epilepsy through the Ages: When is the Die Cast? Introduction*.

Hong, Seok-Jun, Boris C Bernhardt, Dewi S Schrader, Neda Bernasconi, and Andrea Bernasconi (2016). „Whole-brain MRI phenotyping in dysplasia-related frontal lobe epilepsy“. In: *Neurology* 86.7, pp. 643–650.

Iglesias, Juan Eugenio, Jean C Augustinack, Khoa Nguyen, Christopher M Player, Allison Player, Michelle Wright, Nicole Roy, Matthew P Frosch, Ann C McKee, Lawrence L Wald, *et al.* (2015). „A computational atlas of the hippocampal formation using ex vivo, ultra-high resolution MRI: application to adaptive segmentation of in vivo MRI“. In: *Neuroimage* 115, pp. 117–137.

Jack Jr, Clifford R, Frank W Sharbrough, Gregory D Cascino, Kathryn A Hirschorn, Peter C O'Brien, and W Richard Marsh (1992). „Magnetic resonance image–based hippocampal volumentry: Correlation with outcome after temporal lobectomy“. In: *Annals of Neurology: Official Journal of the American Neurological Association and the Child Neurology Society* 31.2, pp. 138–146.

Jardim, Anaclara Prada, Jeana Torres Corso, Maria Teresa Fernandes Castilho Garcia, Larissa Botelho Gaça, Sandra Mara Comper, Carmen Lúcia Penteado Lancellotti, Ricardo Silva Centeno, Henrique Carrete Júnior, Esper Abrão Cavalheiro, Carla Alessandra Scorza, *et al.* (2016). „Hippocampal atrophy on MRI is predictive of histopathological patterns and surgical prognosis in mesial temporal lobe epilepsy with hippocampal sclerosis“. In: *Epilepsy Research* 128, pp. 169–175.

Jette, Nathalie, Aylin Y Reid, and Samuel Wiebe (2014). „Surgical management of epilepsy“. In: *Canada Med Assoc Journal* 186.13, pp. 997–1004.

Kim, Minjeong, Guorong Wu, Wei Li, Li Wang, Young-Don Son, Zang-Hee Cho, and Dinggang Shen (2011). „Segmenting hippocampus from 7.0 Tesla MR images by combining multiple atlases and auto-context models". In: *International Workshop on Machine Learning in Medical Imaging*. Springer, pp. 100–108.

Kinney, Michael Owen, Stjepana Kovac, and Beate Diehl (2019). „Structured testing during seizures: A practical guide for assessing and interpreting ictal and postictal signs during video EEG long term monitoring". In: *Seizure* 72, pp. 13–22.

Knudsen, Gitte M, Peter S Jensen, David Erritzoe, William FC Baaré, Anders Ettrup, Patrick M Fisher, Nic Gillings, Hanne D Hansen, Lars Kai Hansen, Steen G Hasselbalch, *et al.* (2016). „The center for integrated molecular brain imaging (Cimbi) database". In: *Neuroimage* 124, pp. 1213–1219.

Kwan, Benjamin YM, Fateme Salehi, Pavlo Ohorodnyk, Donald H Lee, Jorge G Burneo, Seyed M Mirsattari, David Steven, Robert Hammond, Terry M Peters, and Ali R Khan (2016). „Usage of SWI (susceptibility weighted imaging) acquired at 7 T for qualitative evaluation of temporal lobe epilepsy patients with histopathological and clinical correlation: An initial pilot study". In: *Journal of the neurological sciences* 369, pp. 82–87.

Langfitt, JT (1995). „Comparison of the psychometric characteristics of three quality of life measures in intractable epilepsy". In: *Quality of Life Research* 4.2, pp. 101–114.

Larroza, Andrés, Vicente Bodı, David Moratal, *et al.* (2016). „Texture analysis in magnetic resonance imaging: review and considerations for future applications". In: *Assessment of cellular and organ function and dysfunction using direct and derived MRI methodologies*, pp. 75–106.

Lüders, Hans O, Imad Najm, Dileep Nair, Peter Widdess-Walsh, and William Bingman (2006). „The epileptogenic zone: general principles". In: *Epileptic disorders* 8.2, pp. 1–9.

Lüders, Hans, Naoki Akamatsu, Shahram Amina, Christoph Baumgartner, Selim Benbadis, Adriana Bermeo-Ovalle, Andrew Bleasel, Alireza Bozorgi, Mar Carreño, Michael Devereaux, *et al.* (2019). „Critique of the 2017 epileptic seizure and epilepsy classifications". In: *Epilepsia* 60.6, pp. 1032–1039.

Lüsebrink, Falk, Astrid Wollrab, and Oliver Speck (2013). „Cortical thickness determination of the human brain using high resolution 3 T and 7 T MRI data". In: *Neuroimage* 70, pp. 122–131.

Malmgren, Kristina and Maria Thom (2012). „Hippocampal sclerosis—origins and imaging". In: *Epilepsia* 53, pp. 19–33.

Mathon, Bertrand, Franck Bielle, Séverine Samson, Odile Plaisant, Sophie Dupont, Anne Bertrand, Richard Miles, Vi-Huong Nguyen-Michel, Virginie Lambrecq, Ana Laura Calderon-Garcidueñas, *et al.* (2017). „Predictive factors of long-term outcomes of surgery for mesial temporal lobe epilepsy associated with hippocampal sclerosis". In: *Epilepsia* 58.8, pp. 1473–1485.

Memarian, Negar, Sally Kim, Sandra Dewar, Jerome Engel Jr, and Richard J Staba (2015). „Multimodal data and machine learning for surgery outcome prediction in complicated cases of mesial temporal lobe epilepsy". In: *Computers in biology and medicine* 64, pp. 67–78.

Miller, John W and Shahin Hakimian (2013). „Surgical treatment of epilepsy". In: *Continuum: Lifelong Learning in Neurology* 19.3 Epilepsy, p. 730.

Mo, Jia-Jie, Jian-Guo Zhang, Wen-Ling Li, Chao Chen, Na-Jing Zhou, Wen-Han Hu, Chao Zhang, Yao Wang, Xiu Wang, Chang Liu, *et al.* (2019). „Clinical Value of Machine Learning in the Automated Detection of Focal Cortical Dysplasia Using Quantitative Multimodal Surface-Based Features". In: *Frontiers in neuroscience* 12, p. 1008.

Mueller, Susanne G, Paul A Yushkevich, Sandhitsu Das, Lei Wang, Koen Van Leemput, Juan Eugenio Iglesias, Kate Alpert, Adam Mezher, Peter Ng, Katrina Paz, *et al.* (2018). „Systematic comparison of different techniques to measure hippocampal subfield volumes in ADNI2". In: *NeuroImage: Clinical* 17, pp. 1006–1018.

Muhlhofer, Wolfgang, Yee-Leng Tan, Susanne G Mueller, and Robert Knowlton (2017). „MRI-negative temporal lobe epilepsy—What do we know?" In: *Epilepsia* 58.5, pp. 727–742.

Najm, Imad, Lara Jehi, Andre Palmini, Jorge Gonzalez-Martinez, Eliseu Paglioli, and William Bingaman (2013). „Temporal patterns and mechanisms of epilepsy surgery failure". In: *Epilepsia* 54.5, pp. 772–782.

Nishimura, Dwight G (2010). *Principles of magnetic resonance imaging*. Standford Univ.

Obusez, Emmanuel C, Mark Lowe, Se-Hong Oh, Irene Wang, Jennifer Bullen, Paul Ruggieri, Virginia Hill, Daniel Lockwood, Todd Emch, Doksu Moon, *et al.* (2018). „7T MR of intracranial pathology: Preliminary observations and comparisons to 3T and 1.5 T". In: *Neuroimage* 168, pp. 459–476.

Opheim, Giske, Oula Puonti, Jan Ole Pedersen, Vincent O. Boer, Ane Kloster, Martin Prener, *et al.* (2020). „Optimizing a preprocessing pipeline for structural 7T MR analyses in FreeSurfer, program no. 3667". In: Annual ISMRM Meeting, 2020.

Papayannis, CE, D Consalvo, MA Kauffman, G Seifer, S Oddo, L D'Alessio, P Saidon, and S Kochen (2012). „Malformations of cortical development and epilepsy in adult patients". In: *Seizure* 21.5, pp. 377–384.

Pardoe, Heath R, Gaby S Pell, David F Abbott, and Graeme D Jackson (2009). „Hippocampal volume assessment in temporal lobe epilepsy: how good is automated segmentation?" In: *Epilepsia* 50.12, pp. 2586–2592.

Parvizi, Josef and Sabine Kastner (2018). „Promises and limitations of human intracranial electroencephalography". In: *Nature neuroscience* 21.4, pp. 474–483.

Rondinoni, Carlo, Celso Magnun, Alexandre Vallota da Silva, Helmut Manfred Heinsen, and Edson Amaro Jr (2019). „Epilepsy under the scope of ultra-high field MRI". In: *Epilepsy & Behavior,* p. 106366.

Rüber, Theodor, Bastian David, and Christian E Elger (2018). „MRI in epilepsy: clinical standard and evolution". In: *Current opinion in neurology* 31.2, pp. 223–231.

Ryvlin, Philippe, Michel Cucherat, and Sylvain Rheims (2011). „Risk of sudden unexpected death in epilepsy in patients given adjunctive antiepileptic treatment for refractory seizures: a meta-analysis of placebo-controlled randomised trials". In: *The Lancet Neurology* 10.11, pp. 961–968.

Ryvlin, Philippe and Sylvain Rheims (2008). „Epilepsy surgery: eligibility criteria and presurgical evaluation". In: *Dialogues in clinical neuroscience* 10.1, p. 91.

Ryvlin, Philippe and Sylvain Rheims (2016). „Predicting epilepsy surgery outcome". In: *Current opinion in neurology* 29.2, pp. 182–188.

Sánchez, AM Granados and JF Orejuela Zapata (2018). „Diagnosis of mesial temporal sclerosis: sensitivity, specificity and predictive values of the quantitative analysis of magnetic resonance imaging". In: *Neuroradiol J* 31.1, pp. 50–59.

Sankar, Tejas, Neda Bernasconi, Hosung Kim, and Andrea Bernasconi (2008). „Temporal lobe epilepsy: differential pattern of damage in temporopolar cortex and white matter". In: *Human brain mapping* 29.8, pp. 931–944.

Santyr, Brendan G, Maged Goubran, Jonathan C Lau, Benjamin YM Kwan, Fateme Salehi, Donald H Lee, Seyed M Mirsattari, Jorge G Burneo, David A Steven, Andrew G Parrent, *et al.* (2017). „Investigation of hippocampal substructures in focal temporal lobe epilepsy with and without hippocampal sclerosis at 7T". In: *Journal of Magnetic Resonance Imaging* 45.5, pp. 1359–1370.

Scanlon, Cathy, Susanne G Mueller, Ian Cheong, Miriam Hartig, Michael W Weiner, and Kenneth D Laxer (2013). „Grey and white matter abnormalities in temporal lobe epilepsy with and without mesial temporal sclerosis". In: *Journal of neurology* 260.9, pp. 2320–2329.

Scheffer, Ingrid E, Samuel Berkovic, Giuseppe Capovilla, Mary B Connolly, Jacqueline French, Laura Guilhoto, Edouard Hirsch, Satish Jain, Gary W Mathern, Solomon L Moshé, *et al.* (2017). „ILAE classification of the epilepsies: position paper of the ILAE Commission for Classification and Terminology". In: *Epilepsia* 58.4, pp. 512–521.

Schmeiser, Barbara, Jinmei Li, Armin Brandt, Josef Zentner, Soroush Doostkam, and Thomas M Freiman (2017). „Different mossy fiber sprouting patterns in ILAE hippocampal sclerosis types". In: *Epilepsy Research* 136, pp. 115–122.

Shaw, Thomas, Ashley York, Maryam Ziaei, Markus Barth, Steffen Bollmann, Alzheimer's Disease Neuroimaging Initiative, *et al.* (2020). „Longitudinal Automatic Segmentation of Hippocampal Subfields (LASHiS) using Multi-Contrast MRI". In: *NeuroImage*, p. 116798.

Shorvon, Simon and Torbjorn Tomson (2011). „Sudden unexpected death in epilepsy". In: *The Lancet* 378.9808, pp. 2028–2038.

Sperling, Michael R (2004). „The consequences of uncontrolled epilepsy". In: *CNS spectrums* 9.2, pp. 98–109.

Springer, Elisabeth, Barbara Dymerska, Pedro Lima Cardoso, Simon Daniel Robinson, Christian Weisstanner, Roland Wiest, Benjamin Schmitt, and Siegfried Trattnig (2016). „Comparison of routine brain imaging at 3 T and 7 T". In: *Investigative radiology* 51.8, p. 469.

Staba, Richard J, Arne D Ekstrom, Nanthia A Suthana, Alison Burggren, Itzhak Fried, Jerome Engel Jr, and Susan Y Bookheimer (2012). „Gray matter loss correlates with mesial temporal lobe neuronal hyperexcitability inside the human seizure-onset zone". In: *Epilepsia* 53.1, pp. 25–34.

Steve, Trevor A, Jeffrey D Jirsch, and Donald W Gross (2014). „Quantification of subfield pathology in hippocampal sclerosis: a systematic review and meta-analysis". In: *Epilepsy research* 108.8, pp. 1279–1285.

Strzelczyk, Adam, Claudia Griebel, Wolfram Lux, Felix Rosenow, and Jens-Peter Reese (2017). „The burden of severely drug-refractory epilepsy: a comparative longitudinal evaluation of mortality, morbidity, resource use, and cost using German health insurance data". In: *Frontiers in neurology* 8, p. 712.

Téllez-Zenteno, José F, Lizbeth Hernández Ronquillo, Farzad Moien-Afshari, and Samuel Wiebe (2010). „Surgical outcomes in lesional and non-lesional

epilepsy: a systematic review and meta-analysis". In: *Epilepsy research* 89.2-3, pp. 310–318.

Thom, Maria (2014). „Hippocampal sclerosis in epilepsy: a neuropathology review". In: *Neuropathology and applied neurobiology* 40.5, pp. 520–543.

Thom, Maria, Ioannis Liagkouras, Lillian Martinian, Joan Liu, Claudia B Catarino, and Sanjay M Sisodiya (2012). „Variability of sclerosis along the longitudinal hippocampal axis in epilepsy: a post mortem study". In: *Epilepsy research* 102.1-2, pp. 45–59.

Trattnig, Siegfried, Elisabeth Springer, Wolfgang Bogner, Gilbert Hangel, Bernhard Strasser, Barbara Dymerska, Pedro Lima Cardoso, and Simon Daniel Robinson (2018). „Key clinical benefits of neuroimaging at 7 T". In: *Neuroimage* 168, pp. 477–489.

Tripathi, Manjari, Sucharita Ray, and P Sarat Chandra (2016). „Presurgical evaluation for drug refractory epilepsy". In: *International Journal of Surgery* 36, pp. 405–410.

Van der Kolk, Anja G, Jeroen Hendrikse, Jaco JM Zwanenburg, Fredy Visser, and Peter R Luijten (2013). „Clinical applications of 7 T MRI in the brain". In: *European journal of radiology* 82.5, pp. 708–718.

Veersema, Tim J, Pieter van Eijsden, Peter H Gosselaar, Jeroen Hendrikse, Jaco JM Zwanenburg, Wim GM Spliet, Eleonora Aronica, Kees PJ Braun, and Cyrille H Ferrier (2016). „7 tesla T2*-weighted MRI as a tool to improve detection of focal cortical dysplasia". In: *Epileptic Disorders* 18.3, pp. 315–323.

Veersema, Tim J, Cyrille H Ferrier, Pieter van Eijsden, Peter H Gosselaar, Eleonora Aronica, Fredy Visser, Jaco M Zwanenburg, Gerard AP de Kort, Jeroen Hendrikse, Peter R Luijten, *et al.* (2017). „Seven tesla MRI improves detection of focal cortical dysplasia in patients with refractory focal epilepsy". In: *Epilepsia Open* 2.2, pp. 162–171.

Voets, Natalie L, Carl J Hodgetts, Arjune Sen, Jane E Adcock, and Uzay Emir (2017). „Hippocampal MRS and subfield volumetry at 7T detects dysfunction not specific to seizure focus". In: *Scientific reports* 7.1, pp. 1–14.

Wagstyl, Konrad, Sophie Adler, Birgit Pimpel, Aswin Chari, Kiran Seunarine, Sara Lorio, Rachel Thornton, Torsten Baldeweg, and Martin Tisdall (2020). „Planning stereoelectroencephalography using automated lesion detection: Retrospective feasibility study". In: *Epilepsia*.

Wang, Irene, Sehong Oh, Ingmar Blümcke, Roland Coras, Balu Krishnan, Sanghoon Kim, Aaron McBride, Olesya Grinenko, Yicong Lin, Margit Overmyer,

et al. (2020). „Value of 7T MRI and post-processing in patients with nonlesional 3T MRI undergoing epilepsy presurgical evaluation". In: *Epilepsia*.

Wang, Xiu, Chao Zhang, Yao Wang, Wenhan Hu, Xiaoqiu Shao, Jian-guo Zhang, and Kai Zhang (2016). „Prognostic factors for seizure outcome in patients with MRI-negative temporal lobe epilepsy: A meta-analysis and systematic review". In: *Seizure* 38, pp. 54–62.

Wang, Z Irene, Stephen E Jones, Zeenat Jaisani, Imad M Najm, Richard A Prayson, Richard C Burgess, Balu Krishnan, Aleksandar Ristic, Chong H Wong, William Bingaman, *et al.* (2015). „Voxel-based morphometric magnetic resonance imaging (MRI) postprocessing in MRI-negative epilepsies". In: *Annals of neurology* 77.6, pp. 1060–1075.

West, Siobhan, Sarah J Nolan, and Richard Newton (2016). „Surgery for epilepsy: a systematic review of current evidence". In: *Epileptic Disorders* 18.2, pp. 113–121.

Wiebe, Samuel and Nathalie Jette (2012). „Pharmacoresistance and the role of surgery in difficult to treat epilepsy". In: *Nature Reviews Neurology* 8.12, p. 669.

Wieser, HG, WT Blume, D Fish, E Goldensohn, A Hufnagel, D King, MR Sperling, and H Lüders (2001). „Proposal for a new classification of outcome with respect to epileptic seizures following epilepsy surgery". In: *Epilepsia* 42, pp. 282–286.

Wiesinger, Florian, Pierre-Francois Van de Moortele, Gregor Adriany, Nicola De Zanche, Kamil Ugurbil, and Klaas P Pruessmann (2006). „Potential and feasibility of parallel MRI at high field". In: *NMR in Biomedicine: An International Journal Devoted to the Development and Application of Magnetic Resonance In vivo* 19.3, pp. 368–378.

Wisse, Laura EM, Hugo J Kuijf, Anita M Honingh, Hongzhi Wang, John B Pluta, Sandhitsu R Das, David A Wolk, Jaco JM Zwanenburg, Paul A Yushkevich, and Mirjam I Geerlings (2016). „Automated hippocampal subfield segmentation at 7T MRI". In: *American Journal of Neuroradiology* 37.6, pp. 1050–1057.

Yu, O, Y Mauss, IJ Namer, and J Chambron (2001). „Existence of contralateral abnormalities revealed by texture analysis in unilateral intractable hippocampal epilepsy". In: *Magnetic resonance imaging* 19.10, pp. 1305–1310.

Yushkevich, Paul A, John B Pluta, Hongzhi Wang, Long Xie, Song-Lin Ding, Eske C Gertje, Lauren Mancuso, Daria Kliot, Sandhitsu R Das, and David A Wolk (2015). „Automated volumetry and regional thickness analysis

of hippocampal subfields and medial temporal cortical structures in mild cognitive impairment". In: *Human brain mapping* 36.1, pp. 258–287.

Zhang, Chunbo and Patrick Kwan (2019). „The concept of drug-resistant epileptogenic zone". In: *Frontiers in Neurology* 10, p. 558.

Zhang, Yiwei, Yuelei Lv, Hui You, Wanchen Dou, Bo Hou, Lin Shi, Zhentao Zuo, Weiyu Mao, and Feng Feng (2019). „Study of the hippocampal internal architecture in temporal lobe epilepsy using 7 T and 3 T MRI". In: *Seizure* 71, pp. 116–123.

Zijlmans, Maeike, Willemiek Zweiphenning, and Nicole van Klink (2019). „Changing concepts in presurgical assessment for epilepsy surgery". In: *Nature Reviews Neurology* 15.10, pp. 594–606.

Appendix

<div style="text-align: right">A</div>

A.1 Article 1

Ane Kloster*, Giske Opheim*, Emil Holm, Philip Fink-Jensen, Bo Jespersen, Camilla G. Madsen, Karen B. Larsen, Olaf B. Paulson, Melanie Ganz, Lars H. Pinborg, *"Automated hippocampal segmentations in histopathologically classified HS ILAE type 1 and 2"*, 2020, **In prep.**

Shared first-authors

Working title: Automated hippocampal segmentations in histopathologically classified HS ILAE type 1 and 2

Authors:
Ane Kloster[1]*, Giske Opheim[1,2]*, Emil Holm[1], Philip Fink-Jensen[1,2], Bo Jespersen[3], Camilla G. Madsen[4], Karen B. Larsen[5], Olaf B. Paulson[1,2], Melanie Ganz[1,6], Lars H. Pinborg[1,2,7]

     *shared first authors

Affiliations:
1.   Neurobiology Research Unit, Neuro Centre, Copenhagen University Hospital Rigshospitalet, Denmark
2.   Faculty of Health and Medical Sciences, University of Copenhagen, Denmark
3   Dept. of Neurosurgery, Copenhagen University Hospital Rigshospitalet, Denmark
4   Functional and Diagnostic Imaging Unit, Dept. of Radiology, Copenhagen University Hospital Hvidovre, Denmark
5   Dept. of Pathology, Copenhagen University Hospital Rigshospitalet, Denmark
6   Dept. of Computer Science, University of Copenhagen, Denmark
7   Epilepsy Clinic, Dept of Neurology, Copenhagen University Hospital Rigshospitalet, Denmark

Corresponding author: Lars H. Pinborg, MD, DMSc, Associate Professor
                  Epilepsy Clinic & Neurobiology Research Unit
                  Department of Neurology
                  6-8 Inge Lehmanns Vej
                  Rigshospitalet, Unit 8057
                  DK-2100 Copenhagen, Denmark
                  email: lars.pinborg@nru.dk
                  phone: +45 3545 6712

Abstract

Introduction

Temporal lobe epilepsy (TLE) is the most common type of drug-resistant epilepsy. The archetypal histopathological abnormality in mesial TLE is hippocampal sclerosis (HS). HS is histopathologically classified according to international consensus into three types, depending on the pattern of neuronal cell loss in different hippocampal subfields. Preoperative subclassification of HS is desirable because different types are associated with different seizure outcomes and post-surgical memory performances. The aim of the study was to test the feasibility of an automated hippocampal segmentation tool implemented in FreeSurfer v. 6.0 and a simple volume asymmetry ratio (VAR) to detect patterns of subfield volume abnormalities concordant with the histopathological diagnosis.

Methods

Fifty-two TLE patients underwent an anterior temporal lobe resection and 52 healthy controls were analysed. As part of the standard Danish epilepsy surgery program all patients were 3T MRI scanned and hippocampal resected samples were histopathologically classified according to recommendations from the International League Against Epilepsy (ILAE). We calculated absolute VAR for whole hippocampus and subfields CA1 and CA4, and used Wilcoxon rank-sum test with Bonferroni correction for multiple comparisons to assess group differences between HS patients, non-HS and HC.

Results

Patients were categorized as HS ILAE type 1 (n=25), HS ILAE type 2 (n=18), HS-ILAE type 3 (n=1, thus excluded from group comparisons) and non-HS (n=8). There was a significant difference in mean VAR in whole hippocampus, CA1 and CA4 for both HS ILAE type 1 and type 2 compared to healthy controls and the non-HS group, respectively. There was no significant difference in mean

VAR in whole hippocampus, CA1 and CA4 when comparing HS ILAE type 1 with HS ILAE type 2.

Conclusion

The hippocampal segmentation tool implemented in FreeSurfer v. 6.0 and a simple volume asymmetry ratio are excellent at identifying patients histopathologically diagnosed with HS. It was not possible to identify subfield volume asymmetry patterns that separately identify HS ILAE type 1 from HS ILAE type 2 patients. Contrary to expectations CA4 VAR was not significantly different in HS ILAE type 1 versus HS ILAE type 2 patients.

Key words: [MRI], [hippocampal sclerosis], [temporal lobe epilepsy], [automated segmentation], [hippocampal subfields]

1. Introduction

Epilepsy is a disabling seizure disorder that affects ~1% of the population[1,2]. One third of epilepsy patients are drug-resistant, debilitated by recurring seizures despite best possible antiseizure drug treatment[3]. Temporal lobe epilepsy (TLE) is the most prevalent form of drug-resistant epilepsy[4,5,7]. In patients with focal onset epilepsy such as TLE, localization of the cortical area necessary for initiating a seizure (the epileptogenic zone, EZ) allows for modifying or even curing epilepsy by surgical resection of the putative EZ. In TLE-patients, 53-84% of patients remain seizure free one year after anteromesial temporal lobe resections[6,7]. The probability of obtaining seizure freedom is significantly increased if an epileptogenic lesion is identified on the preoperative magnetic resonance image (MRI) of the brain[8].

The archetypal histopathological abnormality in mesial TLE-patients is hippocampal sclerosis (HS)[9,10]. HS is characterized by segmental loss of pyramidal neuronal cells and increased gliosis, i.e., sclerosis of the hippocampus. According to the International League Against Epilepsy (ILAE)[10], HS is histopathologically classified into three types, depending on the specific pattern of neuronal cell loss within the four different subfields of the Cornu ammonis (CA). HS ILAE type 1 is characterized by severe neuronal cell loss in the CA1 and CA4. HS ILAE type 2 and HS ILAE type 3 are characterized by predominant neuronal loss in CA1 and CA4, respectively.

Preoperative information on HS ILAE subtypes would be of clinical value in the evaluation of epilepsy surgery candidates, as they correlate to postoperative seizure outcomes[11,19] and memory impairment[17,18]. If specific patterns of atrophy in hippocampal subfields can be identified on presurgical MRIs, as a proxy for the HS ILAE neuropathological diagnosis of neuronal loss, it

could add importantly both to the surgical decision-making and the information to the patient regarding risks and benefits from the proposed operation.

Preoperatively, reduced hippocampal volume and increased T2 or FLAIR signal intensity are well-recognized surrogate MR imaging markers for the histopathological hallmarks of HS[10,12-14] .The degree of hippocampal volume reduction in T1-weighted images relates to the severity of neuronal cell loss, and the increased T2 or FLAIR signal intensity relates to tissue disruptions or gliosis[13,15,16]. But even in the hands of highly specialized MR neuroradiologists, the diagnosis of HS can be challenging in cases with discrete morphological alterations, and the identification of HS ILAE subtypes are not considered feasible by visual inspection of presurgical MRI scans[17]. This has led to investigations on the use of automated hippocampal subfield segmentation of MRIs in patients with temporal lobe epilepsy[15,16,20-23]. Jardim et al. (2016) demonstrated significant positive correlations between total hippocampal volumes obtain from MRI (1.5 T and FreeSurfer v. 5.3) and neuronal cell densities in CA1, CA3 and CA4 (but not CA2) obtained from histopathological evaluation[20]. The authors did not report correlations between subfield hippocampal volumes and neuronal densities. Sone et al. (2016) reported that FreeSurfer v. 6.0 was superior to FreeSurfer v. 5.3 in demonstrating volume reductions in CA1 and CA4 using 3T MRI[21]. In the updated FreeSurfer v. 6.0 segmentation tool, volumes of subfields are closer to the histologically defined hippocampal subfields[25]. The authors urged further investigations with the use of histopathology from individual patients[21]. Peixoto-Santos et al. (2018) were not able to separate 22 HS ILAE type 1 patients from 6 HS ILAE type 2 patients using 3T MRI and FreeSurfer v. 6.0[22]. The authors used the subfield volumes of separate hemispheres instead of left-right asymmetry ratios, which could make data more susceptible to bias such as differences in intracranial volumes or scanner effects such as hemispheric inhomogeneities. Schoene-Bake et al (2014) did not use the HS ILAE

classification but demonstrated a significant positive correlation (r = 0.38, p = 0.004) between

neuronal density in CA1 and CA1 volume (3T MRI, FreeSurfer older version) in 51 patients with a

histopathological diagnosis of HS, but failed to demonstrate similar correlations for other subfields

of hippocampus[23].

We studied 51 epilepsy patients operated in the mesial temporal lobe and 52 healthy controls. For

image analysis we used 3T MRI and the updated automated hippocampal segmentation tool

implemented in FreeSurfer v. 6.0. For histopathological diagnosis we used the international

consensus classification of hippocampal sclerosis in temporal lobe epilepsy[10]. We hypothesize that

we will be able to separate groups with HS ILAE type 1 and 2 using high quality 3T MRI, the

updated automated hippocampal segmentation tool and a simple volume asymmetry ratio.

2.   Materials and methods

2.1   Patients

This is a retrospective study where we identified 203 TLE patients who underwent surgical

resection at Rigshospitalet in Denmark between January 2009 and October 2018. The Danish

Patient Safety Authority approved the study (case numbers 3-3013-1030/1 and 3-3013-3074/1).

A thorough and rigorous inclusion process led to exclusion of patients due to failed quality control

of MRI (n=89), bilateral pathology (n=4), other pathology hampering image segmentation (n=1), re-

operation within first year of follow-up (n=2), lesionectomies not including hippocampal tissue

(n=23), hampered hippocampal tissue preventing histological assessment (n=13), and clinically

significant segmentation errors (n=10) .

From the histopathological examination the remaining 60 TLE-patients were diagnosed with either

HS (n = 52) or non-HS (n = 8) (figure 1). The HS patients were further subdivided according to the international consensus classification of hippocampal sclerosis in temporal lobe epilepsy[10]. In eight patients, no HS ILAE classification was possible, due to fragmented tissue samples, and were therefore excluded. Only one patient was classified as HS ILAE type 3, and was excluded from group comparisons. This resulted in the following test groups: HS ILAE type 1 (n=25), HS ILAE type 2 (n=18) and non-HS (n=8).
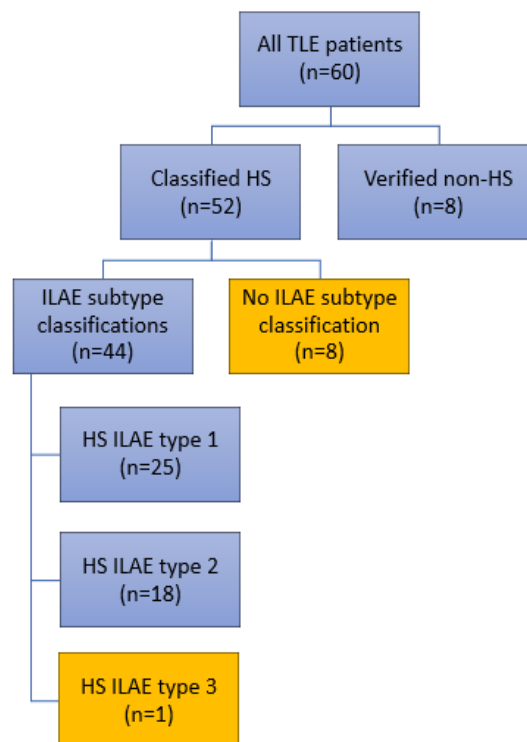
Figure 1: Overview of patients. Patients included after completion of MRI quality control (QC), hippocampal segmentation QC, and histopathological inclusion criteria. The orange boxes show patients excluded from group analysis. *TLE=temporal lobe epilepsy, HS=hippocampal sclerosis, ILAE=International League Against Epilepsy.*

2.2   Healthy controls

From the Center for Integrated Molecular Brain Imaging (CIMBI) database[24] we identified 59

healthy controls (HC) who were age- and sex-matched with the epilepsy patients, and scanned in a 3T Siemens scanner (see subsection 2.4) using both 3D T1 and 3D T2 sequences. All scans complied with quality control standards for segmentation using FreeSurfer, but seven subjects failed quality control of segmentation outputs. This resulted in n=52 HC for group comparisons.

2.3 Histopathology

The surgical specimen (hippocampus) was fixated in 10% buffered formalin for 12-24 hours. After macroscopic examination, the tissue was sectioned into 4-mm interval parallel slices according to coronal planes along an anterior-posterior axis. All slices were proceeded. Tissue blocks were post fixed, transferred to 10 % buffered formalin, dehydrated, and embedded in paraffin wax. Then the blocks were cut into 4 micrometer thick sections on a sledge microtome. After deparaffinizing, alternate sections were stained with hematoxylin and eosin (as in routine histology) or used for immunohistochemistry (NeuN, neuronal marker). The reagents used for immunostaining came from EnVision^{TM} FLEX+, High pH kit (K8012), Dako. Antigen retrieval was carried out at pH 9 for 20 minutes with a PT link module. Staining was done according to manufacture instructions: Sections were incubated with peroxidase for 5 minutes, mouse linker (K8022) for 15 minutes and then anti-NeuN (1:800, Millipore, MAB377) for 20 minutes. Antibody binding visualization was performed by incubation with a labelled HRP-polymer for 20 minutes and a signal as generated with a 3,3`-diaminobenzidine-tetrahydrochloride (DAB chromogene) for 10 minutes. Hematoxylin was used for counterstaining. Neuropathologists classified the patients with HS according to the international consensus classification of hippocampal sclerosis in temporal lobe epilepsy[10]. Figure 2 shows microscopic anatomy of patients categorized as HS ILAE type 1, HS ILAE type 2, and non-HS.
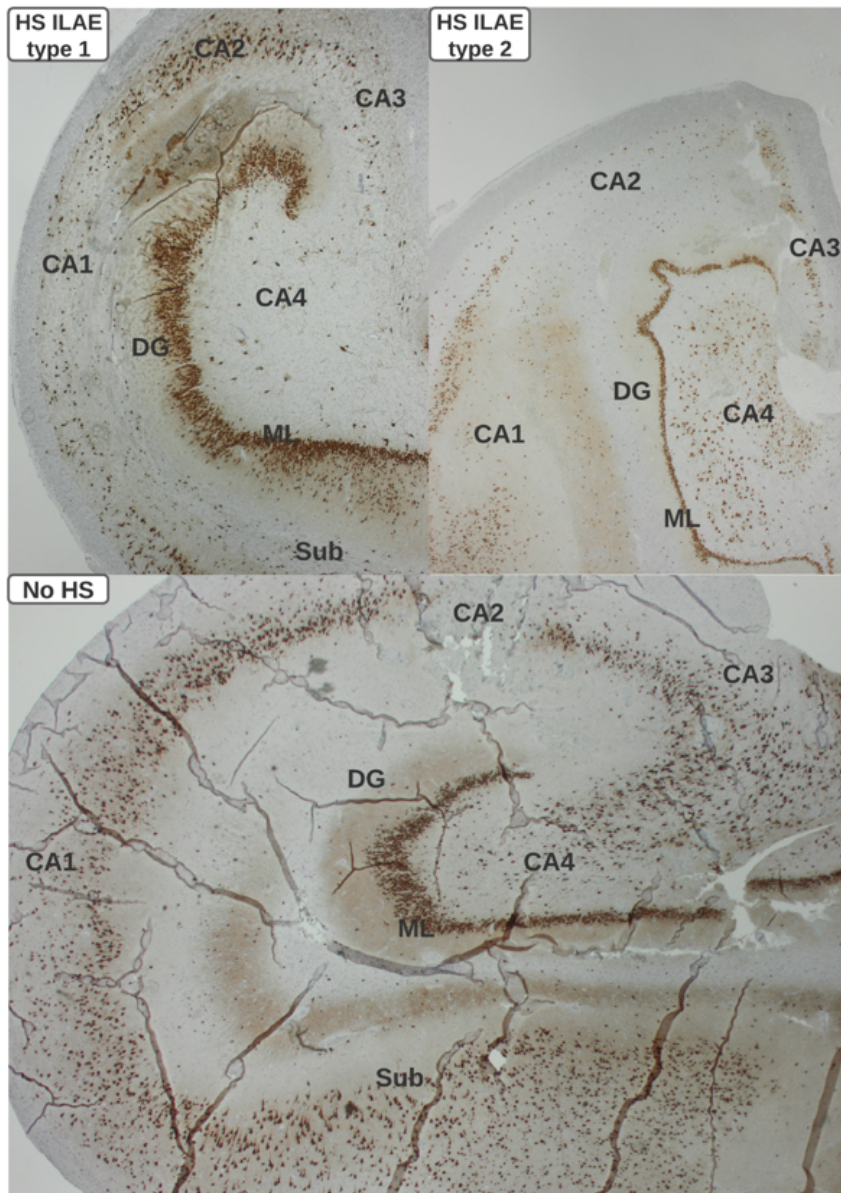
Figure 2: Microscopic anatomy of human hippocampi in three patients from the study with HS ILAE type 1, HS ILAE type 2 and no-HS. HS ILAE type 1 with severe neuronal cell loss in CA1 and CA4, HS ILAE type 2 with preferential cell loss in CA1 and relatively unaffected CA4, and non-HS with no significant cell loss in any subfields. CA2, CA3 and DG show variable but mild cell loss across HS ILAE subtypes 1 and 2. *CA=cornu ammonis, DG=dentate gyrus, ML=molecular layer, Sub=subiculum.*

2.4   MRI scan protocol

We used whole brain MRI sequences; 3D T1-weighted MPRAGE (magnetization-prepared rapid

acquisition gradient echo) with 1 mm isotropic acquisition resolution (acquisition time 5 min 32

sec, TI = 900 ms, TE = 2.23 ms, TR = 1900 ms, flip angle = 9 deg). Coronal 2D FSE (fast spin

echo) T2, perpendicular to hippocampi (acquisition resolution 0.5 x 0.4 x 3 mm, acquisition time: 3

min 50 sec, TE = 79 ms, TR = 6180 ms, flip angle = 120 deg). All patient MRI scans were acquired

in a Siemens Magnetom Verio 3T system with a 32-channel receive head coil. HC were scanned in

a Siemens Magnetom Prisma 3T system with a 64-channel receive head coil. All scans were

performed at Copenhagen University Hospital Hvidovre.

2.5   Data Analysis

Image processing was performed in the *FreeSurfer version 6.0[25]*, with the built-in cross-sectional

hippocampal subfield segmentation tool[26]. All hippocampal segmentations were performed with the

multispectral option of adding T2-weighted images as overlays to the T1-weighted images to

increase boundary tracing accuracy in the outer hippocampi as well as in subfields. All hippocampal

subfield segmentation outputs were visually quality assessed by the same observer. Hippocampal

volumes (whole-hippocampal (WH), CA1 and CA4) were exported for statistical analysis. An

example of segmentation outlines for the various subfields is seen in figure 3.
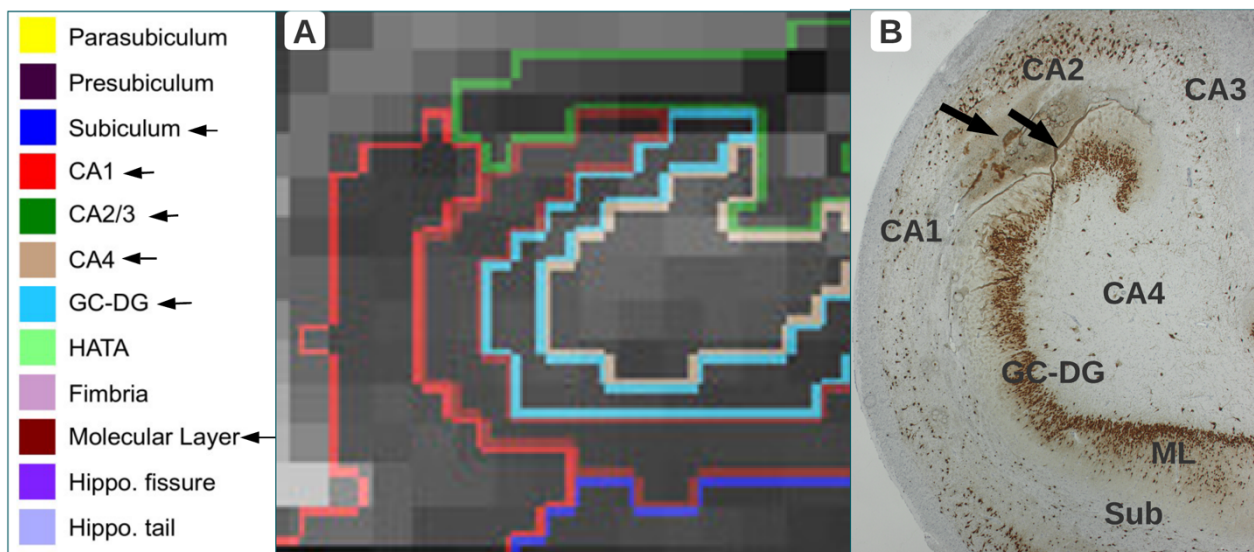
Figure 3: Example of subfield segmentation outlines (A) and corresponding microscopic anatomy in a HS ILAE type 1 patient (B). All 12 labels in the color legend comprise whole-hippocampal volumes, but not all are present in the cross-section of the hippocampal head in **(A)**. The colored outlines in **(A)** correspond to the subfields in the color legend to the left (also indicated with small arrows in the legend), and are enhanced for the purpose of demonstrating shape and approximate locations of subfield labels. Of note, these outlines represent discrete and non-continuous labels, but give a good notion of how the boundaries in individual subfields are separated. In the visual quality assessment of subfield segmentations, these outlines are viewed in 3D T1, with careful visualization across all MR slices covering the hippocampi. The hippocampal cross-section in A is from the coronal 2D T2 MR image, which is best suited for visualizing hippocampal layers. **(A)** does not represent the exact location of the microscopic image in **(B)** - each coronal 2D MRI slice thickness is 3 mm, which makes a one-to-one comparison infeasible. Black arrows in **(B)** indicate artefacts occurring during immunohistochemical staining.

Hippo=hippocampal, CA=cornu ammonis, DG=dentate gyrus, HATA=hippocampus-amygdala transfer area. ML=molecular layer, Sub=subiculum.

2.6   Statistical Analysis

For each subject, an absolute volume asymmetry ratio was calculated for all three hippocampal

regions (WH, CA1 and CA4), where the absolute difference between right and left field was

divided by the sum of both fields. The FreeSurfer subfield segmentation tool labels many regions of

interest (see figure 3), but to reduce the number of comparisons we chose WH, CA1 and CA4

before statistical analysis, since these regions determine the international consensus classification of

HS in temporal lobe epilepsy[10]. Significant atrophy suggestive of HS was defined as an asymmetry

ratio greater than approximately 99.3% of asymmetry ratios observed in the HC group (upper

whiskers in figure 4). This allowed for pooling of right- and left-sided TLE patients in all patient

groups. All patient subgroups were compared against each other as well as to HC. This was done

with a two-tailed Wilcoxon rank-sum test with Bonferroni correction for multiple comparisons, and

by visual inspection of asymmetry distributions. The significance threshold after Bonferroni

correction was $p<0.0083$. We also used Wilcoxon rank-sum test to test for differences between CA1

and CA4 within each group of HS ILAE type 1 and 2.

3.   Results

In table 1, we show mean and standard deviation values of VAR in WH, CA1 and CA4 for the three

categories of patients (HS ILAE type 1 (n = 25), HS ILAE type 2 (n = 18), non-HS (n = 8)) and

healthy controls (n = 52). There was a significant difference in VAR in WH, CA1 and CA4 for both

HS ILAE type 1 and type 2 compared to healthy controls and the non-HS group respectively (p-

values are listed in table 2). There was no significant difference in VAR in WH, CA1 and CA4

when comparing HS ILAE type 1 with HS ILAE type 2. There was no significant difference in

VAR in WH, CA1 and CA4 when comparing healthy controls with the non-HS group.

Table 1: Hippocampal volume asymmetry ratios (VAR) in patients and healthy controls.

HS=hippocampal sclerosis, HC=healthy controls, Std=standard deviations, WH=whole hippocampus, CA=cornu ammonis, ILAE=International League Against Epilepsy.

Volume asymmetry ratios	WH		CA1		CA4	
	mean	std	mean	std	mean	std
HS ILAE type 1	0.1431	0.0603	0.1588	0.0816	0.1876	0.0934
HS ILAE type 2	0.1538	0.0595	0.2026	0.0804	0.1840	0.0667
Non-HS	0.0295	0.0250	0.0408	0.0234	0.0374	0.0307
Healthy controls	0.0213	0.0169	0.0352	0.0332	0.0333	0.0240

Table 2: P-values from group comparisons with Bonferroni correction for multiple comparisons.

Significant differences after Bonferroni correction (p < 8.3e-03) are highlighted in light gray.

HS=hippocampal sclerosis, , HC=healthy controls, WH=whole hippocampus ,CA=cornu ammonis.

Group comparisons (p-values)	WH	CA1	CA4
HS ILAE type 1 vs. non-HS	1.21e-04	3.29e-04	2.79e-04
HS ILAE type 1 vs. HC	1.27e-11	1.23e-09	3.33e-10
HS ILAE type 1 vs. HS ILAE type 2	7.58e-01	1.24e-01	7.77e-01
HS ILAE type 2 vs. non-HS	8.98e-05	7.12e-05	7.12e-05
HS ILAE type 2 vs. HC	3.97e-10	1.01e-09	3.34e-10
HC vs. non-HS	4.80e-01	3.67e-01	9.91e-01

In figure 4 the data is graphically depicted as a box-plot. There were 23/25 HS ILAE type 1 and 18/18 HS ILAE type 2 patients who had WH VAR larger than 99.3% of WH volume asymmetries ratios observed in healthy controls (threshold = 0.048). Among HS ILAE type 1 patients 21/25 and among ILAE type 2 patients 18/18 patients had VAR larger than the upper limit (99.3%) of CA1 asymmetries in healthy controls (threshold = 0.067). 21/25 HS ILAE type 1 patients and 17/18 HS ILAE type 2 patients had VAR larger than the upper limit (99.3%) of CA4 asymmetries in healthy controls (threshold = 0.095).
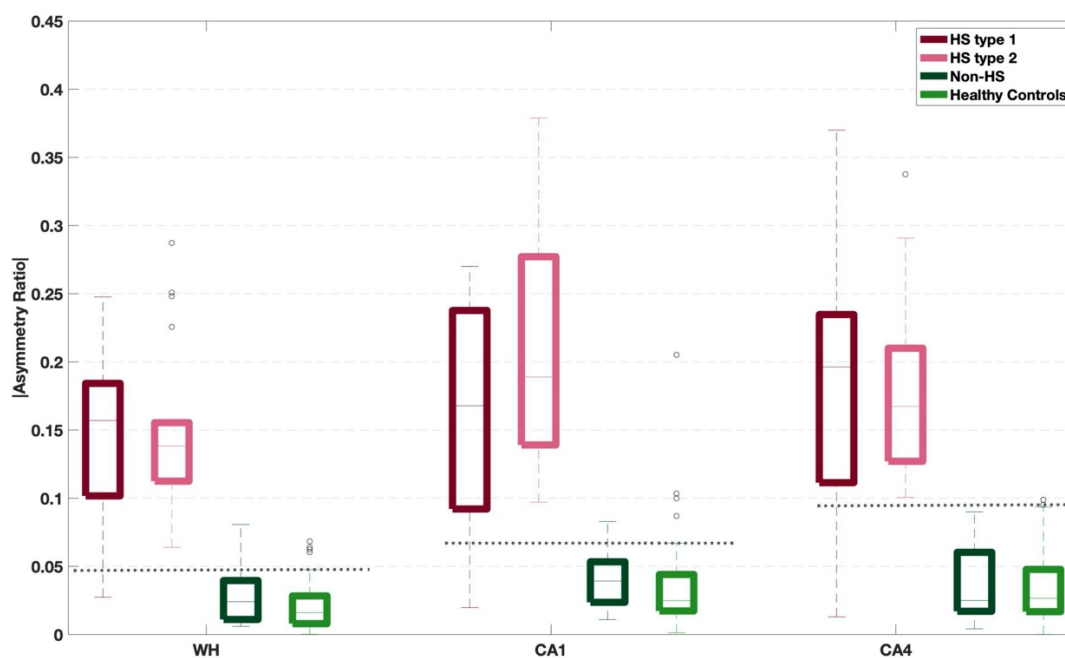
Figure 4*:* Boxplots displaying distributions of volume asymmetry ratios in all four groups across the three hippocampal regions. The four groups are HS ILAE type 1 (dark red) and HS ILAE type 2 (light red), non-HS patients (dark green) and healthy controls (light green). The three hippocampal regions are *WH = whole hippocampus, CA = cornu ammonis and HS = hippocampal sclerosis.* The dark grey dash lines show the thresholds for abnormal asymmetry ratio determined by VAR above 99.3% (the upper adjacent whisker) of those observed in the healthy controls.

We found no significant differences in CA1 VAR in HS ILAE type 1 versus HS ILAE type 2 patients (p=0.124), no significant differences in CA4 VAR in HS ILAE type 1 versus HS ILAE type 2 patients (p=0.777), and no significant differences in WH VAR between HS ILAE type 1 and HS ILAE type 2 patients (p=0.758). Mean and standard deviations are found in table 2. When testing within each HS ILAE subtype group, we found no significant differences between CA1 and CA4 VAR in HS ILAE type 1 (p= 0.3224) and in HS ILAE type 2 patients (p= 0.5166).

4.   Discussions

Evaluating drug-resistant epilepsy patients for epilepsy surgery is a highly complex multi-modal and interdisciplinary process and most likely among the most complex in clinical practice. The aim is to collect and integrate data to identify the minimum amount of cortex that will render the patient seizure free after surgery, and to empower the clinician to inform patients and relatives about potential benefits and harms in relation to surgery. In 2013, a task force from ILAE reported a new international consensus classification of hippocampal sclerosis based on semiquantitative hippocampal cell loss in particular in CA1 and CA4, with the aim of improving prediction of postsurgical outcome[10]. Subsequently, several groups reported that histopathological subgroups correlated to postoperative seizure outcomes[11,20] and memory impairment[18,19]. However, histopathological classification is labor-intensive and complicated, even in the hands of experienced neuropathologists[10]. Furthermore, the access to suitable en-bloc resections for histopathological subclassification are likely to decrease in the years to come with the implementation of minimal invasive surgery techniques such as stereotactic laser amygdalohippocampectomy for mesial TLE[27,28]. Thus, in this study we evaluated whether it is possible to use presurgical high-quality 3T MRI, the updated automated hippocampal segmentation tool implemented in FreeSurfer v. 6.0., and

a simple volume asymmetry ratio to separately identify groups histopathologically classified as HS ILAE type 1 and HS ILAE type 2, respectively. Our results show that we definitely are able to separate almost all patients with HS from TLE-patients with histopathologically normal appearing hippocampus (non-HS patient group) and healthy controls, but we were unable to separately identify patients with HS ILAE type 1 from patients with HS ILAE type 2. Especially, it is depicted clearly in figure 4 that contrary to expectations, the CA4 VAR in HS ILAE type 2 patients was significantly larger than in healthy controls and non-HS patients, and not significantly different from HS ILAE type 1 patients.

There may be several factors contributing to the failure of automatic hippocampal segmentation to identify specific patterns of volume loss in CA1 and CA4 concordant with histopathological diagnosis:

i)   Histopathological classification:

The fact that qualitative histopathological assessments are prone to both interobserver and intraobserver variability is well-known by neuropathologists and explicitly addressed in the original consensus article by Blümcke et al. (2013)[10]. The ILAE HS classification is non-categorical, where the degree of neuronal cell loss observed in different subtypes presents with certain overlap: a combination of *>80%* neuronal loss in CA1 and *40-90%* neuronal loss in CA4 defines HS ILAE type 1, whereas in HS ILAE type 2 the neuronal loss is *almost* 80% in CA1 in combination with *mild cell loss barely visible* in CA4. The fact that the first detectable neuronal loss in Hematoxylin and Eosin (H&E) stains corresponds to approximately 30-40% cell loss[10] is likely to contribute to uncertainties in histopathological subclassification and is definitely important to keep in mind when interpreting the results of this study: in H&E stains *A mild cell loss barely visible* in CA4 may correspond to a 40-50% neuronal loss. A cell loss of this magnitude will most likely result in CA4

VARs in HS ILAE type 2 patients definitely larger than non-HS patients and healthy controls, and in some patients similar to CA4 VAR in HS ILAE type 1 patients (*40-90% neuronal loss*). Variability of histopathological changes in subfields along the long axis of the hippocampus has also been demonstrated[28]. Thus, it is emphasized in the consensus article that classification requires en-bloc resected hippocampal tissue and complete anatomic representation of all subfields[10]. In our study we excluded patients where the hippocampal tissue did not include both CA1 and CA4, however, sometimes hippocampal where not delivered en bloc for histopathological examination often since part of the tissue where used for scientific purposes. The tissue could be fragmented, damaged and difficult to orient when cutting slices in the microtome. In our study, HS ILAE type 1 was diagnosed in 25/44 patients (56 %), which is lower than the 60-80 % of HS patients reported in the literature[10,29]. Contrarily, 18/44 (41 %) of HS patients were classified as HS ILAE type 2, which is far higher than the 5-10 % expected from the literature[10,29] . This could imply that some of our patients were histopathologically misclassified.

ii)   <u>FreeSurfer hippocampal subfield classification:</u>

Peixoto-Santos et al. (2018) initially studied 22 HS ILAE type 1 patients and two HS ILAE type 2 patients using 3T MRI and FreeSurfer v. 6.0[22]. Despite the relative distribution of HS ILAE type 1 and HS ILAE type 2 in this study being in line with literature values, the authors were likewise not able to separate HS ILAE type 1 patients from HS ILAE type 2 patients; a result that was unchanged after adding additional four HS ILAE type 2 patients to the study material. Interestingly, the authors subsequently did ex vivo imaging of the hippocampal body in the same 3T MR scanner as the presurgical MRI. Contrarily, it was possible to separate HS ILAE type 1 patients from HS ILAE type 2 patients using the ex vivo high resolution 3T MRIs and manual delineations of hippocampal subfields. This could imply that some of our HS patients are misclassified when using the automated delineation of hippocampal subfields in vivo in 3T presurgical MRIs. An explanation

could be that the probability atlas that the subfield segmentation algorithm is trained on, is based upon manual delineations from ex vivo and in vivo scans from ten healthy and four demented subjects, as well as one subjects with mild cognitive impairment[26]. While these subjects are displaying some volume reduction due to age and dementia, the a priori information may not be applicable to epilepsy and HS patients, where the reduction in subfield volumes will be severe and often quite segmental – not respecting anatomical borders between hippocampal subfields in the longitudinal direction[29]. This would lead to overestimations of all subfields as a consequence of any volume reduction in the WH region, as the information from the probability atlas means it is more likely that the subfields are reduced proportionally relative to WH volumes (as they would due to age), while they in fact are disproportionally reduced in HS. As a consequence, the segmentation is highly sensitive to volume reduction, but without the specificity to detect the variations in subfield volumes. This could be tested in a group of HS ILAE type 3 patients (predominant neuronal loss in CA4) and falsified if CA1 VAR is significantly lower than CA1 VARs in HS ILAE type 1 and 2.

iii)   <u>Neuronal loss at microscopic examination does not translate into volume loss in MRI</u>
Several studies in epilepsy patients have demonstrated significant positive correlations between subfield volume on MRI and neuronal density based upon counting neurons in histoanatomical images representative for each subfield: Schoene-Bake et al (2014) demonstrated a significant positive correlation in CA1 ($r = 0.38$, $p = 0.004$) but not in CA4[23]. The authors used an older version than FreeSurfer v. 6.0. Peixoto-Santos et al. (2018) used FreeSurfer v. 6.0 and demonstrated a significant positive correlation in both CA1 ($r = 0.658$, $p < 0.0019$) and CA4 ($r = 0.461$, $p = 0.010$)[22]. Despite demonstrating significant correlations between subfield volume on MRI and neuronal density, it is also clear from regression fits that only a smaller proportion of the variation in CA1/CA4 volume is actually attributed to the CA1/CA4 neuronal density, which will hamper the

use of CA1/CA4 volume as a proxy for CA1/CA4 neuronal density in the individual patient. In that context it is noteworthy that Peixoto-Santos et al. (2018) were unable to separate 22 HS ILAE type 1 patients from 6 HS ILAE type 2 patients[22].

In our study, we looked carefully at the four HS ILAE type 1 patients with CA1 and CA4 VAR within the normal range (defined by the upper whiskers of the healthy controls, see figure 4). All patients were classified as HS ILAE type 1. From the expert neuroradiological description, one patient had contralesional incomplete inverted hippocampus which may hamper automatic delineation of hippocampal subfields. One patient had central areas in the anterior part of hippocampus with increased volume and other peripheral areas with reduced volume, and two patients had normal hippocampal volume but increased T2 signal intensity. Depicted in figure 5 is histopathology and MRI in one of these two patients with normal hippocampal volume. The histopathological image (figure 5A) is rather poor in quality, but shows a clear reduction in neuronal cells in CA1 and CA4. Marked astrogliosis in Glial fibrillary acidic protein (GFAB) stains was also demonstrated. In the MRI part of figure 5 (C, B, D) both labelled and unlabelled MR images are shown. Subfield segmentations look correctly placed and with similar volumes on both sides. Thus, discrepancy between neuronal density demonstrated in H&E stains and volume demonstrated in MRI may be related to a reduction in neuronal cells being counteracted by concurrent astrogliosis and leaving the tissue volume relatively unaffected, and, as discussed in section **i)** above, contrary to MRI - the poor sensitivity of H&E stains to detect neuronal loss below 30-40% of normal values.
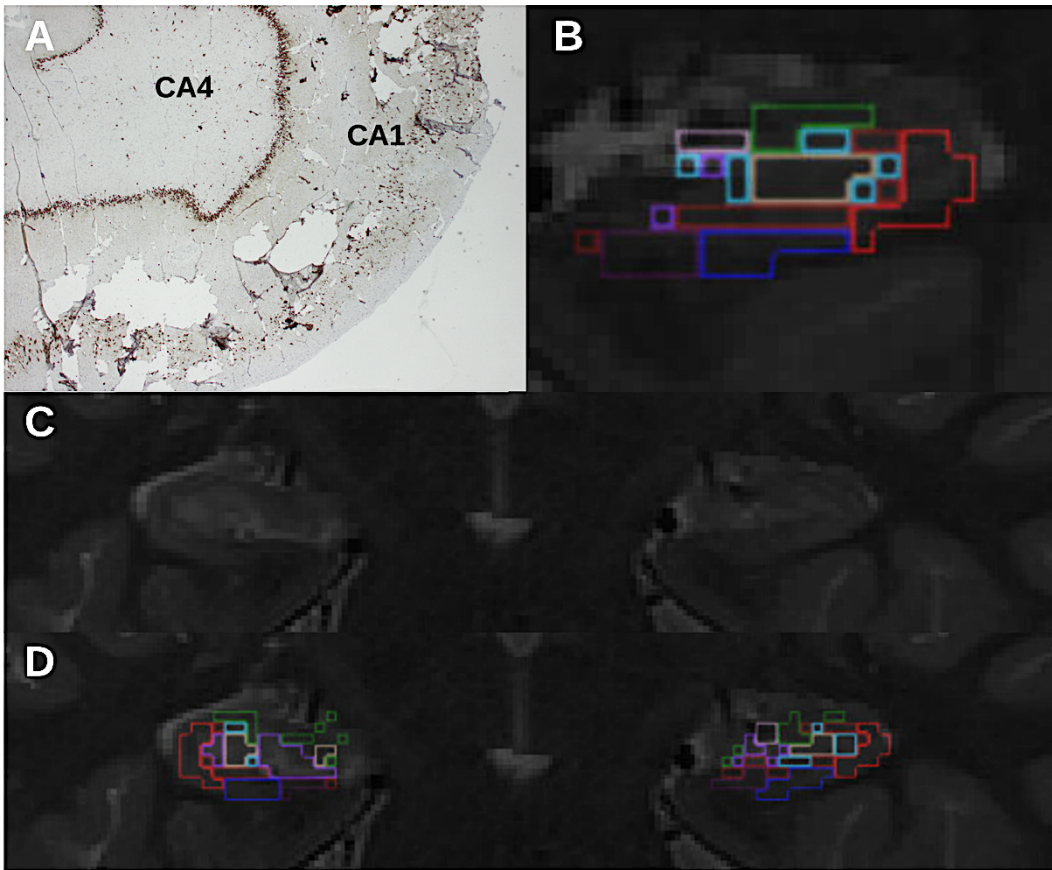
Figure 5: Histopathology and MR images of hippocampus in a HS ILAE type 1 outlier. The sectional microscopy image from the stained hippocampal specimen in **A** clearly depicts neuronal loss in CA1 and CA4. The bright red and beige colored outlines in **B** and **D** correspond to the CA1 and CA4 segments, respectively. The hippocampal cross-section in **B**, **C** and **D** are from the coronal 2D T2 MR image, in a place of the hippocampal proper that was resected, and thus represent the approximately same areas as the thin-sliced hippocampal specimens. *CA=cornu ammonis.*

4.1 Limitations

Though, the current study is the largest study so far to test how hippocampal subfield VAR compare to the expected pattern from the histopathological examination using the ILAE consensus classification of HS we planned the study to be larger by including patients from the Norwegian

epilepsy surgery program. This collaboration was put on hold in relation to the COVID-19 pandemic. A larger data set would allow us to better discriminate and understand the relative contribution of the three main factors possibly causing the failure of automatic hippocampal segmentation to identify specific patterns of volume loss in CA1 and CA4 concordant the HS ILAE subtypes. A larger data set are likely to result in more patients with HS ILAE type 3 than in our material.

4.2 Future perspectives

In a larger data set it would be of immense interest directly test the use of MRI against histopathological classification for predicting seizure outcome, psychiatric and cognitive dysfunction in TLE patients. In addition, MRI is not restricted to the analysis of hippocampus but allows for analyzing large scale networks and the interaction between hippocampus and adjacent and remote neocortical volumes. Finally, the use of ultra-high field MRI at 7T may improve the delineation of hippocampal subfields in the direction of result obtained with ex vivo MRI as described above.

5. Conclusions

In this study in 52 patients with mesial TLE and 52 healthy controls we show that a simple volume asymmetry ratio generated by automated hippocampal subfield segmentation in *FreeSurfer* v.6.0 from the presurgical MRIs is an excellent marker of the histopathological diagnosis of HS. Segmentation of hippocampal subfields generated results that imply more widespread and less subfield specific VAR than expected from the HS ILAE histopathological subclassification.

Acknowledgements

Competing interests

None of the authors declare any competing interests.

References:

1. Christensen J, Vestergaard M, Pedersen MG, Pedersen CB, Olsen J, Sidenius P. Incidence and prevalence of epilepsy in Denmark. *Epilepsy Res*. 2007;76(1):60-65. doi:10.1016/j.eplepsyres.2007.06.012

2. Thijs RD, Surges R, O'Brien TJ, Sander JW. Epilepsy in adults. *Lancet*. 2019;393(10172):689-701. doi:10.1016/S0140-6736(18)32596-0

3. Chen Z, Brodie MJ, Liew D, Kwan P. Treatment outcomes in patients with newly diagnosed epilepsy treated with established and new antiepileptic drugs a 30-year longitudinal cohort study. *JAMA Neurol*. 2018;75(3):279-286. doi:10.1001/jamaneurol.2017.3949

4. Shukla G, Prasad AN. Natural History of Temporal Lobe Epilepsy: Antecedents and Progression. *Epilepsy Res Treat*. 2012;2012:1-8. doi:10.1155/2012/195073

5. Wiebe S, Jette N. Pharmacoresistance and the role of surgery in difficult to treat epilepsy. *Nat*

Rev Neurol. 2012;8(12):669-677. doi:10.1038/nrneurol.2012.181

6. Ryvlin P, Cross JH, Rheims S. Epilepsy surgery in children and adults. *Lancet Neurol*. 2014;13(11):1114-1126. doi:10.1016/S1474-4422(14)70156-5

7. West S, Nolan SJ, Cotton J, et al. Surgery for epilepsy. *Cochrane Database Syst Rev*. 2015;(3). doi:10.1002/14651858.CD010541.pub2

8. Spencer S, Huh L. Outcomes of epilepsy surgery in adults and children. *Lancet Neurol*. 2008;7(6):525-537. doi:10.1016/S1474-4422(08)70109-1

9. Blümcke I, Mrcpath MT, Wiestler D. Blümcke, Mrcpath, Wiestler_Ammon ' s Horn Sclerosis A Maldevelopmental Disorder Associated with Temporal Lobe Epilepsy.pdf. 2002;1.

10. Blümcke I, Thom M, Aronica E, et al. International consensus classification of hippocampal sclerosis in temporal lobe epilepsy: A Task Force report from the ILAE Commission on Diagnostic Methods. *Epilepsia*. 2013;54(7):1315-1329. doi:10.1111/epi.12220

11. Kreilkamp BAK, Weber B, Elkommos SB, Richardson MP, Keller SS. Hippocampal subfield segmentation in temporal lobe epilepsy: Relation to outcomes. *Acta Neurol Scand*. 2018;137(6):598-608. doi:10.1111/ane.12926

12. Bernasconi A, Cendes F, Theodore WH, et al. Recommendations for the use of structural magnetic resonance imaging in the care of patients with epilepsy: A consensus report from the International League Against Epilepsy Neuroimaging Task Force. *Epilepsia*. 2019;60(6):1054-1068. doi:10.1111/epi.15612

13. Malmgren K, Thom M. Hippocampal sclerosis-Origins and imaging. *Epilepsia*. 2012;53(SUPPL. 4):19-33. doi:10.1111/j.1528-1167.2012.03610.x

14. Jackson, G. D., Berkovic, S. F., Tress, B. M., Kalnins, R. M., Fabinyi, G. C. A., & Bladin, P. F. (1990). Hippocampal sclerosis can be reliably detected by magnetic resonance imaging. *Neurology*, *40*(12), 1869-1869.

15. Van Paesschen W, Revesz T, Duncan JS, King MD, Connelly A. Quantitative neuropathology and quantitative magnetic resonance imaging of the hippocampus in temporal lobe epilepsy. *Ann Neurol*. 1997;42(5):756-766. doi:10.1002/ana.410420512

16. Van Paesschen W, Sisodiya S, Connelly A, et al. Quantitative hippocampal MRI and intractable temporal lobe epilepsy. *Neurology*. 2001;57(11 SUPPL. 4).

17. Van Strien, Niels M., et al. "Imaging hippocampal subregions with in vivo MRI: advances and limitations." *Nature Reviews Neuroscience* 13.1 (2012): 70-70.

18. Comper, Sandra Mara, et al. "Impact of hippocampal subfield histopathology in episodic memory impairment in mesial temporal lobe epilepsy and hippocampal sclerosis." *Epilepsy & Behavior* 75 (2017): 183-189.

19. Coras, Roland, et al. "Differential influence of hippocampal subfields to memory formation: insights from patients with temporal lobe epilepsy." *Brain* 137.7 (2014): 1945-1957.

20. Jardim, Anaclara Prada, et al. "Hippocampal atrophy on MRI is predictive of histopathological patterns and surgical prognosis in mesial temporal lobe epilepsy with hippocampal sclerosis." *Epilepsy Research* 128 (2016): 169-175.

21. Sone, Daichi, et al. "Automated subfield volumetric analysis of hippocampus in temporal lobe epilepsy using high-resolution T2-weighed MR imaging." *NeuroImage: Clinical* 12 (2016): 57-64.

22. Peixoto-Santos JE, De Carvalho LED, Kandratavicius L, et al. Manual hippocampal subfield segmentation using high -field MRI: Impact of different subfields in hippocampal volume loss of temporal lobe epilepsy patients. *Front Neurol*. 2018;9(NOV):1-12. doi:10.3389/fneur.2018.00927

23. Schoene-Bake JC, Keller SS, Niehusmann P, et al. In vivo mapping of hippocampal subfields in mesial temporal lobe epilepsy: Relation to histopathology. *Hum Brain Mapp*.

2014;35(9):4718-4728. doi:10.1002/hbm.22506

24. Knudsen GM, Jensen PS, Erritzoe D, et al. The Center for Integrated Molecular Brain Imaging (Cimbi) database. *Neuroimage*. 2016;124:1213-1219. doi:10.1016/j.neuroimage.2015.04.025

25. Fischl B. FreeSurfer Authos Manuscript. *Neuroimage*. 2012;62(2):774-781. doi:10.1016/j.neuroimage.2012.01.021.FreeSurfer

26. Iglesias JE, Augustinack JC, Nguyen K, et al. A computational atlas of the hippocampal formation using ex vivo, ultra-high resolution MRI: Application to adaptive segmentation of in vivo MRI. *Neuroimage*. 2015;115:117-137. doi:10.1016/j.neuroimage.2015.04.042

27. Gross, R. E., et.al. Stereotactic laser amygdalohippocampectomy for mesial temporal lobe epilepsy. *Annals of neurology*, (2018); *83*(3), 575-587.

28. Donos C, Breier J, Friedman E, Rollo P, Johnson J, Moss L, et al. Laser ablation for mesial temporal lobe epilepsy: Surgical and cognitive outcomes with and without mesial temporal sclerosis. Epilepsia. 2018;59(7):1421-32.

29. Thom M. Review: Hippocampal sclerosis in epilepsy: A neuropathology review. *Neuropathol Appl Neurobiol*. 2014;40(5):520-543. doi:10.1111/nan.12150

A.1.1 Co-author declarations Article 1

UNIVERSITY OF COPENHAGEN
FACULTY OF HEALTH AND MEDICAL SCIENCES

DECLARATION OF CO-AUTHORSHIP

The declaration is for PhD students and must be completed for each conjointly authored article. Please note that if a manuscript or published paper has ten or less co-authors, all co-authors must sign the declaration of co-authorship. If it has more than ten co-authors, declarations of co-authorship from the corresponding author(s), the senior author and the principal supervisor (if relevant) are a minimum requirement.

1. Declaration by	
Name of PhD student	Giske F. Opheim
E-mail	giskeopheim@nru.dk
Name of principal supervisor	Lars H.Pinborg
Title of the PhD thesis	Utilizing 7 Tesla MRI and automated segmentation– A new era in

2. The declaration applies to the following article	
Title of article	Automated hippocampal segmentations in histopathologically classified HS ILAE type 1 and 2

Article status

Published ☐ Date:	Accepted for publication ☐ Date:
Manuscript submitted ☐ Date:	Manuscript not submitted ☒
If the article is published or accepted for publication, please state the name of journal, year, volume, page and DOI (if you have the information).	

3. The PhD student's contribution to the article *(please use the scale A-F as benchmark)* Benchmark scale of the PhD-student's contribution to the article **A**. Has essentially done all the work (> 90 %) **B**. Has done most of the work (60-90 %) **C**. Has contributed considerably (30-60 %) **D.** Has contributed (10-30 %) **E.** No or little contribution (<10 %) **F.** Not relevant	A, B, C, D, E, F
1. Formulation/identification of the scientific problem	C
2. Development of the key methods	F
3. Planning of the experiments and methodology design and development	C
4. Conducting the experimental work/clinical studies/data collection/obtaining access to data	C

1

3. The PhD student's contribution to the article *(please use the scale A-F as benchmark)*	A, B, C, D, E, F
Benchmark scale of the PhD-student's contribution to the article **A**. Has essentially done all the work (> 90 %) **B**. Has done most of the work (60-90 %) **C**. Has contributed considerably (30-60 %) **D.** Has contributed (10-30 %) **E.** No or little contribution (<10 %) **F.** Not relevant	
5. Conducting the analysis of data	B
6. Interpretation of the results	C
7. Writing of the first draft of the manuscript	C
8. Finalisation of the manuscript and submission	C

Provide a short description of the PhD student´s specific contribution to the article.[i]

The PhD student has co-supervised the master student (Ane Kloster, now MD) during the project work, and participated in all stages from conceptualization to finalization of manuscript draft. The PhD student has also conducted additional analyses of data from Norwegian collaborator during her mandatory external research stay, and collaborated closely with Dr Ane Kloster and main supervisor Lars H. Pinborg.

---

4. Material from another thesis / dissertation[ii]	
Does the article contain work which has also formed part of another thesis, e.g. master's thesis, PhD thesis or doctoral dissertation (the PhD student's or another person's)?	Yes: ■ No: ☐
If yes, please state name of the author and title of thesis / dissertation.	"The clinical value of automated volume-based analysis of MR images before epilepsy surgery in the temporal lobe", Master Thesis, by Ane Kloster
If the article is part of another author's academic degree, please describe the PhD student´s and the author´s contributions to the article so that the individual contributions are clearly distinguishable from one another.	Ane Kloster has collected the vast majority of data. The PhD student has conducted all data analyses and produced figures and data for tables. The PhD student and Ane Kloster have finalized the manuscript together.

---

5. Signatures of the co-authors[iii]				
	Date	Name	Title	Signature
1.	7/11 -2020	Lars H. Pinborg	MD,Assoc Professor	
2.	7/11 -2020	Ane Kloster	MD	

5. Signatures of the co-authors[iii]

3.				
4.				
5.				
6.				
7.				
8.				
9.				
10.				

6. Signature of the principal supervisor

I solemnly declare that the information provided in this declaration is accurate to the best of my knowledge.

Date: 2020-11-07

Principal supervisor: Lars H. Pinborg

7. Signature of the PhD student

I solemnly declare that the information provided in this declaration is accurate to the best of my knowledge.

Date: 2020-11-07

PhD student: Giske F. Pinborg

Please learn more about responsible conduct of research on the Faculty of Health and Medical Sciences' website.

---

[i] This can be supplemented with an additional letter if needed.

[ii] Please see Ministerial Order on the PhD Programme at the Universities and Certain Higher Artistic Educational Institutions (PhD Order) § 12 (4):

3

"Any articles included in the thesis may be written in cooperation with others, provided that each of the co-authors submits a written declaration stating the PhD student's or the author's contribution to the work."

[iii] If more signatures are needed please add an extra sheet.

A.2 Article 2

Giske Opheim, Erik B. Dam, Oula Puonti, Ane Kloster, Martin Prener, Raghaven-dra Selvan, Minna H. Litman, Helle J. Simonsen, Olaf B. Paulson, Lars H. Pinborg, Melanie Ganz, *"Exploring radiomic features in clinical 3T and 7T MRI of mesial temporal sclerosis in an open presurgical patient cohort."*, 2020, **In prep.**

Title: Exploring radiomic features in clinical 3T and 7T MRI of mesial temporal sclerosis in an open presurgical patient cohort.

Running title: Quantitative 7T and 3T MRI features in MTS

Authors: Giske Opheim[1,2], Erik B. Dam[3], Oula Puonti[4,5], Ane Kloster[1,2], Martin Prener[1,2], Raghavendra Selvan[3], Minna H. Litman[1], Helle J. Simonsen[6], Olaf B. Paulson[1,2], Lars H. Pinborg[1,2], Melanie Ganz[1,3]

Affiliations: [1] Neurobiology Research Unit, Copenhagen University Hospital Rigshospitalet, Denmark; [2] Faculty of Health and Medical Sciences, University of Copenhagen, Denmark; [3]Department of Computer Science, University of Copenhagen, Denmark; [4]Danish Research Centre for Magnetic Resonance, Centre for Functional and Diagnostic Imaging and Research, Copenhagen University Hospital Hvidovre, Denmark; [5] Department of Health Technology, Technical University of Denmark, Kgs. Lyngby, Denmark, [6] Functional Imaging Unit, Dept. of Clinical Physiology, Nuclear Medicine and PET, Rigshospitalet, Copenhagen University Hospital

Corresponding author: Giske Opheim

                                             Rigshospitalet, Unit 8057

                                             Blegdamsvej 9, 2100 Copenhagen, Denmark

                                             email: giskeopheim@nru.dk

                                             Telephone: +45 42303710

ORCID: Giske Opheim, 0000-0002-1516-0838

                        Lars H. Pinborg, 0000-0001-9024-7936

                        Melanie Ganz, 0000-0002-9120-8098

Key words: epilepsy surgery, hippocampus, post-processing, 7T MRI, clinical MRI

No. of text pages: 24 (page 1-24, including references, figures and tables)

No. of tables: 2

No. of figures: 3

Summary

To compare quantitative measures of hippocampal volume, intensity, and texture changes in ultra-high-field magnetic resonance imaging (MRI) at 7 Tesla (7T) versus MRI at 3 Tesla (3T) between patients with mesial temporal sclerosis (MTS) and other patients in an ongoing presurgical evaluation cohort.

MRI at 3T and 7T were acquired in 48 patients. All patients were divided according to radiological diagnosis (MTS=15, non-MTS=33). T1-weighted and T2-weighted MRIs were analyzed in FreeSurfer (FS) v. 6.0 with the hippocampal subfield segmentation tool. Whole-hippocampal, cornu ammonis (CA) 1, CA2/3, CA4 and granular-cell dentate gyrus (GC-DG) segments were exported for further image processing. We calculated absolute asymmetry ratios and used Wilcoxon rank-sum test with Bonferroni correction for multiple comparisons to test for group differences (MTS vs non-MTS) in mean, standard deviation, and entropy (a texture measure) of T2 signal intensity, and volume.

Group differences in MTS versus non-MTS patients were statistically significant for volume and entropy, for both 3T and 7T MRI. For the mean and standard deviations of T2 signal intensity values, only CA4 in 7T data showed a significant group difference.

By comparing MTS and non-MTS patient groups with descriptive statistics, our findings demonstrated similar discriminative ability of 7T and 3T MRI. This is valuable information for decisions on what MRI modality to refer presurgical patients to, particularly when planning to include automated hippocampal MRI segmentations as add-on quantitative information for surgical decision support.

1 Introduction

In drug-resistant focal epilepsy, identification and surgical removal of the epileptogenic zone is the only treatment offering seizure freedom[1]. During the complex presurgical evaluation, a visually confirmed epileptogenic lesion on the magnetic resonance images (MRIs) remains one of the most important preoperative predictors of seizure freedom[2].

In attempts to aid the localization process, the focus on magnetic resonance imaging (MRI) biomarkers of mesial temporal sclerosis (MTS) has gained interest in the last couple of decades[4-8]. In MTS with a sclerotic hippocampus, the radiological diagnosis depends on two hallmark signs: atrophy and either T2 or fluid-attenuation inversion-recovery (FLAIR) hyperintensities on the affected side[5]. For MTS diagnosis, it is therefore of particular interest to automatically compute asymmetries of volumes and signal intensities[4,6,7-10], in efforts to further support presurgical decision-making, precisely inform patients about chances of seizure freedom/reduction after surgery, or to automatize radiological workflow. Such analyses may help radiologists categorize the MRIs prior to visual assessment with automatic sorting of patients, and become increasingly relevant for individual patients where clinical investigations point to diverging hypotheses of seizure origin and/or visual assessment is inconclusive. For these reasons, post-processing of MRIs is pointed out as an emerging concept in presurgical evaluation[11].

Previous work includes employing automated segmentation and correlate outputs with radiological diagnosis, manual segmentations, and/or histological verifications on ex vivo data[3-10,12-18]. Some studies suggested an improved accuracy of manual and automated segmentations in high-resolution MRIs from 7T when compared to MRIs from conventional, clinical field strengths, though they are performed in low sample sizes and it is unclear how the results differ from 3T[12-18]. Of importance,

25 further segmentation of hippocampal subfields is of interest since different patterns of subfield

26 atrophy correlate with different surgery outcomes[19] and memory impairment[20]. Visual evaluation

27 and manual segmentations of subfields are infeasible to obtain as part of clinical workflow based on

28 in vivo MRI scans. Furthermore, there is potential clinical value in quantitative signal intensity and

29 texture information; attributes that are difficult to assess with the human eye, both in clear MTS

30 cases and when volumetric asymmetry at WH level is inconclusive[21,22].

31

32 Algorithms for MTS detection make use of several radiomic features from post-processing of 1.5 or

33 3T MRI along with other clinical investigations are well-studied[23-26]. Still, there are limitations that

34 any epilepsy surgery center might encounter when implementing these computational approaches:

35 Clinical datasets may not match the data employed in the literature studies, which would prevent

36 algorithms from reaching an automated detection accuracy high enough to be of diagnostic value.

37 Additionally, many centers will not have access to large retrospective datasets, and will inherently

38 lack a subset of "ground truths" such as histopathological verifications in an open, ongoing cohort

39 such as presented here.

40

41 Hence, as MRI will often be the first modality at hand in the starting phase of presurgical

42 evaluation, it is prudent to focus on evaluating the stand-alone radiomic MRI features further. It is

43 relevant to validate how well these quantitative MRI features discriminate clear cases of MTS from

44 non-MTS, since this information may reflect strengths and weaknesses of the MRI acquisitions.

45 Furthermore, it may be relevant to consider referral to 7T MRI whenever radiological assessment of

46 hippocampus is targeted together with post-processing. But it is still unclear whether automated

47 hippocampal segmentations from 7T MRI are superior at discriminating between known MTS and

48 suspected non-MTS in a side-by-side comparison with 3T MRI. Our objective was to explore

49   radiomic MRI features in the hippocampi of a group of radiologically diagnosed MTS patients, and

50   compare findings in clinical 3T and 7T MRIs. Given previous study results, we hypothesized that

51   7T MRI offers better group discrimination of volume, T2 signal intensity, and texture changes

52   compared to 3T MRI.

53

54   2 Methods

55   The project was approved by the Ethics Committee of the Capital Region of Copenhagen Denmark

56   (H-2-2013-038), and all patients signed consent forms prior to scanning. Further, as the 7T scanner

57   is not CE-marked the study was also approved by the Danish Medicines Agency (2016101738,

58   2017081122).

59

60   2.1 Patient population

61   Patients (n=68) with drug-resistant epilepsy were referred from the presurgical evaluation team at

62   Rigshospitalet, Copenhagen, Denmark (see *figure 1*), between November 2017 and January 2020.

63   Of these, 12 were excluded due to tattoos (n=10) or implants (n=2) within a 30 cm distance from

64   the coil, according to local 7T MRI safety regulations. This and other exclusion steps are given in

65   *figure 1,* which shows that additional eight patients were excluded. Of the remaining 48 patients, 15

66   were radiologically diagnosed with mesial temporal sclerosis (MTS) based on 3T MRIs. The

67   diagnoses were performed by a neuroradiologists specialized within epilepsy diagnostics on MRI,

68   with more than 15 years of experience. The 33 non-MTS patients had: normal appearing 3T MRI

69   (n=19), other suspected hippocampal pathology (n=1, dysplasia), suspected focal extra-

70   hippocampal dysplasia (n=5), polymicrogyria (n=2), nodular heterotopias (n=2), gangliogliomas

71   (n=2) and other cysts (n=2). Age-span was 12-78 years (mean: 35.5 std: 16.0), whereof 30 were

72   males.

68 patients referred from presurgical evaluation

1 excluded (dropped out)

12 excluded (safety screening)

3T + 7T MRI of 55 patients

2 excluded: 1 7T scan with poor quality + 1 large ventricles

5 excluded (faulty segments)

Mesial Temporal Sclerosis (n=15)

Other radiological diagnoses (n=33)
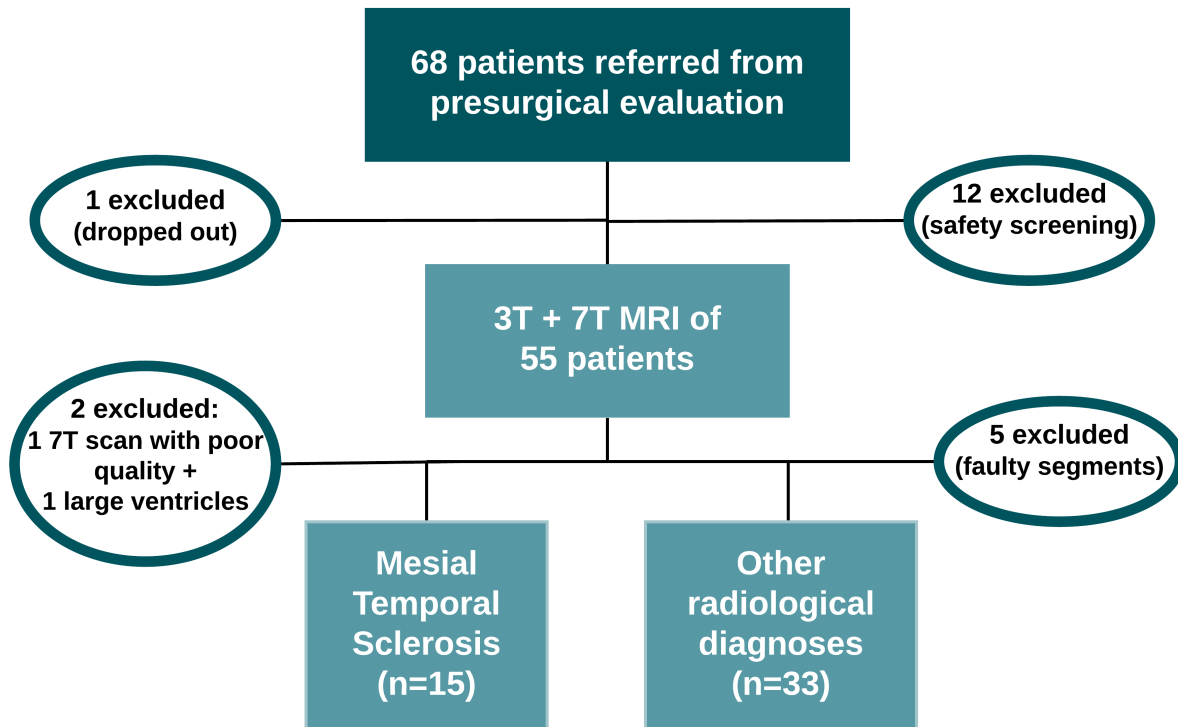
Figure 1: Starting with 68 patients, 12 were excluded during 7T MR safety screening, and one was excluded between 7T and 3T MR scans due to dropout from presurgical evaluation. One was excluded to poor 7T scan quality, and one due to large ventricles hampering the segmentations and affecting the hippocampal volume and shape. Additionally, five we excluded during quality control of segmentation output. The remaining 48 patients were divided in MTS (n=15) and other diagnoses (n=33).

2.2 MRI scans

All patients had the same sets of MRI scans at 3T and 7T. For 3T, scans were acquired on a Siemens Prisma system *(Siemens Ltd., Erlangen, Germany),* with 32-channel receive coil. For 7T, scans were acquired on an actively shielded Philips Achieva 7T MR system (*Philips Ltd, Best, The*

85   *Netherlands*), with 19x19cm dielectric pads on both sides, and a quadrature 32/2 Rx/Tx coil (Nova

86   Medical, Wilmington, MA). Sequence parameters from the two scans are shown in *table 1*.

87   **Tables:**

Image	3T specifications	7T specifications
T1-weighted	Sag. 3D MPRAGE / 1x1x1 mm	Sag. 3D MPRAGE / 0.7x0.7x0.7 mm
T2-weighted	Cor. 2D TSE T2 / 0.5x0.4x3 mm	Sag. 3D TSE T2 / 0.7x0.7x0.7 mm

88   **Table 1:** Overview of sequences and spatial resolutions in the 3T and 7T datasets.

89

90   **2.3 Data processing**

91   The data were processed using FreeSurfer[27] v.6.0 prior to using the FreeSurfer hippocampal

92   subfield segmentation tool[28]. T2-weighted images were added to allow multispectral hippocampal

93   subfield segmentations where boundary tracing accuracy is increased[28]. For 7T data, the high-

94   resolution-adapted FreeSurfer processing stream was used

95   (https://ftp.nmr.mgh.harvard.edu/pub/dist/freesurfer/6.0.0-patch/hcp/conf2hires). Outputs were

96   visually quality controlled by the same observer, with more than three years of experience in

97   viewing FreeSurfer segmentation outputs on 3T and 7T MR data. Hippocampal masks were created

98   and exported for further image analyses and statistics along with the volumes for WH (consisting of

99   all subfields depicted in the color legend on *figure 2*) and the regions of hippocampus proper

100   (Cornu Ammonis (CA) 1, CA2/3, CA4, and the granular-cell dentate gyrus (GC--DG)), as depicted

101   on *figure 2*.

102
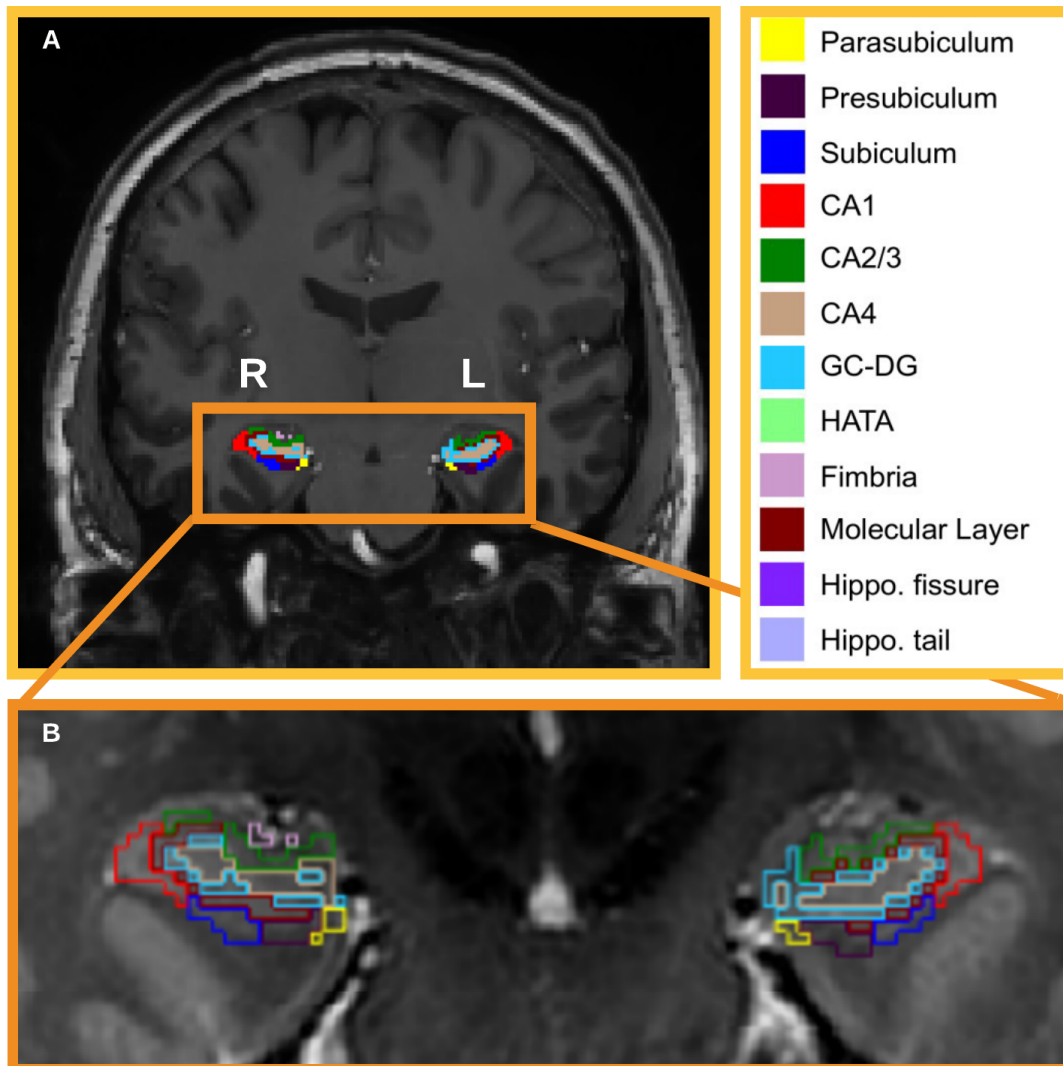
Figure 2: Illustration of hippocampal segmentations. **A)** Coronal slice of a T1-weighted 7T image

from one of our non-MTS subjects. The colored labels depict various subfields visualized in this

part of the hippocampal head. The orange box encapsulates the hippocampi with segmentation

labels. **B)** Zoomed-in coronal view of the corresponding label outlines from slice in **A),** but on a T2-

weighted scan**.** Volumes were computed from the soft segmentations rather than these discrete

labels. ***Upper right:*** Color chart for all the subfields, where the WH volume is the sum of all the

subfield volumes.

110

111   *7T-specific preprocessing:* The T1-weighted images were first bias-field corrected and then

112   denoised to correct for B1 inhomogeneities across the temporal lobes before running the

113   segmentation pipeline[29]. Bias-field correction was done in SPM12 (Wellcome Department of

114   Cognitive Neurology)[30] with a down-sampling factor of 3, light regularization and full-width half-

115   maximum set to 60 mm. Denoising was done with a spatially adaptive non-local means (SANLM)

116   filter provided in the SPM12 CAT12 toolbox[31].

117   **2.4 Analyses of FreeSurfer outputs**

118   Volumes were directly exported from FreeSurfer. Masks for the hippocampal subfields were

119   converted to binary masks. T2-weighted scans were rigidly co-registered and resampled to match

120   the T1-weighted scans. Mean and standard deviation values of the signal intensities inside the

121   masks as well as entropy (a texture measure) were calculated from the T2-weighted MRIs in Matlab

122   (Release 2019b, The MathWorks, Inc., Natick, MA, US).

123

124   We used the absolute hippocampal asymmetry ratios for each subject (equation on *figure 2d*) for all

125   parameters, as this compensated for the different scaling factors in 3T and 7T MRI T2 intensity

126   values. Using an absolute asymmetry ratio allowed us to group both left- and right-sided MTS into

127   one group of unilateral MTS.

128

129   **2.5 Statistics**

130   Groups were divided into MTS and non-MTS, with the patients with other radiological diagnoses

131   than MTS pooled together into one group. We used the Wilcoxon rank-sum (Mann-Whitney) test to

132   test for differences in absolute asymmetry ratios of all four parameters between the groups, with a

133   Bonferroni-corrected p-value. The conservative Bonferroni correction would suggest a significance

134   threshold at p<0.00125.

135

3 Results

137   The resulting groups were MTS (n=15) and non-MTS (n=33). One case in the MTS group was

138   suspected for bilateral pathology, but deemed unilateral after visual inspection of 7T MRI.

139

3.1 Group differences 3T and 7T MRI

141   There were significant differences between asymmetries in MTS and non-MTS in both entropy and

142   volume for all five hippocampal regions for 3T MRI (*see table 2*). For standard deviations of T2

143   signal intensities, group difference (after Bonferroni correction) was close to significant for CA2/3.

144   See *figure 3a-c* for distributions of asymmetry ratios for entropy, mean signal intensity and volume.

145

Parameter_Region	3T	7T
Entropy_WH	1.2×10^{-5}***	1.4×10^{-5}***
Entropy_CA1	7.0×10^{-6}***	2.2×10^{-6}***
Entropy_CA3/2	9.1×10^{-5}***	1.1×10^{-2}
Entropy_CA4	2.2×10^{-6}***	3.3×10^{-6}***
Entropy_GC-DG	4.1×10^{-6}***	3.5×10^{-5}***
MeanSig_WH	1.5×10^{-1}	1.6×10^{-2}
MeanSig_CA1	3.3×10^{-1}	3.5×10^{-2}
MeanSig_CA3/2	1.3×10^{-1}	1.9×10^{-3}
MeanSig_CA4	4.8×10^{-2}	4.8×10^{-4}**
MeanSig_GC-DG	4.4×10^{-1}	1.9×10^{-3}
StdSig_WH	1.61×10^{-1}	4.23×10^{-1}

StdSig_CA1	4.3×10^{-2}	4×10^{-1}
StdSig_CA3/2	1.6×10^{-3}	5.2×10^{-1}
StdSig_CA4	3.9×10^{-2}	7.5×10^{-2}
StdSig_GC-DG	1.8×10^{-1}	2.9×10^{-1}
Volume_WH	7.8×10^{-6}***	9.6×10^{-6}***
Volume_CA1	2.2×10^{-6}***	3.3×10^{-6}***
Volume_CA3/2	5.1×10^{-6}***	9.2×10^{-4}**
Volume_CA4	5.7×10^{-5}***	5.7×10^{-6}***
Volume_GC-DG	1.8×10^{-5}***	6.3×10^{-6}***

146 **Table 2:** P-values from Wilcoxon rank-sum tests of group differences (MTS vs non-MTS). WH =

147 whole hippocampus, CA = cornu ammonis, GC-DG = granular-cell dentate gyrus, MeanSig = mean

148 signal intensity, and StdSig = standard deviations of signal intensities. Statistical significance is

149 given as ** for $p < 0.00125$ and *** for $p < 0.0005$ after Bonferroni correction.

150

151 For entropy, there were significant differences for WH, CA1, CA4 and GC-DG for 7T MRI after

152 Bonferroni correction (*figure 3d, table 2*). For mean signal intensity, 7T differences were significant

153 in CA4, and borderline significant for CA2/3 and GC-DG (*figure 3e, table 2*). Group differences

154 were also significant for volume in all hippocampal regions (*figure 3f, table 2*). However, the

155 difference in CA2/3 in terms of entropy is significant for 3T, but not for 7T. In addition, when

156 examining volumes, the separation between MTS and non-MTS is more pronounced for CA2/3 in

157 3T, than in 7T. Standard deviations of T2 signal intensity values were not significantly different in

158 either of the regions.
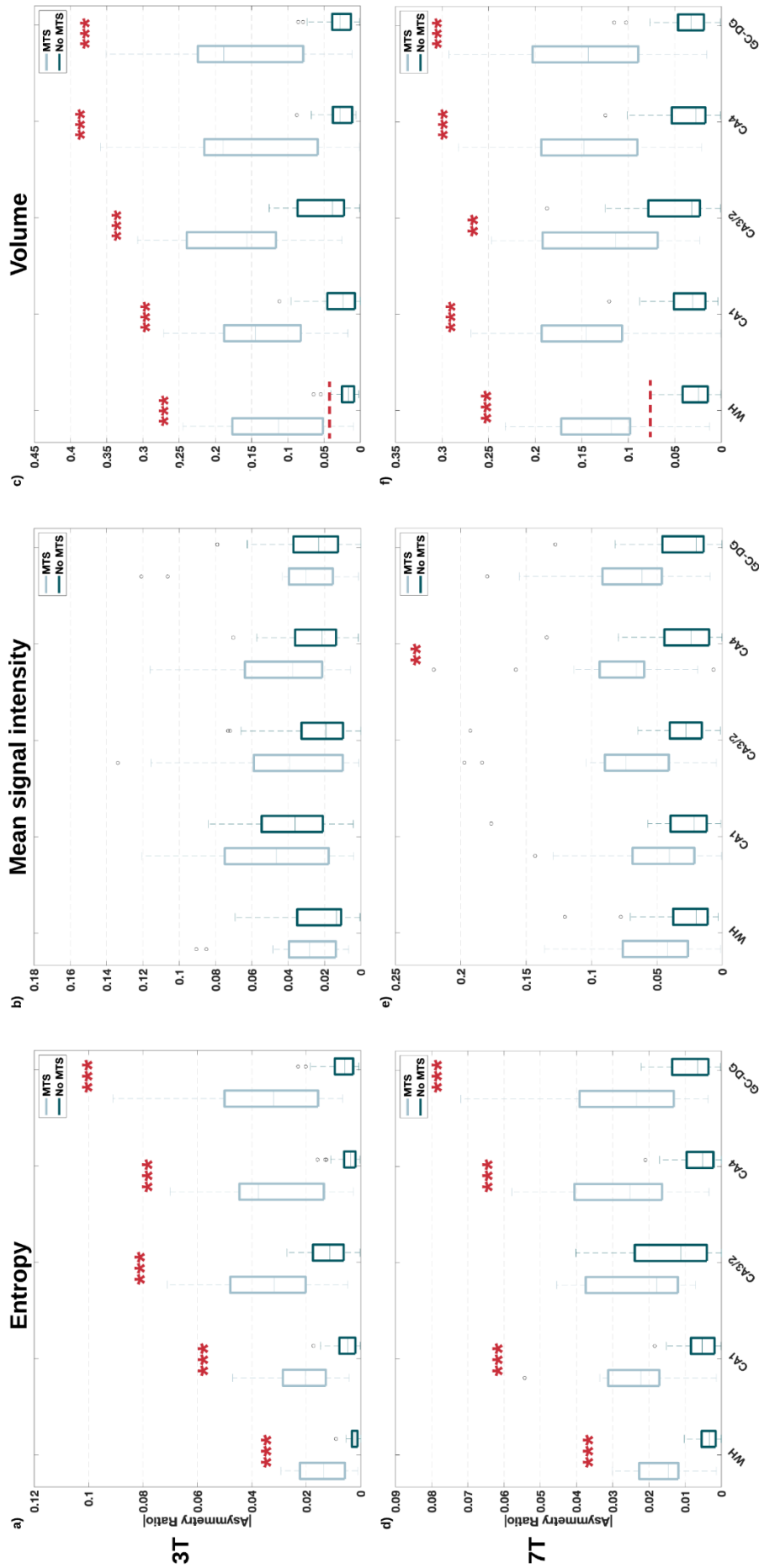
160 **Figure 3:** Boxplots for entropy and volume asymmetry ratios across the two patient groups and five

161 regions. **a-c) (upper row)** are 3T data**,** and **d-f) (lower row)** are 7T data. Statistical significance

162 after Bonferroni correction is given as ** for $p<0.00125$ and *** for $p<0.0005$. The central box

163 marks indicate the median, and the upper and lower edges of the box indicate the 75th and 25th

164 percentiles, respectively. The whiskers extend to the most extreme data points not considered

165 outliers, which corresponds to 2.5% and 97.5% in a normally distributed group.

166 WH = whole hippocampus, CA = cornu ammonis, GC-DG = granular-cell dentate gyrus, MTS =

167 mesial temporal sclerosis.

168

169 **4 Discussion**

170 In this study we assessed quantitative MRI measures of MTS at 3T and 7T, and compared

171 differences in asymmetry between epilepsy patients with and without MTS in the two MRI sets.

172

173 **4.1 Volumetric asymmetry ratios in radiologically diagnosed MTS**

174 From the semiquantitative microscopic examination of TLE surgical cases[19] we expected to find

175 significant differences in volume asymmetry ratios in CA1 and CA4 and possibly in CA2/3 when

176 comparing the patients visually diagnosed with MTS and those without MTS. We found significant

177 group differences in all subfields in both 7T and in 3T MRI data. This is in accordance with "pure"

178 3T studies that utilized automatic hippocampal segmentations in MTS cohorts[3-6,9,10]. The similar

179 group differences for 7T MRI, albeit with overall smaller asymmetry values, are also in agreement

180 with studies on segmentations performed on 7T MRI[12,13,18].

181

182 The radiological diagnosis of MTS by visual assessment of WH volumes is a well-established

183 marker for histopathological neuronal cell loss in the ipsilateral hippocampus[5,13]. Any missed MTS

184 case during visual evaluation is likely due to very subtle changes possibly at the subfield level

185 before it is detectable in the WH region on clinical 3T data[5]. Some of the non-MTS patients by

186 visual evaluation may therefore be true MTS patients. Also, non-MTS patients by visual evaluation

187 might display true asymmetry changes due to their hippocampus being a hub in the seizure

188 propagation pathway, thus affecting hippocampal tissue *without* being the primary epileptogenic

189 lesion. Furthermore, a previous study has shown consistently overestimated automated

190 segmentations occurring in both MTS and non-MTS groups with various degrees of volumetric

191 asymmetry, when compared to manual delineations by experienced radiologists[9]. This also occurs

192 in healthy populations[32], and albeit the Hadar et.al. study[9] used a different tool, it is also based on a

193 probability atlas derived from patients with Alzheimer's disease (AD) and not epilepsy-specific.

194 This likely affects any segmentation tool's ability to capture subtle changes, perhaps only occurring

195 on subfield level, When comparing distributions of volumetric asymmetries (*figure 3c and f*), both

196 mean and max values are higher for 3T than for 7T. This may indicate that there might still be

197 minute volume changes, particularly in the hippocampal subfields, that have been more precisely

198 automatically delineated on 7T data due to stronger signal and higher spatial resolution. The causes

199 of these differences in segmentations between 3T and 7T need to be better understood based on

200 cases with known MTS diagnosis, in order to further investigate the yield of 7T in subtle and

201 visually missed MTS.

202

203 **4.2 Differences in mean T2 signal intensities**

204 As for the volumetric asymmetry data we expected to find asymmetry differences in mean T2 signal

205 intensities in both CA1 and CA4. However, after Bonferroni correction for multiple comparisons a

206 significant difference only in CA4 and only in the 7T MRI data was demonstrated. These findings

207 are not in accordance with previous 3T[4,6,10,21] and 7T MRI-studies[13,17]. Tissue disruptions should be

208 bigger and more frequent in the MTS group, which might be detected with another T2 signal

209 intensity parameter than the mean value, e.g. T2 relaxometry[34], or our texture measure entropy,

210 which is based on the varying distributions of the T2 signal intensities (*see section 4.3)* inside the

211 hippocampal region of interest. To what extent it applies in this real-time cohort is only possible to

212 confirm with histopathological evaluation postoperatively.

213

214 Frequent movement artefacts affected many of our 7T 2D T2 images, which is the reason for

215 analyzing 3D T2 images in the 7T dataset. This might have introduced a bias, from which we

216 cannot really investigate the effects, since the standard 3T MR scan protocol only provides us with

217 2D T2 images.

218

219 **4.3 Texture analysis**

220 Entropy was significantly different when comparing the visually diagnosed MTS to the non-MTS

221 group for both 7T and 3T data, with the exception of CA2/3 where no significant difference was

222 found in the 7T MRI data. It is known that spatial resolution and signal-to-noise-ratio influence

223 ability to discriminate texture features from MRIs[35], which is not supported by the similarity in

224 differences we observe in 3T and 7T data. Previous studies on texture changes in MTS on lower

225 field-strength MRI conclude there are significant differences both in ipsi- and contralateral

226 hippocampi when compared to healthy controls[20,36-37]. One other study points to texture changes

227 that follows the seizure propagation pathway in TLE[37]. Without histological ground truth, it can

228 only be speculated whether the lack of significant differences in CA2/3 for 7T reflects true

229 histological appearance, i.e. less to no pronounced neuronal changes in CA2/3 compared to other

230 subfields. That is why we still conclude that the two MRI modalities display similar group

231 differences at large. However, this type of group assessment results does not transfer to machine

232   learning approaches like classification of MTS, where a model may still perform better when

233   classifying MTS based on 7T data than on 3T.

234

235   **4.4 Concordance of asymmetry outliers and clinical findings**

236   A closer examination of individual data points considered outliers in figure 3 was also done.

237   Outliers may represent patients incorrectly classified by visual inspection of MRIs by the expert

238   neuroradiologist or patients incorrectly classified according to the asymmetry ratios calculated after

239   FreeSurfer analysis. Thus, investigating outliers using additional multimodal information have

240   direct implications for understanding to what extent the automated segmentations correspond to

241   clinically supporting information. In the non-MTS group, no patients had a WH volume asymmetry

242   ratio measured with 7T indicating MTS. This is in contrast to 3T, where two patients had a higher

243   volume asymmetry ratio than expected. In both patients neither seizure semiology, surface EEG,

244   stereo-EEG and FDG-PET findings supported the hypothesis of the mesial temporal lobe as an

245   epileptogenic zone.

246

247   In the MTS group, two observations are noticeable: Firstly, the same patient had a low WH volume

248   asymmetry ratio both at 3T and 7T MRI indicating no MTS. This patient was described by the

249   neuroradiologist as having a small hippocampus on both sides but only changes in signal intensity

250   and texture on the right side. Thus, in this patient the use of a left/right volume asymmetry ratio is

251   not well-suited to classify the patient correctly in the MTS group. Nevertheless, for this patient,

252   entropy asymmetry was abnormal, but we found that the values corresponded to higher entropy on

253   the contralateral (left) hippocampus. Secondly, three patients scanned at 3T and two patients

254   scanned at 7T were outliers with a low WH volume asymmetry ratio. All three outliers classified

255   from 3T MRI had concordant EEG and seizure semiology supporting the visual diagnosis of MTS.

256   In two of these patients, anteromesial temporal lobe resection was performed. In the first patient,

257   histopathology was not available (tissue used for research), but the patient is seizure free 18 months

258   after surgery. The second patient was diagnosed with HS ILAE type 1. Both outliers classified from

259   the 7T MRI had concordant EEG and seizure semi-ology supporting the visual diagnosis of MTS.

260   The first patient was diagnosed with HS ILAE type 2 after epilepsy surgery. The second patient

261   declined the offer of epilepsy surgery. WH volume asymmetry ratio may be considered as a crude

262   index of neuronal loss in hippocampal sclerosis since it is well-known not to be evenly distributed

263   across subfields of the hippocampus[31]. In the MTS group, one of the three additional patients with a

264   lower WH volume asymmetry ratio at 3T than expected, still had an abnormal CA1 volume

265   asymmetry. Of the two additional MTS patients with a lower WH volume asymmetry ratio at 7T,

266   both had an abnormal CA1 volume asymmetry ratio.

267

268   Our results imply that the FS analysis of WH volume asymmetry ratios benefit from higher image

269   resolution, SNR and CNR at 7T. However, the findings also clearly imply that visual diagnosis of

270   MTS by an expert neuroradiologist are superior to FS based group discrimination both at 3T and

271   7T. Nevertheless, 11/15 (73%) at 3T and 12/15 (80%) at 7T of epilepsy patients appear to display

272   abnormal volume asymmetries in the MTS group, which could be helpful for less experienced

273   radiologists.

274

275   **4.5 General limitations and uncertainties**

276   *Bias in segmentations*

277   Segmentation on 3T MRIs is likely to be inherently less accurate than on 7T MRIs due to spatial

278   resolution and signal-to-noise ratio. Furthermore, the hippocampal subfield segmentation tool

279   builds on a probabilistic atlas obtained from manual delineations on ultrahigh resolution ex vivo

280   MR scans from healthy, elderly brain samples (n=10), elderly demented (n=4) and mild cognitive

281   impairment (n=1)[27]. Despite being able to capture some mild asymmetry due to age or Alzheimer's

282   disease, it is not specific to sclerotic hippocampi in TLE. The automated segmentations have been

283   shown to be more reproducible than manual segmentations[32,33], and also show high test-retest

284   reliability within scanners[33]. But these strategies might meet some limitations when the subfields

285   have a high degree of atrophy, as the atlas *a priori* might not capture the larger variability in

286   subfield volumes seen in atrophied hippocampi. There may also be different degree of limitations in

287   performing segmentations on 3T MRIs compared to 7T MRIs in cases of incompletely inverted

288   hippocampi (malrotations), which are more frequently occurring in this patient group[38]. To our

289   knowledge, no study has investigated such effects and differences in performance of the

290   segmentation algorithm between 3T and 7T MRIs in any population type. Notably,

291   histopathological subtypes of HS most often consist of less reduced and affected CA2/3 subfields.

292   When looking at our findings in figure 3c and 3f, one might speculate whether the less well-

293   separated asymmetries in CA2/3 subfield volumes in the 7T data reflect a more precise, yet still

294   biased from using probability atlas from healthy subjects, delineation. Although the volumetric

295   asymmetries in general are larger for our 3T data, there are equally significant group differences at

296   large. The above-mentioned segmentation biases therefore do not seem to have affected our group

297   comparison results in general.

298   ***Investigating MRI features in a cohort currently undergoing presurgical evaluation***

299   The lack of histopathological confirmations and postoperative outcomes challenges the basis for

300   conclusions. A radiological diagnosis of unilateral MTS does not provide final evidence of

301   histopathological hippocampal sclerosis, although it is still an excellent predictor of surgery

302   outcome[21,]. Nor is the absence of radiological MTS diagnosis evidence that there is no hippocampal

303   sclerosis. As far as group differences go, they are significant for both 3T and 7T. But significant

304 group differences do not confirm that the diagnosis is 100% correct, and an "unsignificant"

305 asymmetry ratio would not be a guarantee for a patient not having hippocampal sclerosis. This also

306 was evident when we inspected the outliers for both 3T and 7T data, although there still were subtle

307 indications for a better discriminative ability in CA1 volumetric asymmetry in the 7T set.

308

309 Analysis of group differences from clinical MRIs might be strengthened by inclusion of other

310 imaging modalities and clinical features when available, also with 3T MRI. But a real-time cohort

311 means that patients are at different stages of their presurgical evaluation, with different clinical

312 indications, thus not having a homogeneous set of supplemental neuroimaging to add to

313 computational analyses. This was therefore part of the rationale for comparing stand-alone features

314 from clinical MRI of different field strengths as the only modality.

315 **4.6 Clinical implications**

316 We acknowledge that the findings in this study do not have implications for individual patients. Our

317 impression is, however, that it is of clinical interest to know that both 7T and 3T-based radiomic

318 features seem to discriminate the already well-defined radiologically diagnosed MTS patients.

319 Particularly when considering to use this kind of MR-based information as support to the manual

320 radiology workflow, e.g. crude sorting of which patients have one or the other diagnosis.

321

322 **5 Conclusion**

323 This study provides a unique comparison of ordinary hippocampal 3T and 7T MRI features in a

324 cohort of patients diagnosed with MTS. Automatically quantified asymmetries in hippocampal

325 volumes showed group differences consistent with radiological diagnoses both when performed on

326 7T and on 3T MRIs. Nevertheless, 7T MRI features may potentially still offer better discrimination

327 between radiologically diagnosed groups compared to 3T when training machine learning

328   algorithms with the same quantitative features. The marginally less significant difference in 7T-

329   based CA2/3 volume compared to 3T may be indicative of an increased sensitivity to "true

330   histological changes", since most HS subtypes display the largest reductions and changes in CA1

331   and CA4. The group differences in our texture measure entropy was also not significant in CA2/3

332   for 7T data, albeit with similar differences for all other subfields. Although, without histological

333   confirmations of HS subtypes among the radiological MTS group, this remains speculative. Future

334   investigations of the characteristics of these quantitative techniques, as well as their influence on

335   automatic detection accuracies are warranted.

336

337   **Key Points Box**

- Little is known about how radiomic features compare between 3T and 7T MRI in MTS versus non-MTS patients
- 3T and 7T MRI display equally significant group differences between MTS and non-MTS patient groups
- Outlier inspection of WH volumes suggest 80% of 7T and 73% of 3T data display pathological asymmetry indices
- Hippocampal volume and entropy (texture) seem to discriminate MTS from non-MTS equally well, although only volume is lateralizing

352   Born, Annette Sidaros, Noémi Becser Andersen, Ioannis Tsiropoulos and Birthe Pedersen from the

353   Danish Epilepsy Surgery Group at the Epilepsy Clinic, Dept. of Neurology at Rigshospitalet and the

354   Epilepsy Hospital Filadelfia in Dianalund. Lastly, we thank the patients for bravely participating.

355

356   **Disclosure of conflicts of interest**

357   None of the authors has any conflict of interest to disclose.

358

359   **Ethical publication statement**

360   We confirm that we have read the Journal's position on issues involved in ethical publication and

361   affirm that this report is consistent with those guidelines.

362 **References**

363 1. Ryvlin P, Cross JH, Rheims S. Epilepsy surgery in children and adults. The Lancet

364 Neurology. 2014 Nov 1;13(11):1114-26.

365 2. Vakharia VN, Duncan JS, Witt JA, et.al. Getting the best outcomes from epilepsy surgery.

366 Annals of neurology. 2018 Apr;83(4):676-90.

367 3. Cendes F, Andermann F, Gloor P, et.al. MRI volumetric measurement of amygdala and

368 hippocampus in temporal lobe epilepsy. Neurology. 1993 Apr 1;43(4):719-.

369 4. Coan AC, Kubota B, Bergo FP, et.al. 3T MRI quantification of hippocampal volume and

370 signal in mesial temporal lobe epilepsy improves detection of hippocampal sclerosis.

371 American Journal of Neuroradiology. 2014 Jan 1;35(1):77-83.

372 5. Goubran M, Bernhardt BC, Cantor-Rivera D, et.al. In vivo MRI signatures of hippocampal

373 subfield pathology in intractable epilepsy. Human brain mapping. 2016 Mar;37(3):1103-19.

374 6. Steve TA, Jirsch JD, Gross DW. Quantification of subfield pathology in hippocampal

375 sclerosis: a systematic review and meta-analysis. Epilepsy research. 2014 Oct

376 1;108(8):1279-85.

377 7. Steve TA, Yasuda CL, Coras R, et.al. Development of a histologically validated

378 segmentation protocol for the hippocampal body. Neuroimage. 2017 Aug 15;157:219-32.

379 8. Peixoto-Santos JE, Carvalho LE, Kandratavicius L, et.al. Manual hippocampal subfield

380 segmentation using high-field MRI: Impact of different subfields in hippocampal volume

381 loss of temporal lobe epilepsy patients. Frontiers in neurology. 2018 Nov 20;9:927.

382 9. Hadar PN, Kini LG, Coto C, et.al. Clinical validation of automated hippocampal

383 segmentation in temporal lobe epilepsy. NeuroImage: Clinical. 2018 Jan 1;20:1139-47.

384 10. Focke NK, Yogarajah M, Symms MR, et.al. Automated MR image classification in

385 temporal lobe epilepsy. Neuroimage. 2012 Jan 2;59(1):356-62.

386   11. Zijlmans M, Zweiphenning W, van Klink N. Changing concepts in presurgical assessment

387   for epilepsy surgery. Nature Reviews Neurology. 2019 Oct;15(10):594-606.

388   12. Santyr BG, Goubran M, Lau JC, et.al. Investigation of hippocampal substructures in focal

389   temporal lobe epilepsy with and without hippocampal sclerosis at 7T. Journal of Magnetic

390   Resonance Imaging. 2017 May;45(5):1359-70.

391   13. Henry TR, Chupin M, Lehéricy S, et al. Hippocampal sclerosis in temporal lobe epilepsy:

392   findings at 7 T. Radiology. 2011 Oct;261(1):199-209.

393   14. Wisse LE, Kuijf HJ, Honingh AM, et.al. Automated hippocampal subfield segmentation at

394   7T MRI. American Journal of Neuroradiology. 2016 Jun 1;37(6):1050-7.

395   15. Berron D, Vieweg P, Hochkeppler A, et.al. A protocol for manual segmentation of medial

396   temporal lobe subregions in 7 Tesla MRI. NeuroImage: Clinical. 2017 Jan 1;15:466-82.

397   16. Stefanits H, Springer E, Pataraia E, et.al. Seven-tesla MRI of hippocampal sclerosis: an in

398   vivo feasibility study with histological correlations. Investigative radiology. 2017 Nov

399   1;52(11):666-71.

400   17. Coras R, Milesi G, Zucca I, et.al. 7 T MRI features in control human hippocampus and

401   hippocampal sclerosis: An ex vivo study with histologic correlations. Epilepsia. 2014

402   Dec;55(12):2003-16.

403   18. Gillmann C, Coras R, Rössler K, et.al. Ultra-high field MRI of human hippocampi:

404   Morphological and multiparametric differentiation of hippocampal sclerosis subtypes. PloS

405   one. 2018 Apr 18;13(4):e0196008.

406   19. Blümcke I, Thom M, Aronica E, et.al. International consensus classification of hippocampal

407   sclerosis in temporal lobe epilepsy: a Task Force report from the ILAE Commission on

408   Diagnostic Methods. Epilepsia. 2013 Jul;54(7):1315-29.

409   20. Coras, R., Pauli, E., Li, J., et.al. (2014). Differential influence of hippocampal subfields to

410   memory formation: insights from patients with temporal lobe epilepsy. *Brain*, *137*(7),

411   1945-1957.

412   21. Bonilha L, Kobayashi E, Castellano G, et.al. Texture analysis of hippocampal sclerosis.

413   Epilepsia. 2003 Dec;44(12):1546-50.

414   22. Sánchez AG, Zapata JO. Diagnosis of mesial temporal sclerosis: sensitivity, specificity and

415   predictive values of the quantitative analysis of magnetic resonance imaging. Neuroradiol J.

416   2018 Feb;31(1):50-9.

417   23. Zhou B, An D, Xiao F, et.al. Machine learning for detecting mesial temporal lobe epilepsy

418   by structural and functional neuroimaging. Frontiers of Medicine. 2020 Jan 7:1-2.

419   24. Rudie JD, Colby JB, Salamon N. Machine learning classification of mesial temporal

420   sclerosis in epilepsy patients. Epilepsy research. 2015 Nov 1;117:63-9.

421   25. Keihaninejad S, Heckemann RA, Gousias IS, et.al. Classification and lateralization of

422   temporal lobe epilepsies with and without hippocampal atrophy based on whole-brain

423   automatic MRI segmentation. PloS one. 2012 Apr 16;7(4):e33096.

424   26. Memarian N, Kim S, Dewar S, et.al. Multimodal data and machine learning for surgery

425   outcome prediction in complicated cases of mesial temporal lobe epilepsy. Computers in

426   biology and medicine. 2015 Sep 1;64:67-78.

427   27. Fischl B. FreeSurfer. Neuroimage. 2012 Aug 15;62(2):774-81.

428   28. Iglesias JE, Augustinack JC, Nguyen K, et.al. A computational atlas of the hippocampal

429   formation using ex vivo, ultra-high resolution MRI: application to adaptive segmentation of

430   in vivo MRI. Neuroimage. 2015 Jul 15;115:117-37.

431   29. International Society for Magnetic Resonance in Medicine, Proceedings of the 28th Annual

432   Meeting April 2020, Opheim G. et.al., Abstract submission number 5808, "Optimizing a

433   preprocessing pipeline for structural 7T MR analyses in FreeSurfer"

434   30. Friston KJ, Ashburner J, Frith CD, et.al. Spatial registration and normalization of images.

435   Human brain mapping. 1995;3(3):165-89.

436   31. Ashburner J, Friston KJ. Diffeomorphic registration using geodesic shooting and Gauss–

437   Newton optimisation. NeuroImage. 2011 Apr 1;55(3):954-67.

438   32. Brinkmann, Benjamin H., et al. "Segmentation errors and intertest reliability in automated

439   and manually traced hippocampal volumes." *Annals of clinical and translational neurology*

440   6.9 (2019): 1807-1814.

441   33. Brown EM, Pierce ME, Clark DC, et.al. Test-retest reliability of FreeSurfer automated

442   hippocampal subfield segmentation within and across scanners. Neuroimage. 2020 Apr

443   15;210:116563.

444   34. Bernasconi A, Bernasconi N, Caramanos Z, et.al. T2 relaxometry can lateralize mesial

445   temporal lobe epilepsy in patients with normal MRI. Neuroimage. 2000 Dec 1;12(6):739-46.

446   35. Larroza A, Bodí V, Moratal D. Texture analysis in magnetic resonance imaging: review and

447   considerations for future applications. Assessment of cellular and organ function and

448   dysfunction using direct and derived MRI methodologies. 2016 Oct 26:75-106.

449   36. Yu O, Mauss Y, Namer IJ, Chambron J. Existence of contralateral abnormalities revealed by

450   texture analysis in unilateral intractable hippocampal epilepsy. Magnetic resonance imaging.

451   2001 Dec 1;19(10):1305-10.

452   37. Sankar T, Bernasconi N, Kim H, et.al. Temporal lobe epilepsy: differential pattern of

453   damage in temporopolar cortex and white matter. Human brain mapping. 2008

454   Aug;29(8):931-44.

455   38. Bernasconi N, Kinay D, Andermann F, et.al. Analysis of shape and positioning of the

456   hippocampal formation: an MRI study in patients with partial epilepsy and healthy controls.

457   Brain. 2005 Oct 1;128(10):2442-52.

A.2.1 Co-author declarations Article 2

DECLARATION OF CO-AUTHORSHIP

The declaration is for PhD students and must be completed for each conjointly authored article. Please note that if a manuscript or published paper has ten or less co-authors, all co-authors must sign the declaration of co-authorship. If it has more than ten co-authors, declarations of co-authorship from the corresponding author(s), the senior author and the principal supervisor (if relevant) are a minimum requirement.

1. Declaration by	
Name of PhD student	Giske F. Opheim
E-mail	giskeopheim@nru.dk
Name of principal supervisor	Lars H. Pinborg
Title of the PhD thesis	Utilizing 7 Tesla MRI and automated segmentation - A new era in the presurgical evaluation of severe epilepsy

2. The declaration applies to the following article	
Title of article	Exploring radiomic features in clinical 3T and 7T MRI of mesial temporal sclerosis in an open presurgical patient cohort

Article status	
Published ☐ Date:	Accepted for publication ☐ Date:
Manuscript submitted ■ Date: 13th of October 2020	Manuscript not submitted ☐ *Rejected 28th of October, will be re-submitted to other journal*
If the article is published or accepted for publication, please state the name of journal, year, volume, page and DOI (if you have the information).	

3. The PhD student's contribution to the article *(please use the scale A-F as benchmark)* Benchmark scale of the PhD-student's contribution to the article **A**. Has essentially done all the work (> 90 %) **B**. Has done most of the work (60-90 %) **C**. Has contributed considerably (30-60 %) **D.** Has contributed (10-30 %) **E.** No or little contribution (<10 %) **F.** Not relevant	A, B, C, D, E, F
1. Formulation/identification of the scientific problem	A
2. Development of the key methods	F
3. Planning of the experiments and methodology design and development	A
4. Conducting the experimental work/clinical studies/data collection/obtaining access to data	B

3. The PhD student's contribution to the article *(please use the scale A-F as benchmark)*	A, B, C, D, E, F
Benchmark scale of the PhD-student's contribution to the article **A**. Has essentially done all the work (> 90 %) **B**. Has done most of the work (60-90 %) **C**. Has contributed considerably (30-60 %) **D**. Has contributed (10-30 %) **E**. No or little contribution (<10 %) **F.** Not relevant	
5. Conducting the analysis of data	B
6. Interpretation of the results	B
7. Writing of the first draft of the manuscript	A
8. Finalisation of the manuscript and submission	A

Provide a short description of the PhD student´s specific contribution to the article.[i]

The PhD student has initiated and participated in all parts of the study, as well as writing and finalizing the manuscript. In this article, we used existing software and statistical tests. The study was started as part of the PhD course Machine Learning in Imaging Projects at Dept. of Computer Science, UCPH. Interpretation of results has been supervised by PhD supervisors Lars H. Pinborg and Melanie Ganz-Benjaminsen.

4. Material from another thesis / dissertation[ii]	
Does the article contain work which has also formed part of another thesis, e.g. master's thesis, PhD thesis or doctoral dissertation (the PhD student's or another person's)?	Yes: ☐ No: ■
If yes, please state name of the author and title of thesis / dissertation.	
If the article is part of another author´s academic degree, please describe the PhD student´s and the author´s contributions to the article so that the individual contributions are clearly distinguishable from one another.	

5.	Signatures of the co-authors[iii]			
	Date	Name	Title	Signature
1.	25/10/2020	Melanie Ganz-Benjaminsen (senior author)	PhD, Assistant Prof	*Melanie Ganz-Benjamin*
2.	2020-11-06	Lars H. Pinborg (co-author and main supervisors)	MD, DMSc, Assoc	

5.	Signatures of the co-authors[iii]			
3.				
4.				
5.				
6.				
7.				
8.				
9.				
10.				

6.	Signature of the principal supervisor

I solemnly declare that the information provided in this declaration is accurate to the best of my knowledge.

Date: 2020-11-06
Principal supervisor:

7.	Signature of the PhD student

I solemnly declare that the information provided in this declaration is accurate to the best of my knowledge.

Date: 2020-11-06

PhD student: Gisle F. Opheim

Please learn more about responsible conduct of research on the Faculty of Health and Medical Sciences' website.

---

[i] This can be supplemented with an additional letter if needed.

[ii] Please see Ministerial Order on the PhD Programme at the Universities and Certain Higher Artistic Educational Institutions (PhD Order) § 12 (4):

A.3 Article 3

Giske Opheim, Karin Markenroth-Bloch, Anja van der Kolk, et.al., "*7T Epilepsy Task Force consensus recommendations on the use of 7T in clinical practice*", 2020, **Accepted for publication.**

7T Epilepsy Task Force Consensus Recommendations on the use of 7T in Clinical Practice

Giske Opheim, M.Sc; Anja van der Kolk, MD, PhD; Karin Markenroth Bloch, PhD; Albert J. Colon, MD, PhD; Kathryn A. Davis, MD, MS; Thomas R. Henry, MD; Jacobus F.A. Jansen, PhD; Stephen E. Jones, MD, PhD; Jullie W. Pan, PhD; Karl Rössler, MD, DMSc; Joel M. Stein, MD, PhD; Maria C. Strandberg, MD, PhD; Siegfried Trattnig, MD, DMSc; Pierre-Francois Van de Moortele, PhD; Maria Isabel Vargas, MD; Irene Wang, PhD; Fabrice Bartolomei, MD, PhD; Neda Bernasconi, MD, PhD; Andrea Bernasconi, MD; Boris Bernhardt, PhD; Isabella Björkman-Burtscher, MD, PhD; Mirco Cosottini, MD, PhD; Sandhitsu R. Das, PhD; Lucie Hertz-Pannier, MD, PhD; Sara Inati, MD; Michael T. Jurkiewicz, MD, PhD; Ali R. Khan, PhD; Shuli Liang, MD, PhD; Ruoyun Emily Ma, PhD; Srinivasan Mukundan, MD, PhD; Heath Pardoe, PhD; Lars H. Pinborg, MD, DMSc; Jonathan R. Polimeni, PhD; Jean-Philippe Ranjeva, MD, PhD; Esther Steijvers, B.Sc.; Steven Stufflebeam, MD, PhD; Tim J. Veersema, MD; Alexandre Vignaud, MD, PhD; Natalie Voets, PhD; Serge Vulliemoz, MD, PhD; Christopher J. Wiggins, PhD; Rong Xue, PhD; Renzo Guerrini, MD, FRCP; Maxime Guye, MD, PhD

Corresponding Author:
Giske Opheim
giskeopheim@nru.dk

Affiliation Information for All Authors:
Giske Opheim, Neurobiology Research Unit, Dept. of Neurology, Rigshospitalet Copenhagen University Hospital, and Faculty of Health and Medical Sciences, UCPH, Copenhagen, Denmark
Anja van der Kolk, Dept. of Radiology, University Medical Center Utrecht, Utrecht University, Utrecht, and Dept. of Radiology, Netherlands Cancer Institute Antoni van Leeuwenhoek Hospital, Amsterdam, the Netherlands
Karin Markenroth Bloch, Lund University Bioimaging Center, Lund University, Lund, Sweden;
Albert J. Colon, Dept. of Neurology, Neurophysiology and Neurosurgery, ACE Kempenhaeghe/MUMC, Heeze/Maastricht, the Netherlands
Kathryn Davis, Hospital of the University of Pennsylvania, Penn Epilepsy Center, Philadelphia, PA, USA
Thomas R. Henry, Dept. of Neurology and Center for Magnetic Resonance Research, University of Minnesota, Minneapolis, MN, USA
Jacobus F.A. Jansen, Dept. of Radiology and Nuclear Medicine, Maastricht University Medical Center, Maastricht, and School for Mental Health and Neuroscience, Maastricht University, Maastricht, and Dept. of Electrical Engineering, Eindhoven University of Technology, Eindhoven, the Netherlands
Stephen E. Jones, Imaging Institute, Cleveland Clinic, Cleveland, OH, USA
Jullie W. Pan, Dept. of Neurology and Radiology, University of Pittsburg, Pittsburg, PA, USA
Karl Rössler, Dept. of Neurosurgery, Medical University of Vienna, Vienna, Austria
Joel M. Stein, Dept. of Radiology, Hospital of the University of Pennsylvania, Philadelphia, PA, USA
Maria C.Strandberg, Dept. of Neurology, Dept. of Clinical Sciences, Lund University Hospital, Lund, Sweden
Siegfried Trattnig, High Field MR Center, Dept. of Biomedical Imaging and Image Guided Therapy, Medical University of Vienna, Vienna, Austria

Pierre-Francois Van de Moortele, Center for Magnetic Resonance Research, University of Minnesota, Minneapolis, MN, USA

Maria Isabel Vargas, Neuroradiology Division, Diagnostic Unit, University Hospitals and Faculty of Medicine of Geneva, Switzerland

Irene Wang, Epilepsy Center, Cleveland Clinic, Cleveland, OH, USA

Fabrice Bartolomei, Aix Marseille Univ, APHM, INSERM, INS, Inst Neurosci Syst, Timone Hospital, Epileptology Department, Marseille, France

Neda Bernasconi, Neuroimaging of Epilepsy Laboratory (NOEL), Montreal Neurological Institute and McConnell Brain Imaging Centre, McGill University, Montreal, QC, Canada

Andrea Bernasconi, Neuroimaging of Epilepsy Laboratory (NOEL), Montreal Neurological Institute and McConnell Brain Imaging Centre, McGill University, Montreal, QC, Canada

Boris Bernhardt, Montreal Neurological Institute, McGill University, Montreal, QC, Canada

Isabella Björkman-Burtscher, Dept. of Radiology, Institute of Clinical Sciences, Sahlgrenska Academy, University of Gothenburg, Gothenburg, Sweden

Mirco Cosottini, Dept. of Translational Research and New Technologies in Medicine and Surgery, University of Pisa, Italy

Sandhitsu R. Das, Dept. of Neurology, University of Pennsylvania, Philadelphia, PA, USA

Lucie HertzPannier, Paris-Saclay University, CEA, NeuroSpin, Gif-sur-Yvette, and University of Paris, UMR 1141, Paris, France

Sara Inati, EEG Section, NINDS, NIH, Bethesda, MD, USA

Michael T. Jurkiewicz, Dept. of Medical Imaging, Children's Hospital at London Health Sciences Centre, and Dept. of Medical Biophysics, Schulich School of Medicine and Dentistry, The University of Western Ontario, London, ON, Canada

Ali R. Khan, Dept. of Medical Biophysics, Schulich School of Medicine and Dentistry, The University of Western Ontario, and Imaging Research Laboratories, Robarts Research Institute, London, ON, Canada

Shuli Liang, Functional Neurosurgery Department, Beijing Children's Hospital of Capital Medical University, Beijing, China

Ruoyun Emily Ma, Center for Magnetic Resonance Research, University of Minnesota, Minneapolis, MN, USA

Srinivasan Mukundan, Dept. of Radiology, Brigham and Women's Hospital, Harvard Medical School, Boston, MA, USA

Heath Pardoe, NYU Grossman School of Medicine, New York, NY, USA

Lars H. Pinborg, Neurobiology Research Unit, and Epilepsy Clinic, Dept. of Neurology, Rigshospitalet Copenhagen University Hospital, Copenhagen, Denmark

Jonathan R. Polimeni, HarvardMIT Division of Health Sciences and Technology, Massachusetts Institute of Technology, Cambridge, and Athinoula A. Martinos Center for Biomedical Imaging, Dept. of Radiology, Harvard Medical School, Massachusetts General Hospital, Charlestown, MA, USA

Jean-Philippe Ranjeva, Aix Marseille Univ, CNRS, CRMBM, and APHM, CEMEREM, Timone Hospital, Marseille, France

Esther Steijvers, Scannexus Ultrahigh Field MRI Research Center, Maastricht, the Netherlands

Steven Stufflebeam, Harvard-MIT Division of Health Sciences and Technology, Massachusetts Institute of Technology, Cambridge, and Athinoula A. Martinos Center for Biomedical Imaging, Dept. of Radiology, Harvard Medical School, Massachusetts General Hospital, Charlestown, MA, USA

Tim J. Veersema, Dept. of Neurology and Neurosurgery, UMC Utrecht Brain Center, University Medical Center Utrecht, Utrecht, and Dept. of Radiology and Nuclear Medicine, Meander Medical Center, Amersfoort, the Netherlands
Alexandre Vignaud, Paris-Saclay University, CEA, CNRS, BAOBAB, NeuroSpin, Gif-sur-Yvette, France
Natalie Voets, Wellcome Centre for Integrative Neuroimaging, FMRIB Division, Nuffield Dept. of Clinical Neurosciences, University of Oxford, Oxford, UK; Serge Vulliemoz, EEG and Epilepsy Unit, Neurology, Dept. of Clinical Neurosciences, University Hospitals and Faculty of Medicine of Geneva, Switzerland
Christopher J. Wiggins, Scannexus Ultrahigh Field MRI Research Center, Maastricht, the Netherlands
Rong Xue, State Key Lab. of Brain and Cognitive Science, Beijing MRI Center for Brain Research, Institute of Biophysics, Chinese Academy of Sciences, Beijing, China
Renzo Guerrini, Neuroscience Department, Children's Hospital A. Meyer-University of Florence and IMAGO 7 Foundation, Italy
Maxime Guye, Aix Marseille Univ, CNRS, CRMBM, and APHM, CEMEREM, Timone Hospital, Marseille, France

Number of characters in title: 86
Abstract Word count: 234
Word count of main text: 4728
References: 67
Figures: 6
Tables: 2
Search Terms: [66] Epilepsy surgery, [68] Hippocampal sclerosis, [83] Cortical dysplasia, [120] MRI

Abstract

Identifying a structural brain lesion on MRI has important implications in epilepsy and is the most important correlate to seizure freedom after surgery in patients with drug-resistant focal onset epilepsy. However, at conventional magnetic field strengths (1.5 and 3T) only around 60-85% of MRI examinations reveal such lesions. Over the last decade, studies have demonstrated the added value of 7T MRI in patients with and without known epileptogenic lesions from 1.5 and/or 3T. However, translation of 7T MRI to clinical practice is still challenging, particularly in centers new to 7T, and there is a need for practical recommendations on targeted use of 7T MRI in the clinical management of patients with epilepsy. The 7T Epilepsy Task Force - an international group representing 21 7T MRI centers with experience from scanning over 2000 patients with epilepsy – would hereby like to share its experience with the neurology community regarding the appropriate clinical indications, patient selection and preparation, acquisition protocols and setup, technical challenges, and radiological guidelines for 7T MRI in epilepsy patients. This article mainly addresses structural imaging, but also presents multiple non-structural MRI techniques that benefit from 7T and hold promise as future directions in epilepsy.

Answering to the increased availability of 7T MRI as an approved tool for diagnostic purposes, this article aims to give guidance on clinical 7T MRI epilepsy management by giving recommendations on referral, suitable 7T MRI protocols and image interpretation.

1   Introduction

Epilepsy is drug-resistant in about 30-40% of patients.[1] In drug-resistant focal epilepsy (DRFE), surgical resection, laser ablation or disconnection of the epileptogenic zone or network are the only curative options. The chances of successful post-surgical outcome are 2.5-3 times higher if an epileptogenic lesion is identified by MRI.[2] However, precise identification of the resection margin, which is essential for optimizing surgical outcomes, is often difficult using 1.5 or 3T. Moreover, the absence of an MRI detectable lesion in approximately one third of patients with DRFE is a major limitation to surgical candidacy. Finally, normal appearing MRI also hampers targeting for intracranial electrode implantation, which in addition to seizure onset localization, is also used for chronic brain electrostimulation therapies and targeted laser ablation.

7T MRI, compared to lower field strengths, has increased signal-to-noise ratio (SNR) and susceptibility effects, leading to better image contrast, higher spatial resolution and stronger susceptibility contrast.[3, 4] These advantages offered at 7T may address multiple preoperative and postoperative problems in DRFE, including lesion detection (especially MCD) in 16-32% of previously MRI-negative patients, and identification of residual epileptogenic tissue after surgical failures.[5-10] Notwithstanding these advantages, technical challenges such as inhomogeneous radiofrequency (RF) distributions present limitations on ultrahigh field systems and add certain challenges for its use in epilepsy.

An excellent review article on scientific developments of 7T in epilepsy has recently been published.[11] This paper instead provides guidance for setting up a 7T epilepsy protocol for *clinical use,* based on the collective experience of 21 centers where over 2000 7T MRI epilepsy exams were performed.

2   Clinical indications, patient preparation & safety

When operating a non-CE/FDA approved 7T MRI scanner, clinical patient scanning should be authorized by the local institutional review board (IRB), taking both clinical benefits and possible safety issues into account.

When planning an individual epilepsy patient for clinical 7T MRI, one should pay attention to patient-specific indications for additional enhanced brain imaging, any contraindications to MRI in general and 7T in particular, and other potential issues inherent to the UHF environment. Thorough evaluation of these three factors improves the diagnostic gain of 7T MRI by making optimal use of its advantages – and adapting to its limitations. Given the currently limited availability of clinical 7T MRI platforms, most centers focus on indications for referral of DRFE patients for 7T MRI, as opposed to general diagnostic purposes.

2.1 Clinical indications

The main indications for 7T MRI in epilepsy are to improve imaging to identify a possible morphological lesion responsible for DRFE, and better delineate or classify known lesions. We have identified four main indications based on *a priori* knowledge at the time of 7T MRI referral.

3T MRI negative cases

The objective is to detect possible lesions missed by the currently recommended epilepsy-specific 3T MRI protocol.[12, 13] The presence of so far undetected lesions can be supported by the clinical history, ictal semiology, interictal and especially ictal scalp EEG, PET, or SPECT.

Lesion typing, delineation & false-positives

This includes further characterization of known structural abnormalities deemed suitable for resection by improved profiling of the abnormality, including distinction of neoplastic lesions, optimal delineation of MCD and scarring lesions, and distinguishing pathological lesions from benign or unknown morphological variants. This analysis also includes resolving false-positive 3T MRI (*section 4*), which may lead to misguided clinical management without the added information from 7T MRI.

Electrode positioning

Improved lesion characterization and visualization of adjacent structures may also augment planning of intracranial electrode positioning for electrophysiological measurements or electrostimulation therapy. This is facilitated by the increased anatomical details at 7T that enable consideration of fine structures with subtle signal changes, atrophy or malformations. However, potential increased geometric distortion in some sequences due to stronger magnetic field must be considered.

Eloquent areas

Iatrogenic injury to sites of normal cerebral physiology may be avoided by interictal mapping using stimulation or resting-state fMRI. The greater BOLD SNR performance of 7T MRI affords considerable advantages in mapping eloquent cortex over 1.5T and 3T fMRI.[12, 14]

2.2 Tolerability issues at 7T

While patient motion can be detrimental for image assessment at any field strength, this effect is even more pronounced at 7T. The most efficient way to minimize motion is to prepare patients prior to the MRI examination. However, even patients who have had previous MRI examinations can encounter

specific issues or physical sensations at 7T that we recommend addressing during preparation.[13]

Longer acquisition times

To make optimal use of the advantages of UHF MRI, individual 7T sequences (*Table 1*) – and therefore whole MRI protocols – will often take longer to acquire than at 3T. Lying supine inside the MRI scanner for such long times may cause discomfort and musculoskeletal pain in a subset of patients (approx. 25%).[15] Sleepiness is also more likely to occur and might increase risk of seizures in some patients with DRFE.

Longer scanner bore and smaller head coil

The longer scanner bore may induce claustrophobia. In addition, the most commonly used head coil is smaller than at lower field strengths; patients with larger heads will therefore receive a thinner pillow under the head, which often leads to numbness in the back of the head (Task Force experience; ~40% feels discomfort during the exam).[15, 16] Another consequence of smaller head coils is the lack of space for headphones, which is why most centers use earplugs and/or a soft clay to compensate for the loud noises unavoidable in any MRI scanner.

Peripheral Nerve Stimulation (PNS)

Some patients have reported mild discomfort or anxiety due to PNS, which can present as tingling or twitches in upper limbs or large muscle groups. Most clinical sequences are designed to have limited PNS; however, sensitivity to these physical sensations differs between patients; reported prevalence varies widely from 23-63%.[15-17]

Dizziness

Dizziness caused by movement in and out of the B_0 field is one of the most frequently reported sensations (25-80%).[15-17] To suppress this issue, very slow movement of the patient table into the scanner – which may be preconfigured by vendors – is recommended. Usually, dizziness will pass shortly (30-60 seconds) after positioning. During this movement, patients may also sense a metallic taste.

2.3 Patient safety at 7T

Once the clinical indication for 7T imaging has been established, it should be followed by a critical evaluation of possible contraindications. In this regard, it is important to realize that implants that are MR compatible at 3T may be incompatible at 7T, presenting a serious safety hazard. We therefore recommend thorough safety screening with particular emphasis on potentially hazardous factors that were approved at 3T and might be overlooked upon referral to 7T.

There is no whole-body RF coil in a 7T scanner: brain imaging is obtained with the combined transmit/receive coil, which limits the RF field to the head (plus a safety margin). Generally, for implants, displacement force and torque due to B_0 are higher, and for both implants and tattoos the risk of RF heating is increased due to the shorter RF wavelength. In spite of initiatives on harmonizing approaches[18], there is no global consensus regarding implant safety at 7T yet, and centers differ in their approach to contraindications. Some centers have dedicated safety committees that have scanned phantoms and/or obtained electromagnetic field numerical simulations to assess safety margins of common implants, and might therefore practice less conservative safety margins relative to the head coil. Until official 7T MRI safety guidelines that cover both implant types and safety margins are in place, implants *within* the RF coil volume should be locally approved at 7T

based on literature or local testing.[18] Further statements regarding these and other safety aspects at 7T

will hopefully in the near future complement already existing recommendations.[19]

3 Acquisition protocol & recommended setup

Among other topics, the survey answered by centers in our Task Force contained questions on which sequences they use in epilepsy patients, and to what degree they are useful for radiological evaluation. When comparing protocols, the majority included a subset of structural sequences, which while differing in parameter settings served the same purpose. The contrast weightings in the protocols mirrored those included in the most recent recommendations for 3T MRI of epilepsy patients[12], taking advantage of the increased magnetic field mainly by increasing spatial resolution. Based on frequency of use and radiological rating of importance, eight sequences across four different contrast weightings scored highest, and were presented to the Task Force for consensus voting. These eight sequences will be discussed in detail in the following paragraphs, while major acquisition parameters can be found in Table 1. Specific sequence recommendations based on clinical indication are given in Table 2; a 'general' protocol takes approximately 50 minutes to acquire.

3.1 Most-valued sequences in (clinical) practice

3D T_1-weighted sequences

Because of the significantly longer acquisition times of spin echo-based sequences, gradient echo (GRE)-based MPRAGE[20] or MP2RAGE[21, 22] are the mainstay for T_1-weighted imaging at 7T, with isotropic voxel sizes ranging from 0.6-0.9 mm. The main advantage of using MP2RAGE over MPRAGE is its better resistance to RF field inhomogeneity; MP2RAGE can therefore also be useful in quantitative techniques. However, some 7T platforms are not equipped with an embedded pipeline to process MP2RAGE data and output DICOM images, in which case offline processing is required which hampers clinical workflow with PACS export.

3D Fluid Attenuation Inversion Recovery (FLAIR) sequence

A 3D FLAIR with isotropic reconstructed spatial resolutions of 0.7-0.8 mm and whole-brain coverage is preferred, as it can be reformatted in any orientation. Implementation of FLAIR at 7T is not trivial for several reasons.[23] From a technical point of view, RF-pulses at 7T have to be insensitive to the inhomogeneities of the B_0 and RF field over the brain, while also complying with the restrictions on specific absorption rate (SAR). 3D FLAIR sequences are very sensitive to flip angle (FA) calibrations: if the true FA deviates too much from the set FA – which is spatially different at 7T due to RF field inhomogeneity – signal dropouts will occur and may hamper image assessment. As a consequence, finding the balance between signal intensities across the brain may be subject to radiological priorities, i.e. whether a radiologist wants to focus on medial (prioritize low FA) or lateral (prioritize high FA) structures. These difficulties have led to research into new types of RF pulse strategies and sequence designs[24, 25] to mitigate these problems.

T_2-weighted sequences

The obtainable in-plane spatial resolution of T_2-weighted sequences depends on the requested coverage and is limited by SNR, acquisition time and patient motion. For instance, to cover the hippocampus with a coronal T_2-weighted sequence within a reasonable time, in-plane acquisition resolutions of 0.25-0.50 mm are used, with slice thicknesses of 1-2 mm. However, this will increase sensitivity to patient motion due to the long acquisition times (*Table 1*). These sequences are therefore natural targets for motion correction techniques. The 3D T_2-weighted TSE sequence has less obvious motion artefacts than the multi-slice T_2-weighted sequences, however at the expense of a less pronounced image contrast and higher sensitivity to RF field inhomogeneity. For this 3D sequence, an isotropic spatial resolution of 0.5-0.8 mm and whole-brain coverage is recommended.

T_2*-weighted sequences

Due to more pronounced susceptibility effects at 7T, image contrast in T_2*-weighted sequences increases. Many centers use 3D T_2*-weighted sequences (GRE or susceptibility weighted imaging (SWI)) complementary to other images to assess vascular pathologies and vascularity in given structures. A faster, thus less motion sensitive, alternative to 3D sequences, is to choose 2D T_2*-weighted sequences that cover specific regions with same spatial resolution as 3D sequences.

3.2 Use of dielectric pads

The inhomogeneous RF field often manifests as contrast changes or signal losses in the temporal lobes and cerebellum, an effect which is most pronounced on FLAIR images (*figure 1A,B*), but also apparent on T_2-weighted images (*figure 1C,D*). One straightforward way to increase RF field homogeneity is to apply dielectric pads (<1cm thick) on each side of the head[26], which are used by two thirds of the centers with sizes varying from 10x10 cm^2 to 19x19 cm^2 (*figure 1E)*. The pads are placed as shown in figure 1F. To ensure that the contents are always well-mixed and to verify cracks/dryness in the compound, we recommend to gently massage pads prior to each scan. Renewing the pads annually / biannually prevents suboptimal effects due to degradation of the material over time (depending on the type).

Of note, by introducing dielectric pads into the transmit coil, SAR estimations produced by the scanner are no longer valid. It is therefore important that simulations of pad placements are made to ensure patient safety. Such simulations have been made and published for the standard NOVA head coil (1- and 2-channel transmit, NOVA Medical, Wilmington, MA, USA)[27], which is used in most 7T centers worldwide. When using other coils, new simulations should be performed, and the pads

should not be used if transmission settings are varied between patients unless on-the-fly SAR calculations including the pads are done.

3.3 Deciding on the imaging protocol

The individual patient-specific indications for 7T imaging (*section 2.1*) will drive the selection of sequences, which should be performed in order of priority to preempt motion artefacts from hampering assessment of the most important sequences. Recommendations for a minimum scan protocol can be found in Table 2.

4   Radiological considerations & visual assessment

Moving to 7T requires adaptation of the observer's 'blueprint' of what healthy tissue and pathology looks like. The changes in image quality aspects at 7T can be perceived as an improvement, or sometimes the contrary. For virtually all 7T images, contrast between tissues will be much higher. For instance, the cortex will be more discernible from white matter, basal ganglia will have more heterogeneous signal intensity reflective of substructures that can now be discriminated, and very small vessels, perivascular spaces and u-fibers are clearly identifiable. Although the amount of perivascular spaces has been suggested to correlate with seizure laterality[28], these findings are normal and should not be interpreted as pathology; on the contrary, they can be used for resolving false-positive blurring and transmantle signs at 3T. Another characteristic 7T finding (caused by RF transmit head coils) on T_1-weighted (MPRAGE/MP2RAGE) images is that arteries appear bright even without contrast administration.

RF field inhomogeneity effects (*section 3)* are substantial and remain one of the most significant artefacts at 7T. These effects, however, can be partially suppressed by RF shimming, e.g., through the use of dielectric pads (*figure 1*). Furthermore, susceptibility artefacts will be more pronounced, particularly in areas close to air-containing structures, which may overlap with those affected by RF field inhomogeneities. An additional strategy is to adapt the window width and level, depending on which part of the brain is of interest: this will improve image contrast in, e.g., the temporal lobes while the center of the brain will be less assessable with those same settings. Flow artefacts in and from large vessels are also present, and in cases where such artefacts extend across gray and white matter, care should be taken not to mistake these for pathology. Since there currently does not exist any uniform 7T-specific training material, we recommend surveying several 7T MRI scans, preferably of healthy volunteers, to get acquainted with these characteristics and thus avoid mistaking

them for 7T false positives in the epilepsy examination routine.

The following section provides detailed imaging findings and sequence considerations for selected lesions for which our collective experiences consider 7T MRI particularly helpful.

4.1 Malformations of cortical development (excluding FCD)

Tuberous sclerosis complex (TSC) & long-term epilepsy-associated tumors (LEATS: gangliogliomas and DNET) (Barkovich[29] group I)

The increased spatial resolution and image contrast at 7T improves detection and delineation of cerebral lesions in TSC such as cortical and subependymal tubers, cortical dysplasia, and white matter abnormalities.[30] Also, a new finding first identified at 7T is the presence of tortuous veins associated with subependymal tubers[30, 31]. Next to T_2-weighted/FLAIR imaging for visualization of cortical tubers and white matter abnormalities, and 3D T_1-weighted (MP2RAGE or MPRAGE) imaging for cortical and subependymal tubers (*figure 2*), we particularly recommend a 3D SWI or GRE T_2*-weighted sequence, as the increased sensitivity to susceptibility effects enables better visualization of (frequently encountered) tuber calcification. Image characteristics at 7T are consistent with those seen at lower field strengths; the main advantage is the higher lesion conspicuity leading to both detection of more lesions and better delineation for surgical planning.

LEATS (gangliogliomas and DNET) are low-grade tumors that consist of a composition of mature neuronal cells and glial cells[32]. Imaging characteristics include a solid and/or cystic component, and sometimes edema. At 7T, a 3D T_1-weighted (MP2RAGE or MPRAGE) image will better delineate the solid component due to increased image contrast. Additionally, 3D T_2-weighted sequences excel at both showing the septa (walls) between and around the solid/cystic components as well as more

precisely delineating the extent of any associated edema. Both factors are important when planning the resection margin for surgical intervention. 3D SWI or GRE T_2*-weighted images can additionally evaluate the degree of calcification, which is another common feature of gangliogliomas.

Polymicrogyria (Barkovich[29] group III)

Polymicrogyria is characterized by fused small gyri separated by shallow sulci, with cortical thickness varying from thin to thick, and can be unilateral or bilateral, often with perisylvian predominance. 3D T_1-weighted sequences (MP2RAGE or MPRAGE) are essential for assessing this type of pathology[30], as they permit clear delineation of lesion extent which can guide surgical resection (*figure 3*). On these images, the cortex will appear hypointense and wavy at the grey and white matter interface. While 3D sequences can be used to screen the whole brain for polymicrogyria, 2D sequences with ultrahigh resolution can be an alternative when delineation of a known lesion is requested. In addition, 3D SWI, SWAN and/or GRE T_2*-weighted images enable visualization of small pial vessels, seen as thin hypointense lines in the malformed cortex and sulci with an arboriform distribution as an additional identifying feature; the cortex itself appears extra hyperintense in these sequences.[6, 33]

4.2 Focal cortical dysplasias

Typical MRI findings of FCD include blurring of the gray-white junction with or without increased cortical thickness, and cortical and subcortical signal abnormality on both T_2-weighted /FLAIR and T_1-weighted sequences. Detection of FCD is generally more difficult than with other types of lesions, as the above-mentioned features can be subtle and inconspicuous given the complex convexities of the neocortex. Compared with 3T, lesion conspicuity and boundaries for FCD are typically better visualized at 7T (*figure 4*).[34] 3D SWI or GRE T_2*-weighted sequences allow visualization of

intracortical signal changes ("black line sign") which can improve subtyping FCD type II.[10, 35] Most centers rate 3D T_1-weighted and FLAIR sequences as most helpful for visualizing and diagnosing FCD due to their high image contrast at 7T; reconstructions in all three planes are recommended. Fluid and white matter suppression (FWMS) sequences have also been proposed to detect the transmantle sign in FCD type II.[36] Detection of FCDs at 7T that are completely invisible at lower field strengths seems infrequent[5, 6, 8, 13]; typically, the FCD is significantly less conspicuous at 3T and therefore easily missed. In other words, 7T images make it easier for the human eye to detect these subtle signal changes. Occasionally, *de novo* appearance of new lesions at 7T can be seen, although often in cases of very small lesions not optimally captured by the thicker 3T slices.[13] We suggest scrolling carefully through slices that cover regions where a suspected FCD lesion might be located, as they might still be subtle on 7T images. Finally, 7T can be helpful in ruling out 'FCD-appearing' normal cortex due to, among other factors, reduced partial volume effects compared with 3T (*figure 5*).[13]

4.3 Hippocampal sclerosis

Classic MRI features of HS are hippocampal atrophy, increased T_2-weighted/FLAIR signal intensity, and loss of normal morphology. 7T MRI excels in showing hippocampal morphology, including internal structure and surface features; 2D coronal TSE T_2-weighted and 3D T_1-weighted/FLAIR sequences are particularly suitable for this.[37-39] Hippocampal subfields can be more precisely delineated with training based on landmarks and surface features at 7T, including by automated segmentation methods.[40-42] Though evident at lower field strengths, the stratum radiatum lacunosum moleculare is more consistently identified on 7T T_2-weighted images as a continuous dark band running at the internal aspect of the cornu ammonis in normal hippocampi and variably absent or indistinct in HS (*figure 6*). Prominent infolding can cause the dark band to appear obscured on

coronal 3T images due to partial volume effects, and high-resolution images at 7T help to avoid this pitfall. Absence of digitations along the hippocampal head is another sensitive and specific finding for HS that is considerably more apparent on 7T images[43], as is loss of surface undulations along the inferior aspect of the hippocampal body, which is best assessed in the sagittal plane. In addition, while subclassification of HS is not currently used for presurgical assessment, pathological examination of subfields in postoperative tissue has been shown to provide prognostic information regarding expected surgical outcomes.[44] Overall, these findings suggest that preoperative detailed imaging of the entire hippocampal axis could have a significant impact on both detection and postsurgical outcome prediction.

4.4 Vascular malformations

The most frequent findings with 7T MRI are a higher number of small vascular malformations, particularly venous malformations, and improved visualization and characterization of cavernomas. Some lesions not visible at 1.5 or 3T can be observed with 7T, and angioarchitecture shown with 7T is close to histopathological findings.[45, 46] Sequences taking advantage of the increased spatial resolution *and* susceptibility (SWI/SWAN) are particularly helpful in detecting these lesions and any associated (micro)hemorrhage. SWI sequences at 7T can also clearly delineate the iron-containing gliotic rim, which is important when planning sufficient surgical resection. Care must be taken, however, not to overestimate lesion size: due to the increased susceptibility effects at 7T, cavernomas and other iron-containing structures will appear larger than they really are.[47]

5 Technical issues relevant for clinical practice

Although 7T MRI is already beneficial due to increased image contrast and spatial resolution, it is expected that its utility in epilepsy will be further expanded and optimized. Such progress, however, requires substantial engineering and scientific development to account for challenges posed by working on a UHF platform. Some of these technical challenges and possible solutions will be discussed here.

5.1 RF coils, RF shimming and multi-transmit (pTx) systems

Transmit RF fields represent one of the predominant challenges at 7T. Higher ^{1}H Larmor frequency implies shorter RF wavelengths, translating into strong tissue contrast and signal variations. This may also lead to an increase of SAR for a given target flip angle, with a tendency to form spatially localized hot spots presenting a safety hazard. Proposed solutions can be stratified into a) existing techniques applicable to any 7T platform with single/dual transmit coils; and b) techniques relying on more advanced resources, usable only in specialized research centers with pTx systems. The use of dielectric pads, described in *section 3.2*, perfectly illustrates an existing technique for portable RF shimming. Other existing solutions include specialized sequence designs, e.g., adiabatic pulses that are relatively insensitive to RF field variations[48, 49]. Among advanced solutions, strategies that employ expensive amplifiers and multi-transmit coils are e.g. higher order shimming and calibration-less 'Universal Pulse' models for pTx.[50] The use of the latter methods in clinical settings is pending CE/FDA approval of pTx 7T systems.

5.2 Motion correction

As described in *section 3*, the high-resolution 7T MRI sequences are particularly sensitive to motion.[51] Even small movements or breathing will create artefacts in susceptibility sensitive

techniques such as T_2*-weighted sequences or echo planar imaging (EPI).[52] Several retrospective and prospective correction methods have been suggested, and although promising, tracking of optical markers[53] or NMR-active probes[54] can be challenging due to the tight space in standard head coils, and require a workflow impractical for clinical use. Alternatively, methods based on embedding fat-selective navigators[55] or phase navigators[56] into sequence design have been successfully employed in a variety of applications. To correct for B_0 variation induced by motion, a prospective correction technique that dynamically updates shimming parameters in addition to the imaging geometry will be necessary.[57]

5.3 Susceptibility effects and artefacts

Different tissue types cause variations in susceptibility contrast and local field inhomogeneity. Since this property scales with field strength, tissue components exhibiting increased susceptibility – such as deoxyhemoglobin, ferritin and hemosiderin – can be more readily visualized by 7T T_2*-weighted sequences (including SWI, QSM and BOLD imaging).[58] However, tissues with different susceptibility characteristics can also cause undesirable local inhomogeneity. To minimize these undesired effects at 7T, advanced methods for B_0 shimming (including higher order shims) are needed. As a result, on the majority of new 7T platforms, additional automated B_0 shimming techniques are utilized; however, novel methods continue to be developed.

6   Future directions & concluding remarks

The increased SNR and susceptibility effects at 7T not only improve spatial resolution and image contrast but also facilitate more detailed analysis of functional and molecular aspects of tissues. Several MRI techniques that particularly benefit from these advantages, and have the potential to impact epilepsy MRI, are described below.

6.1 Functional MRI

Functional connectivity studies using 7T fMRI have been conducted to assess network alterations, e.g., by probing the fine-grained function and microstructure of hippocampal subfields in TLE patients. Significantly different patterns of functional network asymmetry in the hippocampus and its subfield CA1 have been found between TLE patients with and without HS using resting state fMRI, possibly improving preoperative lesion localization.[40] In addition, task-related fMRI mapping, which is often used for presurgical planning, benefits from the increased sensitivity to the BOLD effect, improved localization and decreased acquisition time at 7T compared to 3T.[12] Simultaneous EEG/fMRI recordings[59] and laminar fMRI using UHF[60] could also improve the delineation of (intra)cortical hemodynamic correlates of epileptic activity and laminar-specific brain rhythm alterations.

6.2 MR Spectroscopy (MRS) and GluCEST

Molecular imaging at 7T takes advantage of not only the increased spatial resolution, but also the increased spectral resolution of UHF. Both improve sensitivity and specificity of MRS by enabling detection of molecules that are difficult to resolve at lower field strengths, including neurotransmitters like GABA and glutamate. Previous studies have shown that an abnormal metabolism in the surgical resection region was related to outcome after surgery[61], and although

MRS could not demonstrate that metabolic characteristics can consistently lateralize the epileptogenic hippocampus, glutamine concentrations were found to correlate with verbal memory performance in TLE patients.[62] Exploring the concept of neurotransmitter brain networks using 7T MRS, another study investigated interregional GABA and glutamate associations, and found that MRI negative patients displayed an increased number of glutamate and GABA connections and increased average strength of the GABA network.[63] As a whole-brain alternative to MRS, CEST primed to glutamate (GluCEST) has also been used in epilepsy. One study identified increases in glutamate concentration in the hippocampus of seizure onset in a small case series of MRI negative TLE patients.[64]

6.3 X-Nuclei MRI

Increased sensitivity of UHF is particularly valuable for nuclei with lower abundance and SNR compared to ^{1}H-protons. X-nuclei MRI could provide new insights into molecular and cellular dysfunctions beyond the visible lesions. For instance, sodium (^{23}Na) MRI, with which ionic homeostasis and cell viability can be assessed in the human brain, would be a good candidate for epilepsy imaging; a previous study has shown that ^{23}Na MRI is sensitive to pathological processes related to epileptic activity.[65]

6.4 Concluding remarks

In this article, we have presented recommendations on how to set up and evaluate a 7T MRI epilepsy protocol, based on both literature and cumulative experience of the 7T Epilepsy Task Force in clinical practice as well as research. There are still significant technical challenges to be solved, and the field could profit from more clinical studies comparing specifically optimized (instead of clinically used) 3T protocols with 7T sequences. Nevertheless, comparative studies of epileptogenic

lesions between 7T and lower fields have shown better lesion conspicuity and delineation as well as less ambiguous findings at higher field in a clinical setting.[66, 67] Thus, several clinical indications clearly exist for epilepsy patients in whom a lesion is suspected and not convincingly seen at 3T or that requires better characterization. Promising future directions of 7T MRI in epilepsy also include MR techniques beyond structural imaging, although such novel functional and molecular methods need further clinical validation. At a time when approval for use of 7T MRI for diagnostic purposes is becoming a reality on a global level, we hope this article provided useful guidance when setting up a 7T MRI epilepsy protocol in the clinic.

Tables

Table 1 Summary of the eight most useful sequences as identified in a survey from 19 7T MRI centers experienced in examining epilepsy patients for research and/or diagnostic purposes.

Sequence type		Orientation	In-plane spatial resolution in mm, range (median)	Slice thickness in mm, range (median)	Duration in mm:ss, range (median)
Limited coverage					
T_2w #	TSE	Coronal[1]	0.25-0.70 (0.30)	1.00-3.00 (1.35)	3:36-8:48 (5:58)
	TSE	Axial[8]	0.40-0.70 (0.45)	0.75-3.00 (1.55)	3:39-12:00 (6:17)
T_2*w[6]	GRE	Coronal	0.25-0.38 (0.30)	1.65-2.00 (2.00)	5:22-6:12 (5:58)
Whole-brain coverage					
3D T_1w	MPRAGE[4]	Sagittal	0.60-0.90 (0.73)	0.60-1.00 (0.73)	6:47-10:12 (8:27)
	MP2RAGE[2]	Sagittal	0.60-0.80 (0.70)	0.60-0.80 (0.70)	5:20-11:45 (6:21)
3D FLAIR[3]		Sagittal	0.70-1.00 (0.80)	0.70-1.40 (0.80)	5:54-10.38 (7:27)
3D T_2*w[7]	GRE/SWI	Any	0.25-0.80 (0.50)	0.20-2.00 (0.90)	5:17-12:00 (8.27)
3D T_2w[5]	TSE	Sagittal/Axial	0.50-0.80 (0.70)	0.69-2.40 (0.70)	5:32-10:59 (7:11)

In a few centers, the multi-slice T_2-weighted TSE sequences were reconstructed to an even higher spatial resolution. [1-8] The order of importance as scored by the involved radiologists. Abbreviations: FLAIR, fluid attenuated inversion recovery; GRE, gradient recalled echo; MPRAGE, magnetization prepared rapid acquisition gradient echo; SWI, susceptibility-weighted imaging; TSE, turbo spin echo; w, weighted.

Table 2 Summary of sequences of particular interest for certain (known and/or suspected) epileptic lesion types; often used acquisition parameters can be found in the text and in *Table 1*.

Lesion type	Sequences of particular interest
Temporal lobe epilepsy with known or suspected HS	3D T_1w MPRAGE or MP2RAGE
	3D T_2w TSE
	2D T_2w TSE focused on hippocampus and anterior temporal lobe
Focal cortical dysplasia (type I and II)	3D T_1w MPRAGE or MP2RAGE (whole-brain)
	3D FLAIR
	3D T_2*w GRE or SWI
	+/- FWMS sequence
	+/- 2D T_2w TSE focused on suspected cortical lesion
LEAT (Gangliogliomas, DNET)	3D T_1w MPRAGE or MP2RAGE 3D T_2w TSE 3D T_2*w (GRE or SWI)
Polymicrogyria	3D T_1w MPRAGE or MP2RAGE
	3D T_2*w (SWI or SWAN)
	+/- FSPGR
Tuberous sclerosis complex	3D T_1w MPRAGE or MP2RAGE
	3D T_2*w (SWI or SWAN)
	3D FLAIR
Vascular malformations	3D T_2*w (SWI)
MRI negative at 3T	3D T_1w MPRAGE or MP2RAGE 3D FLAIR 3D T_2w TSE 3D T_2*w (GRE or SWI) +/- FWMS sequence +/- 2D T_2w TSE over regions indicated by, e.g., EEG

Abbreviations: FLAIR, fluid attenuated inversion recovery; FWMS, fluid and white matter suppressed; GRE, gradient recalled echo; MPRAGE, magnetization prepared rapid acquisition gradient echo; HS, hippocampal sclerosis; SWAN, susceptibility-weighted angiography; SWI, susceptibility-weighted imaging; TSE, turbo spin echo; w, weighted; LEAT, long-term epilepsy-associate tumors; DNET, dysembryoplastic neuroepithelial tumors

Figures
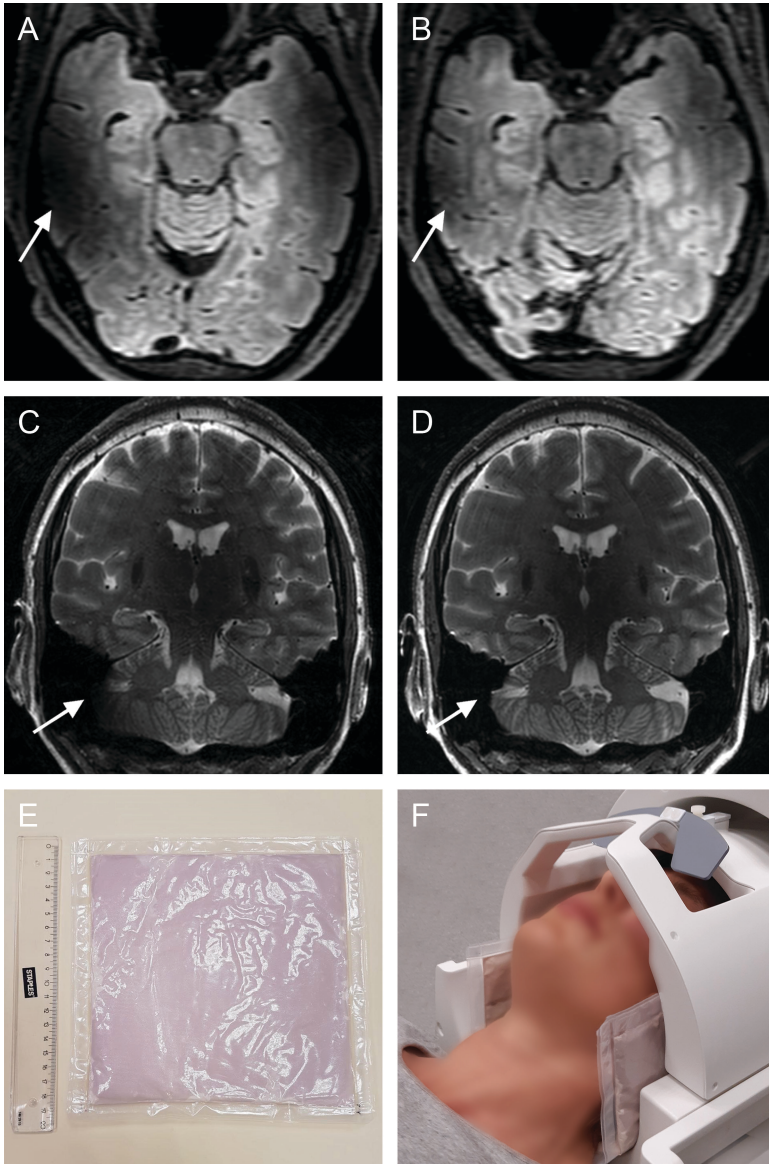
Figure 1 Use of dielectric pads. Illustration of the effect of dielectric pads on (A, B) 3D fluid-attenuated inversion recovery (FLAIR, 0.7^3 mm^3 resolution) and (C, D) T$_2$-weighted sequences (0.3x0.3x1.5 mm^3 resolution). In A and C, no pads are used, while in B and D they are. The dielectric pads used in this case are 19x19 cm^2 (E); pad placement for obtaining images B and D is demonstrated in image F. Of note, optimal pad placement depends on head size and shape.

Figure 2 Example of tuberous sclerosis complex at 7T. 3T T_1-weighted 0.9 mm isotropic MPRAGE (A, D), 7T T_1-weighted 0.6 mm isotropic MPRAGE (B-D) and 0.8 mm isotropic white matter-suppressed T_1-weighted images (F) in an 11-year-old female diagnosed with Tuberous Sclerosis Complex (TSC). Cortical tubers were found throughout the brain both at 3T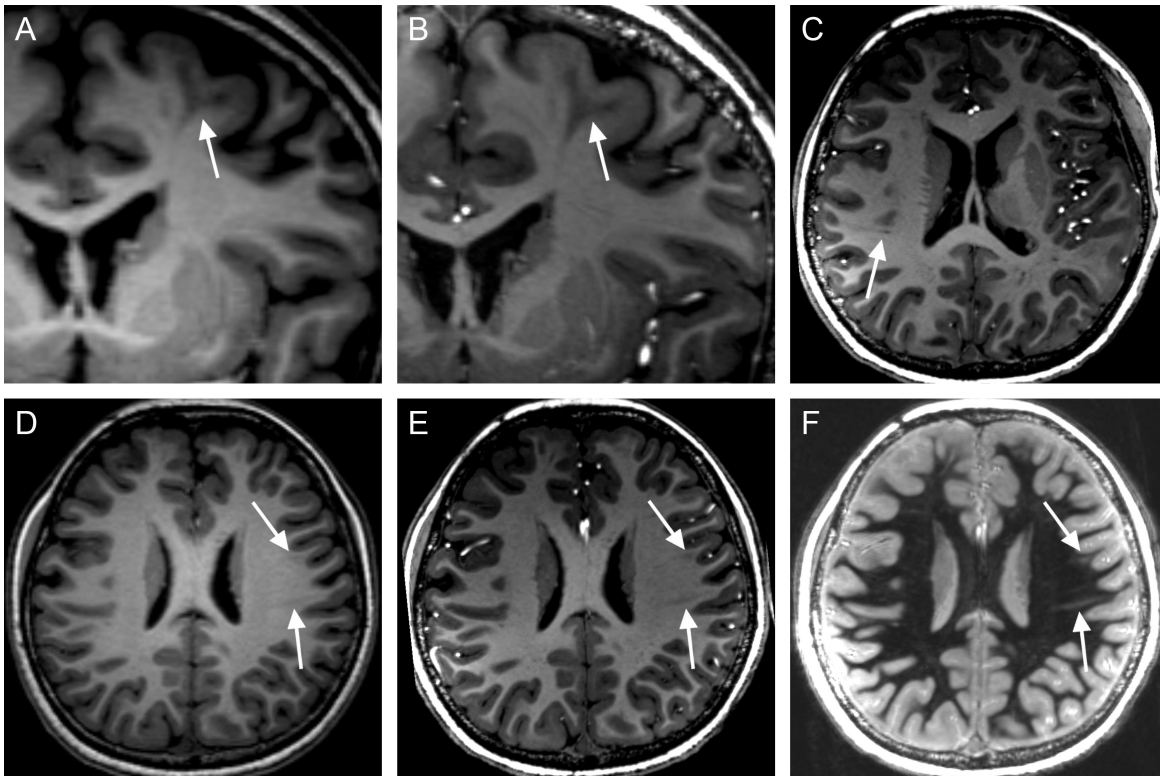 and 7T MRI (arrow in A and B). Radial migration bands, however, were much more difficult to visualize; subtle radial bands could be identified at 7T in the left frontal and parietal lobe (arrows in E and F) which were only retrospectively seen at 3T (D). In addition, more detailed structures surrounding both tubers and radial bands, as well as previously unidentified subtle TSC abnormalities such as a small cyst associated with a radial band in the right parietal lobe (C), were only seen at 7T images. This detailed delineation of TSC abnormalities may improve surgical resection, thereby increasing the likelihood of a seizure-free postoperative outcome. *Courtesy of Kaibao Sun, PhD, Center for MR Research, University of Illinois at Chicago, Chicago, IL, USA. Data was acquired during his*
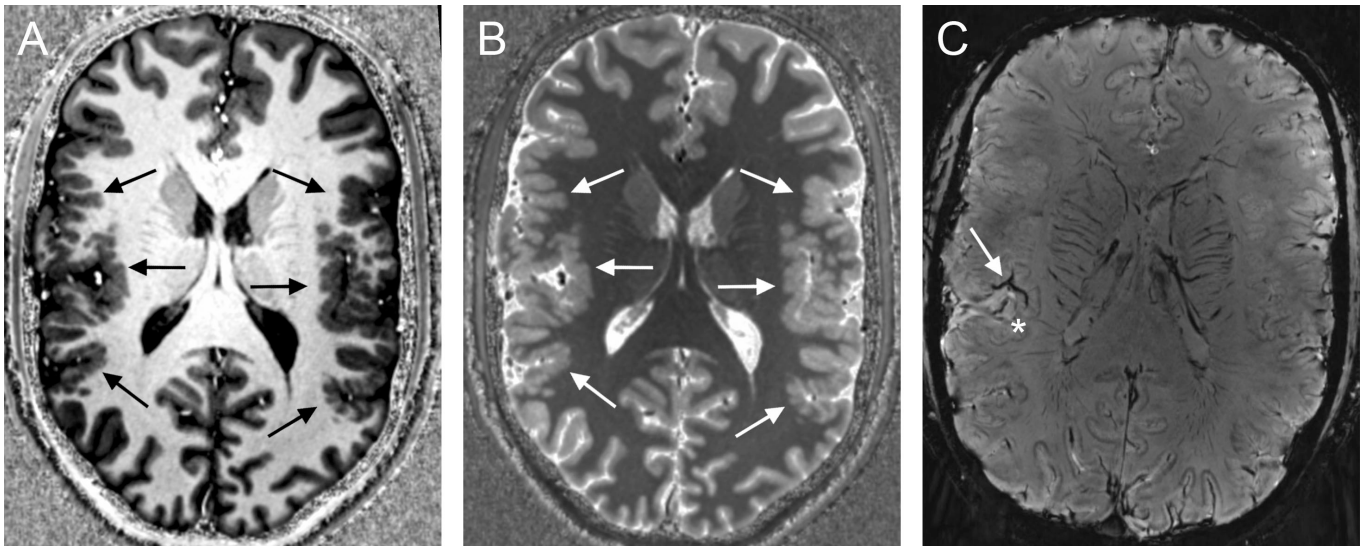
Figure 3 Example of polymicrogyria at 7T. 7T T_1-weighted MP2RAGE (A) and MP2RAGE T_1-map (B) images illustrate thickening of the perisylvian cortex (arrows in A and B) in an 18-year old patient who had known polymicrogyria as already visualized at 3T MRI; clinical indication for 7T imaging was better lesion delineation. An additional 7T T_2*-weighted (SWI) sequence (C) shows hyperintense cortex associated with veins perpendicular to the cortex (* in C) and a tree-like distribution of vessels (arrow in C).
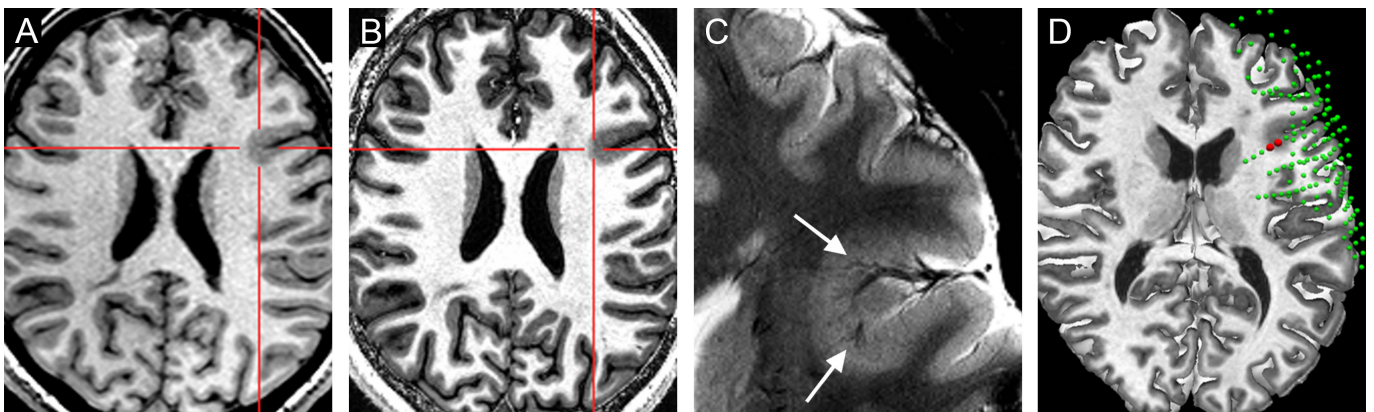
Figure 4 Example of focal cortical dysplasia at 7T. Axial 3T T_1-weighted MPRAGE (A), axial

7T T_1-weighted MP2RAGE (B) and zoomed in axial 7T T_2*-weighted GRE (C) images of a patient

for whom visual review of 7T MRI yielded previously unappreciated subtle findings. The red

crosshairs/arrows pinpoint the location of an area of focal cortical dysplasia (FCD) which was

detected by visual analysis of 7T images. The vascular changes associated with the FCD can be

well appreciated on the T_2*-weighted GRE images in Panel C (arrows). Detection of this subtle

lesion guided subsequent placement of intracranial-EEG (icEEG) with subdural grids and depth

electrodes. The icEEG implantation was devised to confirm the epileptogenicity of the subtle lesion,

map out the lesion extent and its proximity to eloquent cortex with language function. The subtle

lesion location was concordant with ictal onset on the icEEG as shown in the 3D reconstruction of

electrode location and 7T MRI, with 2D axial cut-plane (D). In Panel D, green spheres indicate all

implanted electrodes, red spheres indicate ictal onset.
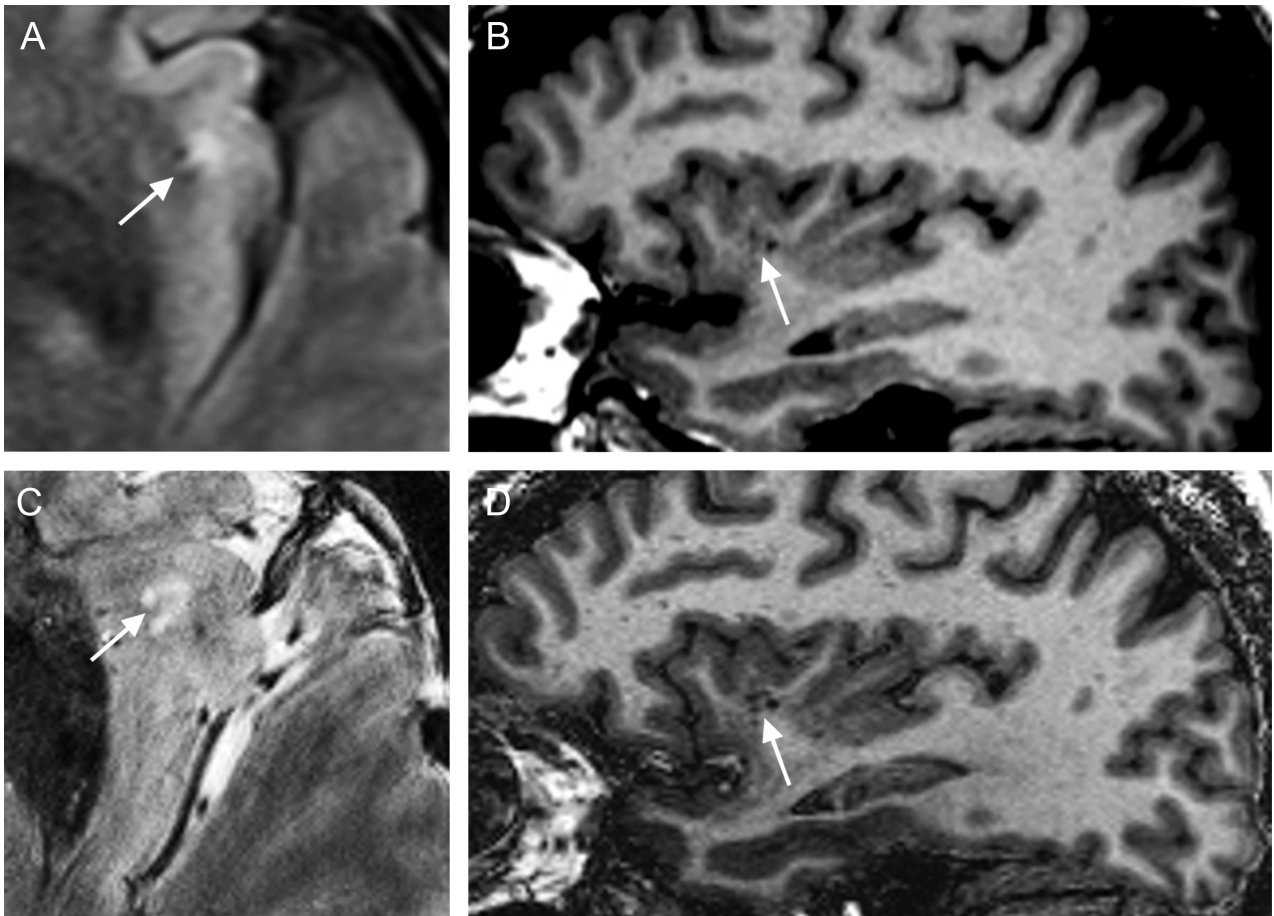
Figure 5 Vascular changes mimicking focal cortical dysplasia. Example of a lesion suspected to be FCD at 3T, but concluded to be vascular changes after reviewing 7T images. The 3T axial FLAIR (A) and 3T sagittal T_1-weighted images (B) suggested subcortical FLAIR hyperintensity and gray-white matter blurring of the left insular cortex, suspicious for FCD. The patient had an SEEG evaluation to explore the suspected area and other possible areas for seizure generation. The suspected area in the left insula was not involved in seizure onset. 7T T_2*-weighted GRE (C) and 7T sagittal T_1-weighted images (D) revealed the lesion to be a vascular abnormality causing adjacent gliosis that mimicked the appearance of FCD. Because of convincing evidence from the 7T images, the patient's surgical plan did not include the left insula.
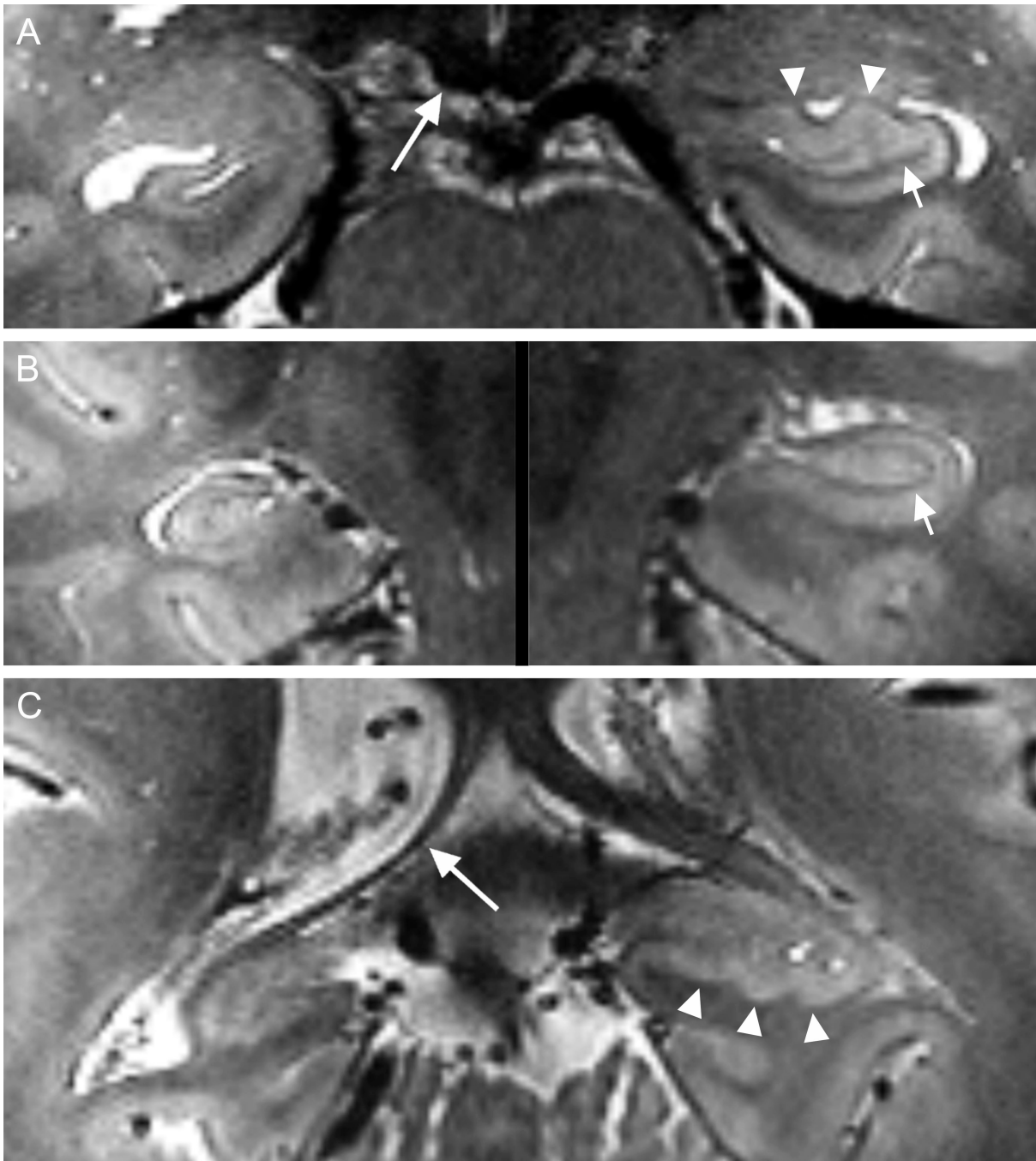
Figure 6 Hippocampal sclerosis (HS) at 7T. Coronal T_2-weighted images at the level of the hippocampal head (A), body (B) and tail (C) show normal appearance of the left hippocampus including a continuous dark band reflecting the stratum radiatum lacunosum moleculare (arrows) and normal digitations along the head and tail (arrowheads). In contrast, the right hippocampus shows features of HS including decreased volume, smooth outer counters, and indistinct internal

architecture. Note also atrophy of the right mammillary body (long arrow in A) and fornix (long arrow in C).

Appendix 1: Authors

Name	Location	Contribution
Giske Opheim, M.Sc.	Neurobiology Research Unit, Dept. Of Neurology, Rigshospitalet Copenhagen University Hospital, Copenhagen, Denmark	Drafting/revision of the manuscript for content, including medical writing for content; Major role in the acquisition of data; Study concept or design; Analysis or interpretation of data
Anja van der Kolk, MD, PhD	Dept. Of Radiology, University Medical Center Utrecht, Utrecht University, Utrecht, the Netherlands; Dept. of Radiology, Netherlands Cancer Institute – Antoni van Leeuwenhoek Hospital, Amsterdam, the Netherlands.	Drafting/revision of the manuscript for content, including medical writing for content; Major role in the acquisition of data; Study concept or design; Analysis or interpretation of data
Karin Markenroth Bloch, PhD	Lund University Bioimaging Center, Lund University, Lund, Sweden	Drafting/revision of the manuscript for content, including medical writing for content; Major role in the acquisition of data; Study concept or design
Albert J. Colon, MD, PhD	Dept. Of Neurology, Neurophysiology and Neurosurgery, ACE Kempenhaeghe/MUMC, Heeze/Maastricht, the Netherlands	Drafting/revision of the manuscript for content, including medical writing for content; Major role in the acquisition of data; Study concept or design
Kathryn A. Davis, MD, MS	Hospital of the University of Pennsylvania, Penn Epilepsy Center, Philadelphia, PA, USA	Drafting/revision of the manuscript for content, including medical writing for content; Major role in the acquisition of data; Study concept or design
Thomas R. Henry, MD	Division of Epilepsy, Dept. Of Neurology, University of Minnesota, Minneapolis, MN, USA	Drafting/revision of the manuscript for content, including medical writing for content; Major role in the acquisition of data; Study concept or design
Jacobus F.A. Jansen, PhD	Dept. Of Radiology and Nuclear Medicine, Maastricht University Medical Center, Maastricht, the Netherlands; School for Mental Health and Neuroscience, Maastricht University, Maastricht, the Netherlands; Dept. Of Electrical Engineering, Eindhoven University of	Drafting/revision of the manuscript for content, including medical writing for content; Major role in the acquisition of data; Study concept or design

	Technology, Eindhoven, the Netherlands	
Stephen E. Jones, MD, PhD	Imaging Institute, Cleveland Clinic, Cleveland, OH, USA	Drafting/revision of the manuscript for content, including medical writing for content; Major role in the acquisition of data; Study concept or design
Jullie W. Pan, PhD	Dept. of Neurology and Radiology, University of Pittsburg, Pittsburg, PA, USA	Drafting/revision of the manuscript for content, including medical writing for content; Major role in the acquisition of data; Study concept or design
Karl Rössler, MD, DMSc	Dept. Of Neurosurgery, Medical University of Vienna, Vienna, Austria	Drafting/revision of the manuscript for content, including medical writing for content; Major role in the acquisition of data
Joel M. Stein, MD, PhD	Dept. Of Radiology, Hospital of the University of Pennsylvania, Philadelphia, PA, USA	Drafting/revision of the manuscript for content, including medical writing for content; Major role in the acquisition of data; Study concept or design
Maria Compagno Strandberg, MD, PhD	Clinical Sciences Lund, Neurology, Lund University, Lund, Sweden	Drafting/revision of the manuscript for content, including medical writing for content; Major role in the acquisition of data
Siegfried Trattnig, MD, DMSc	High Field MR Center, Dept. of Biomedical Imaging and Image Guided Therapy, Medical University of Vienna, Vienna, Austria	Drafting/revision of the manuscript for content, including medical writing for content; Major role in the acquisition of data; Study concept or design
Pierre-Francois Van de Moortele, PhD	Center for Magnetic Resonance Research, University of Minnesota, Minneapolis, MN, USA	Drafting/revision of the manuscript for content, including medical writing for content; Major role in the acquisition of data; Study concept or design
Maria Isabel Vargas, MD	Neuroradiology Division, Diagnostic Unit, University Hospitals and Faculty of Medicine of Geneva, Switzerland	Drafting/revision of the manuscript for content, including medical writing for content; Major role in the acquisition of data; Study concept or design
Irene Wang, PhD	Epilepsy Center, Cleveland Clinic, Cleveland, OH, USA	Drafting/revision of the manuscript for content, including medical writing for content; Major role in the acquisition of data; Study concept or design
Fabrice Bartolomei, MD, PhD	Aix Marseille Univ, APHM, INSERM, INS, Inst Neurosci Syst, Timone Hospital,	Drafting/revision of the manuscript for content, including medical writing for content;

	Epileptology Department, Marseille, France	Major role in the acquisition of data
Neda Bernasconi, MD, PhD	Neuroimaging of Epilepsy Laboratory (NOEL), Montreal Neurological Institute and McConnel Brain Imaging Centre, McGill University, Montreal, QC, Canada	Drafting/revision of the manuscript for content, including medical writing for content
Andrea Bernasconi, MD	Neuroimaging of Epilepsy Laboratory (NOEL), Montreal Neurological Institute and McConnel Brain Imaging Centre, McGill University, Montreal, QC, Canada	Drafting/revision of the manuscript for content, including medical writing for content
Boris Bernhardt, PhD	Montreal Nerological Institute, McGill University, Montreal, QC, Canada	Drafting/revision of the manuscript for content, including medical writing for content
Isabella Björkman-Burtscher, MD, PhD	Dept. of Radiology, Institute of Clinical Sciences, Sahlgrenska Academy, University of Gothenburg, Gothenburg, Sweden	Drafting/revision of the manuscript for content, including medical writing for content; Major role in the acquisition of data; Study concept or design
Mirco Cosottini, MD, PhD	Dept. of Translational Research and New Technologies in Medicine and Surgery, University of Pisa, Italy	Drafting/revision of the manuscript for content, including medical writing for content; Major role in the acquisition of data; Study concept or design
Sandhitsu R. Das, PhD	Dept. of Neurology, University of Pennsylvania, Philadelphia, PA, USA	Drafting/revision of the manuscript for content, including medical writing for content; Major role in the acquisition of data
Lucie Hertz-Pannier, MD, PhD	Paris-Saclay University, CEA, NeuroSpin, Gif-sur-Yvette, France; University of Paris, UMR 1141, 75019 Paris, France	Drafting/revision of the manuscript for content, including medical writing for content; Major role in the acquisition of data; Study concept or design
Sara Inati, MD	EEG Section, NINDS, NIH, Bethesda, MD, USA	Drafting/revision of the manuscript for content, including medical writing for content; Major role in the acquisition of data
Michael T. Jurkiewicz, MD, PhD	Dept. Of Medical Imaging, Children's Hospital at London Health Sciences Centre, London, ON, Canada	Drafting/revision of the manuscript for content, including medical writing for content; Major role in the acquisition of data; Study concept or design

Ali R. Khan, PhD	Dept. of Medical Biophysics, Schulich School of Medicine and Dentistry, The University of Western Ontario, London, ON, Canada; Imaging Research Laboratories, Robarts Research Institute, London, ON, Canada	Drafting/revision of the manuscript for content, including medical writing for content; Major role in the acquisition of data; Study concept or design
Shuli Liang, MD, PhD	Functional Neurosurgery Department, Beijing Children's Hospital of Capital Medical University, Beijing, China	Drafting/revision of the manuscript for content, including medical writing for content; Major role in the acquisition of data; Study concept or design
Ruoyun Ma, PhD	Center for Magnetic Resonance Research, University of Minnesota, Minneapolis, MN, USA	Drafting/revision of the manuscript for content, including medical writing for content; Major role in the acquisition of data; Study concept or design
Srinivasan Mukundan, MD, PhD	Department of Radiology, Brigham and Women's Hospital, Harvard Medical School, Boston, MA, USA	Drafting/revision of the manuscript for content, including medical writing for content; Major role in the acquisition of data
Heath Pardoe, PhD	NYU Grossman School of Medicine, New York, NY, USA	Drafting/revision of the manuscript for content, including medical writing for content; Major role in the acquisition of data; Study concept or design
Lars H. Pinborg, MD, DMSc	Neurobiology Research Unit, Dept. Of Neurology, Rigshospitalet Copenhagen University Hospital, Copenhagen, Denmark; Epilepsy Clinic, Dept. Of Neurology, Rigshospitalet Copenhagen University Hospital, Copenhagen, Denmark	Drafting/revision of the manuscript for content, including medical writing for content; Major role in the acquisition of data; Study concept or design
Jonathan R. Polimeni, PhD	Harvard-MIT Division of Health Sciences and Technology, Massachusetts Institute of Technology, Cambridge, MA, USA; Athinoula A. Martinos Center for Biomedical Imaging, Dept. of Radiology, Harvard Medical	Drafting/revision of the manuscript for content, including medical writing for content

	School, Massachusetts General Hospital, Charlestown, MA, USA	
Jean-Philippe Ranjeva, MD, PhD	Aix Marseille Univ, CNRS, CRMBM, Marseille, France ; APHM, CEMEREM, Timone Hospital, Marseille, France	Drafting/revision of the manuscript for content, including medical writing for content; Major role in the acquisition of data
Esther Steijvers, B.Sc.	Scannexus Ultrahigh Field MRI Research Center, Maastricht, the Netherlands	Drafting/revision of the manuscript for content, including medical writing for content; Major role in the acquisition of data; Study concept or design
Steven Stufflebeam, MD, PhD	Harvard-MIT Division of Health Sciences and Technology, Massachusetts Institute of Technology, Cambridge, MA, USA; Athinoula A. Martinos Center for Biomedical Imaging, Dept. of Radiology, Harvard Medical School, Massachusetts General Hospital, Charlestown, MA, USA	Drafting/revision of the manuscript for content, including medical writing for content
Tim Jeroen Veersema, MD	Dept. Of Neurology and Neurosurgery, UMC Utrecht Brain Center, University Medical Center Utrecht, Utrecht, the Netherlands; Dept. Of Radiology and Nuclear Medicine, Meander Medical Center, Amersfoort, the Netherlands	Drafting/revision of the manuscript for content, including medical writing for content; Major role in the acquisition of data; Study concept or design
Alexandre Vignaud, MD, PhD	Paris-Saclay University, CEA, CNRS, BAOBAB, NeuroSpin, 91191, Gif-sur-Yvette, France	Drafting/revision of the manuscript for content, including medical writing for content; Major role in the acquisition of data
Natalie Voets, PhD	Wellcome Centre for Integrative Neuroimaging, FMRIB Division, Nuffield Dept. Of Clinical Neurosciences, University of Oxford, Oxford, UK	Drafting/revision of the manuscript for content, including medical writing for content; Major role in the acquisition of data
Serge Vulliemoz, MD, PhD	EEG and Epilepsy Unit, Neurology, Dept. of Clinical Neurosciences, University	Drafting/revision of the manuscript for content, including medical writing for content;

	Hospitals and Faculty of Medicine of Geneva, Switzerland	Major role in the acquisition of data
Christopher J. Wiggins, PhD	Scannexus Ultrahigh Field MRI Research Center, Maastricht, the Netherlands	Drafting/revision of the manuscript for content, including medical writing for content; Major role in the acquisition of data; Study concept or design
Rong Xue, PhD	State Key Lab. of Brain and Cognitive Science, Beijing MRI Center for Brain Research, Institute of Biophysics, Chinese Academy of Sciences, Beijing, China	Drafting/revision of the manuscript for content, including medical writing for content; Major role in the acquisition of data
Renzo Guerrini, MD, FRCP	Neuroscience Department, Children's Hospital A. Meyer-University of Florence and IMAGO 7 Foundation, Italy	Drafting/revision of the manuscript for content, including medical writing for content; Major role in the acquisition of data; Study concept or design
Maxime Guye, MD, PhD	Aix Marseille Univ, CNRS, CRMBM, Marseille, France; APHM, CEMEREM, Timone Hospital, Marseille, France	Drafting/revision of the manuscript for content, including medical writing for content; Major role in the acquisition of data; Study concept or design; Analysis or interpretation of data

References:

1.   Ryvlin P, Cross JH, Rheims S. Epilepsy surgery in children and adults. Lancet Neurol 2014;13:1114-1126.

2.   Téllez-Zenteno JF, Hernández Ronquillo L, Moien-Afshari F, Wiebe S. Surgical outcomes in lesional and non-lesional epilepsy: a systematic review and meta-analysis. Epilepsy Res 2010;89:310-318.

3.   van der Zwaag W, Schäfer A, Marques JP, Turner R, Trampel R. Recent applications of UHF-MRI in the study of human brain function and structure: a review. NMR Biomed 2016;29:1274-1288.

4.   Trattnig S, Bogner W, Gruber S, et al. Clinical applications at ultrahigh field (7 T). Where does it make the difference? NMR Biomed 2016;29:1316-1334.

5.   Feldman RE, Delman BN, Pawha PS, et al. 7T MRI in epilepsy patients with previously normal clinical MRI exams compared against healthy controls. PloS One 2019;14:e0213642.

6.   De Ciantis A, Barba C, Tassi L, et al. 7T MRI in focal epilepsy with unrevealing conventional field strength imaging. Epilepsia 2016;57:445-454.

7.   Colon AJ, Osch M, Buijs M, et al. MEG-guided analysis of 7T-MRI in patients with epilepsy. Seizure 2018;60:29-38.

8.   Veersema TJ, Ferrier CH, van Eijsden P, et al. Seven tesla MRI improves detection of focal cortical dysplasia in patients with refractory focal epilepsy. Epilepsia Open 2017;2:162-171.

9.   Englot DJ, Raygor KP, Molinaro AM, et al. Factors associated with failed focal neocortical epilepsy surgery. Neurosurgery 2014;75:648-645;discussion 655;quiz 656.

10.   Bartolini E, Cosottini M, Costagli M, et al. Ultra-High-Field Targeted Imaging of Focal Cortical Dysplasia: The Intracortical Black Line Sign in Type IIb. AJNR Am J Neuroradiol 2019;40:2137-2142.

11.   Rondinoni C, Magnun C, Vallota da Silva A, Heinsen HM, Amaro E, Jr. Epilepsy under the scope of ultra-high field MRI. Epilepsy Behav 2019:106366.

12.   Bernasconi A, Cendes F, Theodore WH, et al. Recommendations for the use of structural magnetic resonance imaging in the care of patients with epilepsy: A consensus report from the International League Against Epilepsy Neuroimaging Task Force. Epilepsia 2019;60:1054-1068.

13.   Wang I, Oh S, Blümcke I, et al. Value of 7T MRI and post-processing in patients with nonlesional 3T MRI undergoing epilepsy presurgical evaluation. Epilepsia 2020.

14.   Beisteiner R, Robinson S, Wurnig M, et al. Clinical fMRI: evidence for a 7T benefit over 3T. NeuroImage 2011;57:1015-1021.

15.   Rauschenberg J, Nagel AM, Ladd SC, et al. Multicenter study of subjective acceptance during magnetic resonance imaging at 7 and 9.4 T. Invest Radiol 2014;49:249-259.

16.   Cosottini M, Frosini D, Biagi L, et al. Short-term side-effects of brain MR examination at 7 T: a single-centre experience. Eur Radiol 2014;24:1923-1928.

17.   Hansson B, Markenroth Bloch K, Owman T, et al. Subjectively Reported Effects Experienced in an Actively Shielded 7T MRI: A Large-Scale Study. J Magn Reson Imaging 2020;52:1265-1276.

18.   Kraff O, Quick HH. 7T: Physics, safety, and potential clinical applications. J Magn Reson Imaging 2017;46:1573-1589.

19.   Hoff MN, McKinney At, Shellock FG, et al. Safety Considerations of 7-T MRI in Clinical Practice. Radiology 2019;292:509-518.

20.   Mugler JP, 3rd, Brookeman JR. Three-dimensional magnetization-prepared rapid gradient-echo imaging (3D MP RAGE). Magn Reson Med 1990;15:152-157.

21.   Van de Moortele PF, Auerbach EJ, Olman C, Yacoub E, Uğurbil K, Moeller S. T1 weighted brain images at 7 Tesla unbiased for Proton Density, T2* contrast and RF coil receive B1 sensitivity with simultaneous vessel visualization. NeuroImage 2009;46:432-446.

22.   Marques JP, Kober T, Krueger G, van der Zwaag W, Van de Moortele PF, Gruetter R. MP2RAGE, a self bias-field corrected sequence for improved segmentation and T1-mapping at high field. NeuroImage 2010;49:1271-1281.

23.   Visser F, Zwanenburg JJ, Hoogduin JM, Luijten PR. High-resolution magnetization-prepared 3D-FLAIR imaging at 7.0 Tesla. Magn Reson Med 2010;64:194-202.

24.   Beqiri A, Hoogduin H, Sbrizzi A, Hajnal JV, Malik SJ. Whole-brain 3D FLAIR at 7T using direct signal control. Magn Reson Med 2018;80:1533-1545.

25.   Pan JW, Moon CH, Hetherington HP. Cerebrospinal fluid-suppressed T(2) -weighted MR imaging at 7 T for human brain. Magn Reson Med 2019;81:2924-2936.

26.   Webb AG. Dielectric materials in magnetic resonance. Concepts in Magnetic Resonance Part A 2011;38A:148-184.

27.   Teeuwisse WM, Brink WM, Haines KN, Webb AG. Simulations of high permittivity materials for 7 T neuroimaging and evaluation of a new barium titanate-based dielectric. Magn Reson Med 2012;67:912-918.

28.   Feldman RE, Rutland JW, Fields MC, et al. Quantification of perivascular spaces at 7T: A potential MRI biomarker for epilepsy. Seizure 2018;54:11-18.

29.   Barkovich AJ, Guerrini R, Kuzniecky RI, Jackson GD, Dobyns WB. A developmental and genetic classification for malformations of cortical development: update 2012. Brain 2012;135:1348-1369.

30.   Pittau F, Baud MO, Jorge J, et al. MP2RAGE and Susceptibility-Weighted Imaging in Lesional Epilepsy at 7T. J Neuroimaging 2018;28:365-369.

31.   Sun K, Cui J, Wang B, et al. Magnetic resonance imaging of tuberous sclerosis complex with or without epilepsy at 7 T. Neuroradiology 2018;60:785-794.

32.   Slegers RJ, Blumcke I. Low-grade developmental and epilepsy associated brain tumors: a critical update 2020. Acta Neuropathol Commun 2020;8:27.

33.   De Ciantis A, Barkovich AJ, Cosottini M, et al. Ultra-high-field MR imaging in polymicrogyria and epilepsy. AJNR Am J Neuroradiol 2015;36:309-316.

34.   Kelley SA, Robinson S, Crone NE, Soares BP. Bottom-of-sulcus focal cortical dysplasia presenting as epilepsia partialis continua multimodality characterization including 7T MRI. Childs Nerv Syst 2018;34:1267-1269.

35.   Thapaliya K, Urriola J, Barth M, Reutens DC, Bollmann S, Vegh V. 7T GRE-MRI signal compartments are sensitive to dysplastic tissue in focal epilepsy. Magn Reson Imaging 2019;61:1-8.

36.   Guye M, Bartolomei F, Ranjeva JP. Malformations of cortical development: The role of 7-Tesla magnetic resonance imaging in diagnosis. Rev Neurol (Paris) 2019;175:157-162.

37.   Stefanits H, Springer E, Pataraia E, et al. Seven-Tesla MRI of Hippocampal Sclerosis: An In Vivo Feasibility Study With Histological Correlations. Invest Radiol 2017;52:666-671.

38.   Gillmann C, Coras R, Rössler K, et al. Ultra-high field MRI of human hippocampi: Morphological and multiparametric differentiation of hippocampal sclerosis subtypes. PloS One 2018;13:e0196008.

39.   Feldman RE, Marcuse LV, Verma G, et al. Seven-tesla susceptibility-weighted analysis of hippocampal venous structures: Application to magnetic-resonance-normal focal epilepsy. Epilepsia 2020;61:287-296.

40.   Shah P, Bassett DS, Wisse LEM, et al. Structural and functional asymmetry of medial temporal subregions in unilateral temporal lobe epilepsy: A 7T MRI study. Hum Brain Mapp 2019;40:2390-2398.

41. Wisse LE, Kuijf HJ, Honingh AM, et al. Automated Hippocampal Subfield Segmentation at 7T MRI. AJNR Am J Neuroradiol 2016;37:1050-1057.

42. DeKraker J, Ferko KM, Lau JC, Köhler S, Khan AR. Unfolding the hippocampus: An intrinsic coordinate system for subfield segmentations and quantitative mapping. NeuroImage 2018;167:408-418.

43. Henry TR, Chupin M, Lehéricy S, et al. Hippocampal sclerosis in temporal lobe epilepsy: findings at 7 T[1]. Radiology 2011;261:199-209.

44. Blümcke I, Thom M, Aronica E, et al. International consensus classification of hippocampal sclerosis in temporal lobe epilepsy: a Task Force report from the ILAE Commission on Diagnostic Methods. Epilepsia 2013;54:1315-1329.

45. Shenkar R, Venkatasubramanian PN, Zhao JC, Batjer HH, Wyrwicz AM, Awad IA. Advanced magnetic resonance imaging of cerebral cavernous malformations: part I. High-field imaging of excised human lesions. Neurosurgery 2008;63:782-789; discussion 789.

46. Shenkar R, Venkatasubramanian PN, Wyrwicz AM, et al. Advanced magnetic resonance imaging of cerebral cavernous malformations: part II. Imaging of lesions in murine models. Neurosurgery 2008;63:790-797; discussion 797-798.

47. Campbell PG, Jabbour P, Yadla S, Awad IA. Emerging clinical imaging techniques for cerebral cavernous malformations: a systematic review. Neurosurg Focus 2010;29:E6.

48. Ma R, Henry TR, Van de Moortele PF. Eliminating susceptibility induced hyperintensities in T1w MPRAGE brain images at 7 T. Magn Reson Imaging 2019;63:274-279.

49. van Veluw SJ, Fracasso A, Visser F, et al. FLAIR images at 7 Tesla MRI highlight the ependyma and the outer layers of the cerebral cortex. NeuroImage 2015;104:100-109.

50. Deniz CM. Parallel Transmission for Ultrahigh Field MRI. Top Magn Reson Imaging 2019;28:159-171.

51.   Ladd ME, Bachert P, Meyerspeer M, et al. Pros and cons of ultra-high-field MRI/MRS for human application. Prog Nucl Magn Reson Spectrosc 2018;109:1-50.

52.   van Gelderen P, de Zwart JA, Starewicz P, Hinks RS, Duyn JH. Real-time shimming to compensate for respiration-induced B0 fluctuations. Magn Reson Med 2007;57:362-368.

53.   DiGiacomo P, Maclaren J, Aksoy M, et al. A within-coil optical prospective motion-correction system for brain imaging at 7T. Magn Reson Med 2020;84:1661-1671.

54.   Aranovitch A, Haeberlin M, Gross S, et al. Prospective motion correction with NMR markers using only native sequence elements. Magn Reson Med 2018;79:2046-2056.

55.   Boer VO, Andersen M, Lind A, Lee NG, Marsman A, Petersen ET. MR spectroscopy using static higher order shimming with dynamic linear terms (HOS-DLT) for improved water suppression, interleaved MRS-fMRI, and navigator-based motion correction at 7T. Magn Reson Med 2020;84:1101-1112.

56.   Liu J, van Gelderen P, de Zwart JA, Duyn JH. Reducing motion sensitivity in 3D high-resolution T(2)*-weighted MRI by navigator-based motion and nonlinear magnetic field correction. NeuroImage 2020;206:116332.

57.   Deelchand DK, Joers JM, Auerbach EJ, Henry PG. Prospective motion and B(0) shim correction for MR spectroscopy in human brain at 7T. Magn Reson Med 2019;82:1984-1992.

58.   Bian W, Hess CP, Chang SM, Nelson SJ, Lupo JM. Susceptibility-weighted MR imaging of radiation therapy-induced cerebral microbleeds in patients with glioma: a comparison between 3T and 7T. Neuroradiology 2014;56:91-96.

59.   Jorge J, Grouiller F, Gruetter R, van der Zwaag W, Figueiredo P. Towards high-quality simultaneous EEG-fMRI at 7 T: Detection and reduction of EEG artifacts due to head motion. NeuroImage 2015;120:143-153.

60.   Norris DG, Polimeni JR. Laminar (f)MRI: A short history and future prospects. NeuroImage 2019;197:643-649.

61.   Pan JW, Duckrow RB, Gerrard J, et al. 7T MR spectroscopic imaging in the localization of surgical epilepsy. Epilepsia 2013;54:1668-1678.

62.   Voets NL, Hodgetts CJ, Sen A, Adcock JE, Emir U. Hippocampal MRS and subfield volumetry at 7T detects dysfunction not specific to seizure focus. Sci Rep 2017;7:16138.

63.   van Veenendaal TM, Backes WH, Tse DHY, et al. High field imaging of large-scale neurotransmitter networks: Proof of concept and initial application to epilepsy. NeuroImage Clinical 2018;19:47-55.

64.   Davis KA, Nanga RP, Das S, et al. Glutamate imaging (GluCEST) lateralizes epileptic foci in nonlesional temporal lobe epilepsy. Sci Transl Med 2015;7:309ra161.

65.   Ridley B, Marchi A, Wirsich J, et al. Brain sodium MRI in human epilepsy: Disturbances of ionic homeostasis reflect the organization of pathological regions. NeuroImage 2017;157:173-183.

66.   Obusez EC, Lowe M, Oh SH, et al. 7T MR of intracranial pathology: Preliminary observations and comparisons to 3T and 1.5T. NeuroImage 2018;168:459-476.

67.   Springer E, Dymerska B, Cardoso PL, et al. Comparison of Routine Brain Imaging at 3 T and 7 T. Invest Radiol 2016;51:469-482.

A.3.1 Co-author declarations Article 3

DECLARATION OF CO-AUTHORSHIP

The declaration is for PhD students and must be completed for each conjointly authored article. Please note that if a manuscript or published paper has ten or less co-authors, all co-authors must sign the declaration of co-authorship. If it has more than ten co-authors, declarations of co-authorship from the corresponding author(s), the senior author and the principal supervisor (if relevant) are a minimum requirement.

1. Declaration by	
Name of PhD student	Giske F. Opheim
E-mail	giskeopheim@nru.dk
Name of principal supervisor	Lars H. Pinborg
Title of the PhD thesis	Utilizing 7 Tesla MRI and automated segmentation - A new era in the presurgical evaluation of patients with severe epilepsy

2. The declaration applies to the following article	
Title of article	7T Epilepsy Task Force Consensus Recommendations on the use of 7T in Clinical Practice

Article status	
Published ☐ Date:	Accepted for publication ☒ Date: October 29th 2020
Manuscript submitted ☑ Date:	Manuscript not submitted ☐
If the article is published or accepted for publication, please state the name of journal, year, volume, page and DOI (if you have the information).	The article is still under embargo, and according to the journal's policy, we are prohibited from releasing information about it until after publication.

3. The PhD student's contribution to the article *(please use the scale A-F as benchmark)* Benchmark scale of the PhD-student's contribution to the article **A.** Has essentially done all the work (> 90 %) **B.** Has done most of the work (60-90 %) **C.** Has contributed considerably (30-60 %) **D.** Has contributed (10-30 %) **E.** No or little contribution (<10 %) **F.** Not relevant	A, B, C, D, E, F
1. Formulation/identification of the scientific problem	C
2. Development of the key methods	F
3. Planning of the experiments and methodology design and development	B
4. Conducting the experimental work/clinical studies/data collection/obtaining access to data	F

3. The PhD student's contribution to the article *(please use the scale A-F as benchmark)*	A, B, C, D, E, F
Benchmark scale of the PhD-student's contribution to the article	
A. Has essentially done all the work (> 90 %) B. Has done most of the work (60-90 %) C. Has contributed considerably (30-60 %) D. Has contributed (10-30 %) E. No or little contribution (<10 %) F. Not relevant	
5. Conducting the analysis of data	A
6. Interpretation of the results	B
7. Writing of the first draft of the manuscript	C
8. Finalisation of the manuscript and submission	B

Provide a short description of the PhD student's specific contribution to the article.[i]

The PhD student has:
- co-initiated and co-organized the project work
- written the survey which laid the basis for our data collection
- collected data and presented overview for concensus voting during teleconferences
- coordinated the discussion groups and drafting process
- finalized the manuscript together with second and senior author

4. Material from another thesis / dissertation[ii]	
Does the article contain work which has also formed part of another thesis, e.g. master's thesis, PhD thesis or doctoral dissertation (the PhD student's or another person's)?	Yes: ☐ No: ☒
If yes, please state name of the author and title of thesis / dissertation.	
If the article is part of another author's academic degree, please describe the PhD student's and the author's contributions to the article so that the individual contributions are clearly distinguishable from one another.	

5.	Signatures of the co-authors[iii]			
	Date	Name	Title	Signature
1.	2020-11-06	Maxime Guye (senior author)	MD, PhD, Prof.	
2.	2020-11-06	Lars H. Pinborg (co-author and main PhD supervisor)	MD, DMSc	

5.	Signatures of the co-authors[iii]			
3.				
4.				
5.				
6.				
7.				
8.				
9.				
10.				

6.	Signature of the principal supervisor
I solemnly declare that the information provided in this declaration is accurate to the best of my knowledge.	
Date: 2020-11-06	
Principal supervisor:	

7.	Signature of the PhD student
I solemnly declare that the information provided in this declaration is accurate to the best of my knowledge.	
Date: 2020-10-30	
PhD student: Gisle F. Opheim	

Please learn more about responsible conduct of research on the Faculty of Health and Medical Sciences' website.

---

[i] This can be supplemented with an additional letter if needed.

[ii] Please see Ministerial Order on the PhD Programme at the Universities and Certain Higher Artistic Educational

"Any articles included in the thesis may be written in cooperation with others, provided that each of the co-authors submits a written declaration stating the PhD student's or the author's contribution to the work."

[iii] If more signatures are needed please add an extra sheet.

A.4 7T Epilepsy Task Force - the survey

7T MR Epilepsy Task Force Survey

The purpose of the following form is to provide us with a systematic overview of both technical as well all clinical details on 7T epilepsy imaging in the institutions participating in this task force. We wish to identify similarities and differences between our 7T MR systems and epilepsy protocols, similarities in how we select patients and assess sequences/images, and any specific experiences that you might have with regard to these 7T examinations.

The form contains three main sections:
1) Vendors, hardware, sequences
2) Radiology – rating of sequences
3) General questions – epilepsy protocol, patients, other details, opinions

Short instructions on how to fill out this form will be given next to each head question. With regards to sequences, you may attach the exam card from the scanner (please export in format readable by all computer platforms) instead of filling out the form. If you wish to attach the exam card, please state if any sequences therein should be disregarded.

Filled out forms can be sent to Giske Opheim (giskeopheim@nru.dk), who will keep track of all data and present findings at the first joint tcon meeting.

 Please do not hesitate to reach out to Giske if you cannot make this deadline or if you have any questions / comments on / suggestions with regard to the form.

Also on behalf of Anja van der Kolk and Maxime Guye,

Giske Opheim

Email: giskeopheim@nru.dk
Skype: gopheim_3
Office phone: +45 35456718
Cellphone: +45 42303710 (also on Whatsapp)
WeChat: GiskeOp

Section 1

VENDORS, HARDWARE

Vendor	
Head Coil (If your head coil enables multi-transmit, state whether you use this)	
Use of dielectric pads – yes/no (if yes, what size?)	
Any hearing protection used? (if yes, please specify, e.g. headphones, ear plugs…)	

SCAN PROTOCOL (If you prefer to send Exam Card instead, please attach to email)

Sequence name	Image contrast (e.g. T_1, FLAIR)	Sampling direction	Acquired resolution	Reconstructed resolution	Reconstructions used (direction + resolution)	Scan duration (min:sec)
			… x … x … mm^3	… x … x … mm^3		… : …

Total scan duration (min:sec)	

Section 2

RADIOLOGY RATING – rate 7T MR sequences according to importance (1 being most and 5 being least important)

This is a relative scale rating to inform us of how important the sequences you use are to your radiologist(s). Please rate each sequence individually; this also means several sequences can get the same rating. Comments are optional but encouraged, e.g. "most often associated with movement artefacts" etc.. A comment may also be whether you use this sequence in a specific subgroup of patients only.

Sequence name	Rate (1 to 5)	Comments

MAIN RADIOLOGICAL CHALLENGES (optional)

If there are any key challenge(s) encountered when viewing the images, please state below. This can for instance be B1 inhomogeneity, artefacts of any kind, or other signal changes specific to the 7T images that are time-consuming to adjust to. Please use key words and short sentences when filling out this box.

Section 3

Please address these questions in a concise way; a comments box is provided at the end of this section.

No. of radiologists at your center	
No. of radiologists responsible for/experienced with 7T MR and epilepsy	
No. of epilepsy patients scanned so far at 7T MR at your institution	
Yearly no. of epilepsy patients yearly who receive surgical treatment	
Any MR negative patients undergoing surgery? (if yes, please state percentage of MR negative patients, OR in case these patients are not scanned at 7T at all, state N/A)	
Do you scan epilepsy patients in a clinical setting, a research setting, or both?	
Type of patients you include(d) – both in research and in clinical setting (e.g, "MR negative only", "presurgical evaluation cohort", "all subgroups")	
If you (also) scan patients in a research setting: Do you use any sequences that you consider as extraordinary sequences? (if yes, please specify)	
Do you (as clinician) / do your radiologists consider 7T MR informative when evaluating epilepsy patients?	
Do radiologists assessing 7T epilepsy cases at your institution also assess 7T data from other patient groups? (if yes, please specify)	
What viewer do you use for 7T MR? (e.g. PACS, in-house software)	
Is the above-mentioned viewer the same as you use for 3T, and integrated with PACS? (yes/no)	
Do you do any additional processing before radiological assessment) (E.g. bias field corrections, extraordinary motion correction schemes, etc.)	
If any, what patient complaints have you encountered that are specific to 7T MR examinations?	
Do you spend extra time preparing epilepsy patients before their 7T exam, compared to a 3T exam?	
Have you assessed the added value of 7T MR in a study, or are currently investigating this? (yes/no/currently)	
Do you consider 7T MR to be ready for clinical use in epilepsy? (yes/no)	

Any other comments for the overview survey (optional):	

Filled out by

Name	Institution	Date